Graduate Student Theses, Dissertations, &
Professional Papers

Graduate School

2019

THE GENETIC MECHANISMS UNDERLYING PIGMENTATION AND THEIR EVOLUTIONARY IMPORTANCE IN BIRDS

Nicholas David Sly

Let us know how access to this document benefits you.

Follow this and additional works at: https://scholarworks.umt.edu/etd

THE GENETIC MECHANISMS UNDERLYING PIGMENTATION AND THEIR

EVOLUTIONARY IMPORTANCE IN BIRDS

By

NICHOLAS DAVID SLY

B.S. Biological Sciences, Cornell University, Ithaca, NY, 2008

Dissertation

presented in partial fulfillment of the requirements
for the degree of

Doctor of Philosophy
in Organismal Biology, Ecology, and Evolution

The University of Montana
Missoula, MT

May 2019

Approved by:

Scott Whittenburg, Dean of The Graduate School
Graduate School

Zachary Cheviron, Chair
Division of Biological Sciences

Creagh Breuner
Division of Biological Sciences

Douglas J. Emlen
Division of Biological Sciences

Jeffrey M. Good
Division of Biological Sciences

Matthew Shawkey
Department of Biology, University of Gent

Sly, Nicholas D., PhD, Spring 2018   Organismal Biology, Ecology, and Evolution

The genetic mechanisms underlying pigmentation and their evolutionary importance in birds

Chairperson: Dr. Zachary Cheviron

ABSTRACT: Integumentary pigmentation is a phenotype of fundamental importance to animals, with major impacts on survival and fitness. Thus, understanding the mechanisms underlying pigmentation can help illuminate general principles about how adaptive variation is generated and maintained in populations. Here, I present a dissertation that is aimed at understanding the developmental, regulatory, and genetic mechanisms that underlie variation in avian plumage color, and their evolutionary importance.

In my first chapter, I addressed how the modular organization of plumage traits may impact their evolution. The production of color in developing feathers is a modular process, with several mechanisms combining to produce the complete feather phenotype. A modular trait organization is predicted to increase phenotypic evolvability by reducing negative pleiotropic interactions with functionally unrelated traits. Through phylogenetic comparative analysis, I show that separate mechanisms producing feather colors show independent, uncorrelated patterns of evolutionary change, consistent with their modular organization. My results show that developmental modularity can have detectable impacts on trait evolution.

For my second chapter, I identified gene expression variation associated with melanin pigmentation in the Zebra Finch. I found differential expression of several functionally important genes that synthesize melanin. In addition, I found changes in expression in the signaling pathways that govern transcription of melanogenesis genes. These signaling pathways differ from those previously reported to drive major pigmentation differences, indicating that the regulation of melanogenesis is flexible in how it generates similar phenotypic outcomes.

For my third chapter, I identified the genetic basis for loss of sexual dimorphism in a domestic color morph of Zebra Finch. With whole-genome sequencing, I found a major divergence peak between dimorphic and monomorphic finches containing the gene Norrie Disease Protein (NDP). NDP is a signaling molecule that regulates transcription of several melanogenesis genes, and is underexpressed when dimorphism is lost. Sexual dimorphism can be lost repeatedly and rapidly in many groups. My work shows that relatively simple genetic changes in the regulation of important signaling molecules can influence sexual dimorphism in a patch-specific manner, facilitating this rapid evolution.

ACKNOWLEDGEMENTS:

I dedicate this dissertation to my grandmothers

Beverley A. Luick (1937-2009)

and

Elizabeth A. Sly (1928-2018)

You shaped who I am today.
You nurtured my passion for the natural world.
You supported me with unconditional love that will always stay with me.
It pains me deeply to not have you here now.
I did this for you.
Nya:weh

TABLE OF CONTENTS

Overview:

Integumentary pigmentation is a phenotype of fundamental importance to animals. Coloration relative to the background governs detectability by visual-oriented predators, and thus influences survival (Hill and McGraw 2006b). Coloration can be an important symbol of quality in intra-species interactions, and can thus be the target of intense sexual selection with profound influence on reproductive success and fitness (Hill and McGraw 2006b). Pigmentation can additionally provide structural support to reduce degradation of the integument (Goldstein et al. 2004) and physiological benefits from antioxidant properties (McGraw 2005). Additionally, coloration can give animals aesthetic and intrinsic value that appeals to human observers, generating interest in their study and conservation (pers. obs.).

Understanding the selective forces operating on pigmentation provides a 'why' that is critical for understanding color evolution, but understanding the 'how' is also important. Identifying the complex genetic and developmental organization of phenotypic traits is necessary for understanding how adaptive variation in these traits can be generated. Importantly, trait organization could introduce constraints on phenotypic evolution, or, alternatively, enhance the evolvability of traits and facilitate their response to selection (Wagner 1996, Wagner and Altenberg 1996, Wagner et al. 2008, Klingenberg 2008). Negative pleiotropic interactions are one type of constraint on trait evolution generated by the genetic and developmental organization of traits. Species are thought to be able to increase the evolvability of complex phenotypes by adopting a modular organization, clustering traits with related function and reducing negative pleiotropic interactions among functionally unrelated traits (Wagner 1996, Wagner and Altenberg 1996, Wagner et al. 2008, Klingenberg 2008). This reduction in pleiotropic constraint is predicted to make modular phenotypes more evolvable, exhibiting higher evolutionary rates and greater morphological diversification.

In Chapter 1, I used a comparative phylogenetic approach to determine whether the modular developmental organization of bird plumage affects the evolvability of bird plumage traits. I found that four mechanisms of color production in feathers (carotenoid and melanin pigments, structural colors, and complex feather patterning) show independent, uncorrelated patterns of evolutionary gain and loss across the plumage in

five bird families. This pattern of trait evolution is consistent with their production by separate mechanisms during feather development (Hill and McGraw 2006a), and shows that the developmental architecture of complex traits can show detectable effects on their evolutionary history. However, I found only weak evidence that higher rates of evolutionary correlation (i.e. correlated evolutionary gains/loss of separate plumage characters) act as a constraint on trait evolvability. The degree of evolutionary correlation was not always negatively associated with the measured indices of evolvability, evolutionary rate or morphological disparity. These results are consistent with the idea that developmental modularity can impact trait evolution, but more work is needed to better understand when such impacts influence the evolvability of traits.

Even in the best-studied and most ubiquitous animal pigment, melanin, the genetic and developmental factors that govern its production and generate phenotypic variation are not fully understood. Integumentary color is rarely a discrete, static phenotype, and variation often exists at multiple scales. For instance, individual feathers may exhibit complex patterns, or feather patches across the body may differ in their phenotypes to produce plumage patterns. While coding-region mutations have been identified in many taxa that effect pigmentation across the integument (Hoekstra 2006), these are insufficient to explain much of these dynamic changes in pigmentation. As a result, a better understanding of the mechanisms that regulate expression of pigmentation are needed. While some recent studies have made important inroads in this area (Poelstra et al. 2015, Abolins-Abols et al. 2018), these studies are limited in their phenotypic and taxonomic scope. Therefore, for my second chapter, I identified gene expression variation associated with a range of melanin pigmentation in a model species, the Zebra Finch (*Taeniopygia guttata*).

In Chapter 2, I describe gene expression variation associated with melanin-based colors in developing feathers of both male and female Zebra Finches. I took advantage of domestic pigment variation to control for confounding expression variation. I found that differences in pigmentation are associated with changes in the regulation of just a few genes of functional importance in the synthesis of melanin. In addition, I found few changes in expression in the signaling pathways that govern transcription of melanogenesis genes. Notably, these signaling pathways differ from those previously

reported to drive major pigmentation differences, indicating that the complex system of regulators of melanogenesis is flexible in how it generates similar phenotypic outcomes. In addition, I investigated sex-specific patterns of gene expression in different plumage patches with the aim of describing potential confounding factors in comparisons of pigment gene expression across the sexes. I found a number of sex-biased genes, but they were largely patch- or color- specific, suggesting that these potential confounding effects are largely context dependent.

For my third chapter, I investigated how genetic variation and gene expression patterns are related to sexual dimorphism in the Zebra Finch. Sexual dimorphism in pigmentation is gained and lost rapidly in many taxonomic groups (Wiens 2001). I investigated the genetic basis for loss of dimorphism in the Blackcheek Zebra Finch, a domesticated color morph with a simple recessive autosomal mutation that changes the color of the sexually dimorphic cheek feathers. I sequenced the genomes of Wild-type and Blackcheek Zebra Finches and identified a major divergence peak containing ten genes. One of those, Norrie Disease Protein (NDP), is differentially expressed between the morphs and has been previously linked to pigment pattern variation in domestic birds (Vickrey et al. 2018). NDP is a signaling molecule that could regulate the transcription of several melanogenesis genes that are differentially expressed between the morphs and likely drive the pigmentation differences observed. Thus, sexual dimorphism can be lost repeatedly and rapidly in finches and other groups through relatively simple genetic changes in the regulation of important signaling molecules in a patch-specific manner.

In my dissertation, I have demonstrated that the genetic and developmental architecture of complex plumage traits have an influence on their patterns of evolution across many species. I additionally worked to understand the genetic and regulatory mechanisms that generate variation in plumage color deeply in a single species, the Zebra Finch. The regulation of melanogenesis genes is complex: while several melanin signaling pathways have been well-characterized in their phenotypic effects (e.g. Agouti and MC1R), I have demonstrated here that pigmentation in some species can produce similar phenotypic outcomes by other signaling inputs. My work has demonstrated both specificity (in relatively few gene expression changes being associated with color changes) and flexibility in the regulation of melanogenesis. In addition, I have identified

candidate signaling pathways for a novel role in contributing to sexual dimorphism in pigmentation. While these discoveries advance our understanding of the mechanisms that give rise to variation in plumage color along several different axes, my work also shows that there is still much to learn about the regulation of pigmentation, and how that regulation can be used to generate the wide variation seen in integumentary pigmentation in animals.

References:

Abolins-Abols, M, E Kornobis, P Ribeca, K Wakamatsu, MP Peterson, ED Ketterson, and B Mila (2018) Differential gene regulation underlies variation in melanic plumage coloration in the dark-eyed junco (Junco hyemalis). *Molecular Ecology* **27**:4501-4515.

Goldstein, G, KR Flory, BA Browne, S Majid, JM Ichida, and EH Burtt Jr. (2004) Bacterial degradation of black and white feathers. *The Auk* **121**:656-660.

Hill, GE, and KJ McGraw (2006a) *Bird Coloration Volume I: Mechanisms and Measurement*. Harvard University Press, Cambridge, MA, USA.

Hill, GE, and KJ McGraw (2006b) *Bird Coloration Volume II: Function and Evolution*. Harvard University Press, Cambridge, MA, USA.

Hoekstra, HE (2006) Genetics, development and evolution of adaptive pigmentation in vertebrates. *Heredity* **97**:222-234.

Klingenberg, CP (2008) Morphological integration and developmental modularity. *Annual Review of Ecology, Evolution, and Systematics* **39**:115-132.

McGraw, KJ (2005) The antioxidant function of many animal pigments: are there consistent health benefits of sexually selected colourants? *Animal Behaviour* **69**:757-764.

Poelstra, JW, N Vijay, MP Hoeppner, and JBW Wolf (2015) Transcriptomics of colour patterning and coloration shifts in crows. *Molecular Ecology* **24**:4617-4628.

Vickrey, AI, R Bruders, Z Kronenberg, E Mackay, RJ Bohlender, ET Maclary, R Maynez, EJ Osborne, KP Johnson, CD Huff, M Yandell, and MD Shapiro (2018) Introgression of regulatory alleles and a missense coding mutation drive plumage pattern diversity in the rock pigeon. *eLife* **7**:e34803

Wagner, GP (1996) Homologues, natural kinds and the evolution of modularity. *American Zoologist* **36**:36-43.

Wagner, GP, and L Altenberg (1996) Perspective: complex adaptations and the evolution of evolvability. *Evolution* **50**:967-976.

Wagner, GP, M Pavlicev, and JM Cheverud (2007) The road to modularity. *Nature Reviews Genetics*. **8**:921-931.

Wiens, JJ (2001) Widespread loss of sexually selected traits: how the peacock lost its spots. *TRENDS in Ecology & Evolution* **16**:517-523.

Chapter 1: The influence of developmental modularity on the evolution of bird plumage

Abstract

The structural organization of complex traits is an important determinant of their evolution. In general, modular organization of the genetic and developmental components of complex traits is thought to increase their evolvability by reducing negative pleiotropic interactions with functionally unrelated traits. We investigated the relationship between modular organization and evolvability using a complex, hierarchically modular trait, avian plumage. First, we tested for correlated evolution among many plumage traits in five families of birds and found evidence that plumage traits produced by separate underlying developmental modules are more likely to show independent, uncorrelated evolutionary change. Four common mechanisms of color production in feathers (carotenoid and melanin pigments, structural colors, and complex feather patterning) show independent patterns of evolutionary gain and loss across the plumage, consistent with their production by separate mechanisms during feather development. Conversely, patches across the plumage within a color type show less evolutionary independence, consistent with the idea that developmental prepatterning can link many different patches together. Second, we found only weak evidence that higher rates of evolutionary correlation are a constraint on trait evolvability, as evolutionary correlation was not negatively associated with evolutionary rate or morphological disparity in many cases. Our results are consistent with the idea that developmental modularity can impact trait evolution, but more work is needed to better understand when such impacts can lead to higher evolvability of traits.

Introduction

The developmental and structural organization of complex phenotypes can constrain or facilitate the direction of phenotypic evolution by altering pleiotropic interactions. In traits linked by negative pleiotropic interactions, selection on one trait can cause maladaptive changes in other linked traits, placing severe constraints on phenotypic

6

evolution (Klingenberg 2008). In contrast, positive pleiotropic interactions among traits that share related functions can facilitate phenotypic evolution because selection on one trait can lead to simultaneous adaptive change in other linked traits (Peiman and Robinson 2017). Antagonistic interactions are often the result when pleiotropy links one trait component to functionally unrelated traits. One way to reduce these interactions is to adopt a modular organization, where phenotypes are comprised of sets of integrated, functionally related modules with tightly correlated trait components, but reduced interactions with other functionally unrelated modules (Wagner 1996, Wagner and Altenberg 1996, Wagner et al. 2008, Klingenberg 2008). Theory and empirical work has shown that this evolutionary optimum frees phenotypes from the evolutionary constraints of antagonistic interactions by compartmentalizing them into modules, and selection can act to make phenotypes more modular (Wagner 1996, Wagner and Altenberg 1996, Wagner et al. 2007, Clune et al. 2013)

Tight integration of genetic, developmental, or functional traits into modules is expected to lead to higher evolutionary rates and higher morphological diversification (Wagner et al. 2007, Klingenberg 2008, Claverie and Patek 2013). While modularity is typically measured at the level of individuals, the predicted evolutionary consequences of modularity can be observed through comparative phylogenetic analysis across many species (Claverie and Patek, Klingenberg 2014). Integration of traits into modules is expected to result in the correlated evolution of those traits within a module (Armbruster and Schwaegerle 1996, Klingenberg 2008, Klingenberg 2014). However, modular organization is not the only cause of correlated evolution among traits. For instance, selection acting on multiple traits simultaneously can result in correlated evolution in the absence of genetic, developmental, or functional linkages underlying their production (Armbruster and Schwaegerle 1996, Klingenberg 2014, example: Monteiro and Nogueira 2010). In this sense, patterns of evolutionary trait correlation can be decoupled from the modular organization of mechanisms that underlie trait expression. Thus, it is not clear that variation in evolutionary modularity as measured through correlated evolution of traits should necessarily be accompanied by variation in evolutionary rate and trait disparity. There have been relatively few direct comparisons of evolutionary modularity with genetic or developmental modularity, so the extent to which evolutionary

correlations reflect underlying trait structure versus alternative processes is not well known (Armbruster et al. 2014, Klingenberg 2014, Peiman and Robinson 2017). More studies are needed to connect the processes generating phenotypic variation and the evolutionary outcomes of such phenotypic organization (Claverie and Patek 2013, Armbruster et al. 2014, Klingenberg 2014, Peiman and Robinson 2017).

Bird plumage is a useful model for interconnecting different organizational levels of modularity in a complex phenotype. Plumage can be modeled as a nested hierarchy of modules. These modules include the genetic and developmental mechanisms involved in feather growth, the morphological structure of individual feathers, and the co-regulation of groups of feathers with different shapes and colors into functional plumage patches (**Figure 1B**; reviewed in Prum and Dyck 2003). Such a highly modular system in plumage may facilitate plumage diversification (Prum and Dyck 2003), but few studies have used phylogenetic tests to determine whether this modular organization influences the evolutionary trajectories and patterns of diversification in plumage traits (e.g. Eliason et al. 2015). Here, we take a phylogenetic approach to test for evolutionary correlations among traits that correspond to two classes of modularity in avian plumage: the modular development of feather color, and the modular parcellation of plumage into separate plumage patches. By examining patterns of evolutionary trait correlations in five families of birds, we address the following questions: 1) do plumage traits show patterns of evolutionary correlation and independence as predicted by their underlying developmental modularity, and 2) is the degree of evolutionary correlation among plumage traits negatively associated with evolutionary rate and morphological diversification of plumage.

Methods

The modular organization of plumage

We estimate evolutionary correlations among plumage traits pertaining to two aspects of the modular organization of plumage: feather color and plumage patches. Birds draw from a diverse set of modular mechanisms during feather development to produce the color and pattern of their plumage (**Figure 1A**; Hill and McGraw 2006). Of these mechanisms, we assess the four most common -- melanin pigmentation, carotenoid

pigmentation, structural colors, and feather patterning -- because of their widespread use in plumage across many groups of birds, the relative ease in qualitatively assigning feather phenotypes to the different mechanisms, and their putative developmental independence. We briefly review each of these four color mechanisms below.

The two most common classes of pigment in plumage, melanins and carotenoids, have separate developmental origins and mechanisms of deposition in developing feathers (Hill and McGraw 2006). Melanin pigments, which produce earth-toned browns, grays, and black, are synthesized from amino acid precursors within specialized cells (melanocytes) in individual feather follicles and are deposited in packed organelles (melanosomes) in the feather keratin during feather development (Hill and McGraw 2006). Carotenoid pigments, which produce vibrant yellow, orange, red, or purple colors, are obtained from the diet and, either directly or after enzymatic modification, are deposited via blood lipid transporters into developing feathers (Hill and McGraw 2006).

In contrast to pigments, structural colors are produced by the reflection of specific wavelengths of light off of feather microstructures. We focus on one type of structural color, in which the feather keratin is filled during development with an ordered spongy array of air vacuoles that coherently scatter light (Dufresne et al. 2009, Prum et al. 2009). In the absence of melanin, these structures produce a bright bluish-tinted white; when combined with different layers of melanin or carotenoid pigment to selectively absorb wavelengths, they reflect green, blue, and violet hues (Prum 2006, Shawkey and Hill 2006). We do not here consider other types of feather structural colors, such as the thin-film iridescence produced by ordered layers of melanin, as these arise from other production mechanisms and are more difficult to definitively assign to mechanism (Hill and McGraw 2006).

The fourth developmental mechanism we investigate is the regulation of pigment deposition in feathers by cyclical expression of activators and inhibitors to induce complex color patterning as feathers grow (Price and Pavelka 1996, Prum and Williamson 2002). Signals controlling these patterning processes originate outside of the pigment and keratin production cells (Lin et al. 2013), and may be responsive to systemic hormone signaling, suggesting that they originate from developmental processes

independent of but interacting with the production of pigments themselves (Prum and Dyck 2003, Hill and McGraw 2006).

The separate developmental origins of these four color mechanisms confers a modular organization to plumage color that may influence the evolvability of plumage color. Modularization of color production could facilitate incorporation of different combinations of mechanisms across the plumage and across species, allowing plumage phenotypes to expand into novel areas of morphospace (Prum and Dyck 2003, Stoddard and Prum 2011, Maia et al. 2013). We test whether this modular organization at the developmental level results in evolutionary independence by testing for evolutionary correlations among the color mechanisms.

We contrast modular evolution of feather color production with another broad level of modular organization of feathers: the parcellation of the whole plumage into multiple patches across the body. Plumage is comprised of thousands of individual feathers, each grown and regrown from separate feather follicles. The follicles are arranged in arrays across the skin, and can be considered replicated morphological modules (Prum and Dyck 2003). This replication creates the potential for independence and diversification among different feather follicles to produce different feather phenotypes. In practice, the plumage is often subdivided into various numbers of plumage patches which produce feathers of a similar color and pattern phenotype (**Figure 1B**; Prum and Dyck 2003). The exact mechanisms by which groups of similar feathers are co-regulated to produce patterns across the whole plumage is not known, but reaction-diffusion models of activators and inhibitors across the body are sufficient to generate a developmental pre-pattern for some common plumage patterns (Price and Pavelka 1996). This, along with the repeated evolution of similar pattern elements across species (Price and Pavelka 1996, Omland and Lanyon 2000), suggests that not all discrete plumage patches are free to evolve independently. However, this has not been investigated comprehensively. To do so, we tested for evolutionary correlations among a nearly comprehensive set of plumage patches to assess the degree to which patches show independence.

Estimating evolutionary correlations

We selected five bird families to represent a diversity of plumage color and pattern for comparative analysis: kingfishers (Alcedinidae), cotingas (Cotingidae), blackbirds (Icteridae), tits (Paridae), and wood-warblers (Parulidae). Each family meets the following criteria: a) each of the four color mechanisms described above are present in the plumage of multiple species (except Icteridae, which lacks species with spongy-keratin-based structural colors), b) has a published species-level multi-locus molecular phylogeny, and c) contains more than fifty species.

We divided the plumage into forty-two patches to evaluate. Each patch was chosen because it forms a discrete pattern element, i.e. is distinct in color and pattern from the surrounding plumage, in multiple species among our chosen families. Combined, the forty-two patches cover the majority of the plumage across the body (**Figure 1C**). For each plumage patch, we scored the presence/absence in each species of the four color mechanisms outlined above – carotenoids, melanin, patterning, and keratin-based structural colors. These mechanisms each produce a characteristic range of colors and occupy distinct portions of plumage colorspace, and combining these mechanisms in different ways can produce additional novel colors (Hill and McGraw 2006, Stoddard and Prum 2011, **Table S4** and references therein). We performed an exhaustive literature search to assemble a list of all species in our five focal families whose plumage colors have been analyzed and assigned to mechanism (34.5% or 162 of 469 species; **Table S4**). These references verify that the color mechanisms of interest occur in each of our focal families and that pigment classes that produce similar hues, such as pterins, psittacofulvins, and turacins, are not known from these families, which reduces the difficulty of assigning color to mechanism (Hill and McGraw 2006; **Table S4**). Additionally, these references allow discrimination of some ambiguous colors and combinations of mechanisms in our focal families, including tawny/ochre in orioles (combination of melanin and carotenoid; Hofmann et al. 2007), pinks and lilacs in kingfishers (keratin-based structural color, Saranathan et al. 2012), blue-gray in kingfishers and warblers (keratin-based structural colors; Auber 1957), violet (carotenoids, Prum et al. 2012), and various shades of green (Auber 1957, Saranathan et al. 2012). All-white feathers were scored as the absence of all four color mechanisms. White feathers are produced structurally by scattered light in the feather keratin, and

11

removing pigmentary layers from structural blues results in a structural white (Barrera-Guzman et al. 2018, Prum 2006, Shawkey and Hill 2006), However, structural white can be produced by multiple mechanisms of incoherent or coherent light scattering (Barrera-Guzman et al. 2018, Prum 2006, Shawkey and Hill 2006) which are beyond our ability to distinguish in this study.

We used descriptions of plumage in the species accounts in del Hoyo et al. (2016) and family-specific books (Curson et al. 1994, Fry and Fry 1992, Harrap and Quinn 1996, Jaramillo and Burke 1999, Kirwan and Green 2012) to assign color mechanisms to the remaining plumage patches based on their characteristic colors. We scored adult male and female alternate plumages separately, for a total of ten datasets of plumage characters, where each character trait is the presence/absence of one color mechanism in one plumage patch. Where geographic variation exists, we scored the subspecies sampled in the molecular phylogenies, or the nominate subspecies if subspecific information was not available from the phylogenetic studies.

We obtained multilocus phylogenies with nearly comprehensive species coverage from the literature for each family (Alcedinidae: Andersen et al. 2018, Cotingidae: Berv and Prum 2015, Icteridae: Powell et al. 2014, Paridae: Johansson et al. 2013, and Parulidae: Lovette et al. 2010). Species not included in the molecular phylogenies were excluded from analysis. We excluded characters whose trait gain or loss in a dataset is restricted to a single taxon, and characters that were invariant within a given dataset, as a partial correction for bias in correlation statistics that result from a low sample size of evolutionary events (Maddison and FitzJohn 2015). Final counts of species and traits analyzed per family and sex are reported in **Table 1**.

We estimated evolutionary correlations among plumage traits using Pagel's test of discrete binary character correlation (Pagel 1994), in which a fitted model of correlated character change is tested against a null uncorrelated model using a likelihood ratio test. We ran Pagel's test on all pairwise character combinations for each dataset separately, using custom R scripts derived from the R package phytools v.0.6-20 (Revell 2012) implemented in R version 3.4.1 (R Core Team 2016). We assembled pairwise evolutionary correlation matrices with binary values indicating the presence or absence of a significant evolutionary correlation between each set of characters as determined by the

test statistics (p <0.05).

Modularity Analysis

We examined the fit of the evolutionary correlation matrices to three *a prior*i hypotheses for modular organization: 1) randomly arranged correlations, 2) perfect independence of plumage patches, and 3) perfect independence of color mechanisms. To test whether our evolutionary correlation matrices deviated from random, we generated 100 matrices with the same dimensions and number of significant correlations as the observed, but the significant correlations are randomly distributed within the matrix. We then compared each random matrix to the observed matrix with a Mantel test, and calculated the percentage of random matrices that are significantly correlated with the observed matrix. To test perfect independence of plumage patches, we generated hypothetical matrices of the same dimension as the observed evolutionary correlation matrix, where each color mechanism within a given plumage patch is correlated, and every comparison of color mechanisms across different plumage patches is uncorrelated. Again, we compared these hypothetical matrices to the observed with a Mantel Test. We repeated this procedure for perfect independence by color mechanism, where in the hypothetical matrix pairwise comparisons of the same color mechanism across different plumage patches are correlated and pairwise comparisons of different color mechanisms are uncorrelated.

Evolutionary rate and morphospace analysis

We used generalized linear mixed-effect models (GLMMs) to examine the influence of evolutionary correlations on evolutionary rate of plumage traits. We extracted the instantaneous transition rates from the Pagel's test, using the independent evolution model for each trait, and compared log-transformed forward and reverse transition rates with the number of significant evolutionary correlations within the same color mechanism and across different color mechanisms. We designated a global model with family, sex, color mechanism, and all interactions as fixed effects and plumage patch as a random effect with random intercepts and slopes. We compared the set of all nested models derived from this global model using an AIC framework to select the best

fitting model. In all four comparisons of transition rate and evolutionary correlation, the best-fit model had significantly better support than the next best fit (delta-AIC >2), so we report the results of each top model without model averaging (Grueber et al 2011). We used the R packages lme4 (Bates et al. 2015), lmerTest (Kuznetsova et al. 2017), AICcmodavg (Mazerolle 2017), and stargazer (Hlavac 2018) for these analyses.

We examined the influence of evolutionary correlations on plumage diversification by calculating two measures of morphological disparity for each dataset and comparing those with the number of evolutionary correlations within and among color mechanisms. We calculated mean pairwise distance (MPD) as the mean of a distance matrix generated among species in each trait dataset using a simple matching coefficient (Sokal & Michener [1958] as implemented in the R function dist.binary in the package ade4 [Dray and Dufour 2007]). We calculated PCO volume as the product of the two largest eigenvalues of a principal coordinate decomposition of the distance matrix for each dataset, normalized by the square of the number of species (Ciampaglio et al. 2001). These two robust measures capture slightly different aspects of disparity: PCO volume being an approximate measure of the total volume of morphospace occupied by the clade and MPD being an approximation of how dispersed individual species are in that morphospace (Ciampaglio et al. 2001). We tested for associations between these two disparity metrics with the proportion of significant pairwise correlations within a given color mechanism, and the proportion of significant pairwise correlations across different color mechanisms. Because color mechanisms putatively evolve independently, we compiled these statistics separately at the whole-family level and at the level of each individual color mechanism in each family and sex. We tested for a relationship between these variables with linear models using sex as a fixed effect.

All statistical analyses were implemented in the software R version 3.2.4 (R Core Team 2016).

Results

Across all five of our focal families, evolutionary gain or loss of a color mechanism in one plumage patch was significantly correlated with gain/loss of that same color mechanism in other plumage patches. Conversely, gain/loss of one color

mechanism in a given plumage patch was rarely correlated with the gain/loss of other color mechanisms in the same patch or in other patches across the rest of the plumage. This pattern is illustrated in **Figure 2**, where the proportion of significantly correlated trait pairs within the same color mechanism is higher (range 0.23-1, median 0.55, mean 0.56; diagonal boxes, **Figure 2**) than the proportion of significant pairwise correlations between color mechanisms (range 0-0.54, median 0.05, mean 0.10; off-diagonal boxes, **Figure 2**). The full matrices with individual pairwise comparisons are shown in **Figures S1-S10**. Mantel tests further demonstrated that the observed structure of the evolutionary correlation matrices was consistent with the hypothesized modular organization of plumage color mechanisms. The evolutionary correlation matrices for all five families were statistically indistinguishable from a hypothetical matrix containing only correlations among traits of the same color mechanism (**Table 1**), indicating that while evolutionary gain or loss of a specific plumage color type in one patch is correlated with gain or loss of that same color type in another patch, each of the four plumage color types were largely evolutionarily independent from one another. In addition to this overarching pattern of evolutionary independence relating to plumage color, we also found more limited support for a model of evolutionary independence of plumage patches. Specifically, four evolutionary correlation matrices were statistically indistinguishable from a hypothetical matrix containing only correlations within but not between plumage patches (**Table 1**). Finally, only three matrices show significant correlation with more than 5% of matrices containing a random assembly of correlated characters, however the proportion is still low (6-8%; **Table 1**) and the mean correlation value with these random matrices is near zero.

We found a general negative relationship between a trait's evolutionary rate and the number of significant correlations with other plumage traits. For forward transition rates, we found a significant ($p < 0.05$) negative relationship with significant correlations with plumage traits of different color mechanisms, but only a marginally insignificant ($p = 0.073$) negative relationship with significant correlations with plumage traits of the same color mechanism (**Table S1**). Reverse transition rates had a significantly ($p < 0.05$) negative relationship with the number of correlated plumage traits of both the same and different color mechanisms (**Table S1**). Although the overall model trends were negative,

there was significant variation in the slopes of the relationship at different factor levels and their interactions (**Figure 3**, **Figure S11**, **Table S1**). Slopes for individual families (**Figure 3**) and color mechanisms within each family (**Figure S11**) showed predominately either a negative relationship between rate and correlation, or no relationship, with positive relationships existing for only a handful of factor levels. Sexes differed in their relationship between rate and correlation in very few of the factor level interactions (i.e. melanin traits in Cotingidae, pattern traits in Icteridae, **Table S1**).

Patterns of evolutionary independence were also associated with the extent of plumage diversification within and among families. For example, PCO volume was significantly and positively related to the degree of correlation within color modules, when considered at both the family level (**Table S2**) and level of individual modules within families (**Table S3**, **Figure 4A**). In addition, there was a marginally significant (p = 0.069) positive relationship between mean pairwise distance and the degree of correlation across color mechanisms (**Table S3**, **Figure 4D**), but not across families (**Table S2**). There was no significant relationship between PCO volume and the degree of correlation across color modules, nor in mean pairwise difference compared to correlation within color modules, and sex had no significant effect in any model (**Tables S2-S3**, **Figure 4B,C**).

Discussion

The structural organization of complex traits is an important consideration in trait evolution, because modular organization of the genetic and developmental components of complex traits is predicted to increase their evolvability (Wagner 1996, Wagner and Altenberg 1996, Wagner et al. 2008, Klingenberg 2008). Here, we investigated the influence of developmental modularity on the evolvability of bird plumage. First, by estimating evolutionary correlations among many plumage traits, we demonstrated plumage traits produced by different underlying modular developmental mechanisms are more likely to evolve independently from one another. Second, we showed that the relationship between measures of proxies for evolvability (evolutionary rate and morphological disparity) and the degree of evolutionary correlations among traits (a

16

proxy for modularity), was generally weak and inconsistent. We discuss the broader implications of these results below.

Do patterns of evolutionary correlation reflect developmental modularity?

Traits within a functional module are generally predicted to show correlated evolutionary change with one another due to tight pleiotropic linkages, while traits in separate functional modules with fewer such linkages are predicted to show more evolutionary independence (Wagner et al. 2007, Klingenberg 2008). However, selection can also link traits in their patterns of evolutionary change, when correlated selection is stronger than the negative pleiotropic interactions of those traits. Correlated selection could then generate evolutionary correlations independent of the developmental mechanisms that underlie their expression. Distinguishing between these hypotheses as alternative explanations for evolutionary correlations can be difficult. We found that developmentally modular mechanisms of feather color production show generally independent evolution from one another, both within and across different plumage patches. In contrast, gain or loss of a given color mechanism is often correlated across a number of plumage patches. Several lines of evidence suggest this pattern of evolutionary correlation reflects a dominant process of evolutionary independence of developmental modules, with correlated selection driving different patterns in special cases.

The patterns of correlational structure we observed across plumage patches are distinctly different from those across color mechanisms, in ways predicted by their underlying developmental modularity. The four color mechanisms we tested have separate origins during feather development. This developmental modularity should allow independent evolutionary transitions of each color mechanism across species. This prediction is supported by the very low number of significant correlations of gain/loss among the different color mechanisms within any given plumage patch, and across plumage patches (**Fig 2**, off-diagonal boxes).

Conversely, there is often relatively high correlation in the gain/loss of any particular color mechanism across multiple plumage patches. The production of individual plumage patches and the patterning of the whole plumage is not as well understood as the production of plumage color, but some mechanisms are known.

17

Developmental pre-patterning mechanisms have the potential to link multiple patches, including non-neighboring regions (Price and Pavelka 1996, Haupaix et al. 2018), and groups of plumage patches may experience repeated and correlated gain and loss (Price and Pavelka 1996, Omland and Lanyon 2000). This suggests that 1) plumage patches are rarely if ever expected to be totally independent of one another, 2) that the independent patches or blocks of patches that do exist are likely to evolve or change across these families, whereas the independence of color production mechanisms is more likely to be consistent across families because they are deeply conserved (Hill and McGraw 2006). This prediction is supported by the pattern of higher levels of correlation among different plumage patches compared to the degree of correlation across color mechanisms (**Fig 2**, diagonal boxes).

The exceptions to these general patterns likely demonstrate instances of correlated selection producing patterns of evolutionary correlation. These exceptions are best illustrated in female cotingas (Cotingidae) which show high levels of evolutionary correlation across many plumage patches in carotenoid and structural color traits, and both sexes of blackbirds (Icteridae) which exhibit a high degree of evolutionary correlation between melanin and carotenoid coloration. Cotingas are Neotropical frugivores that are ecologically similar to one another. Although male cotingas are known for brilliant and variable coloration and displays, females are often plumaged in green and yellow colors, presumably for camouflage (Hill and McGraw 2006, Kirwan and Green 2012). Within Cotingas, there are several separate clades with females showing this general coloration (Kirwan and Green 2012, Berv and Prum 2014), likely indicating that it has evolved multiple times (most other females in the family have drab plumage containing only gray and brown melanin-based colors). In cotingas, green is produced by a combination of blue structural and yellow carotenoid coloration (Hill and McGraw 2006, **Table S4**), so the repeated gain or loss of green across the plumage in the family would produce evolutionary correlations among these two color mechanisms even if they are developmentally independent. It seems unlikely that there would be genetic or developmental constraints unique to cotingas that link carotenoid and structural coloration, because these are deeply conserved mechanisms that are expressed independently of one another in many other species of the family. Moreover, these color

mechanisms are do not show high evolutionary correlation in males. Thus this seems likely an instance of ecological selection for a particular combination of color mechanisms driving patterns of evolutionary correlation.

The blackbirds and allies (Icteridae) show strongly correlated evolution of melanin and carotenoid plumage coloration (**Figure 2**). Icterid plumage in many species consists of large tracts of either melanin or carotenoid based coloration, often without patterning to combine the two in the same patch (Jaramillo and Burke 1999). This largely either/or combination of color mechanisms would result in negative evolutionary correlations of melanin and carotenoid across the family. These patterns of evolutionary correlation are seen in both sexes, likely because many sexually monomorphic icterid species show colorful female plumage rather than cryptic male plumage (Jaramillo and Burke 1999, Price and Eaton 2014). These patterns are unlikely to be due to icterid-specific developmental constraint on feather patterning, as the more cryptic species in the family typically have patterned feathers (Jaramillo and Burke 1999). Neither is it likely a developmental constraint on combining carotenoids and melanin, as a small number of species do combine the two in patterned feathers, and a few species combine the two mechanisms into solid patches of uniform color (tawny/ochre, Hofmann et al. 2007, see **Table S4**). The bright carotenoid coloration of many icterids is likely a result of intense sexual selection across the family (Jaramillo and Burke 1999), a role shared by carotenoid coloration in many taxa (Hill and McGraw 2006). Also of note, icterids as a family lack spongy-keratin based structural colors (Hill and McGraw 2006, Jaramillo and Burke 1999, **Table S4**), which would reduce the possible colorspace that could be occupied by the family (Stoddard and Prum 2011), especially compared to such groups as cotingas with similarly high levels of sexual ornamentation. A reasonable interpretation is that sexual selection for large, bright carotenoid signals in the plumage is driving patterns of evolutionary correlation of melanin and carotenoids in this group.

Does evolutionary integration reflect the evolvability of traits?

In general, modularity among traits is thought to increase evolvability of those traits due to the reduction of antagonistic pleiotropic constraints (Wagner et al. 2007, Klingenberg 2008). We found that, in general, plumage traits evolve faster when they

have fewer evolutionary correlations with other plumage traits. However, this trend is not universal: there are many individual factor levels (family, sex, color mechanism) and their interactions that show no relationship between evolutionary rate and correlation, or even a positive relationship (i.e. traits with more correlations evolve faster; **Figures 3 and S11**, **Table S1**). Contrary to predictions, we did not find a general negative trend between morphological disparity and the degree of evolutionary correlation among plumage traits, indicating that evolutionary correlations do not necessarily constrain the morphospace occupied by a clade (**Figure 4**, **Tables S2, S3**). These results suggest that, while the patterns of evolutionary correlations among plumage traits are reflective of underlying modularity, there is not a clear relationship between the degree of evolutionary correlation and the evolvability of those traits.

We suggest several potential explanations for the lack of a strong relationship between evolvability and evolutionary correlation. First, plumage traits may be linked by underlying developmental integration, but their pleiotropic connections within or across developmental modules may not have antagonistic costs, nullifying the predicted influence of modularity on evolvability. If modularity is associated with the reduction of antagonistic pleiotropy across modules while retaining neutral or positive pleiotropic connections within a module, then correlations across modules should show a stronger negative relationship with evolvability, while correlations within a module should show either no relationship or a net positive relationship with evolvability. We compared these two sets of correlations separately in all our linear models but did not find that more across-module correlations have a stronger relationship with rate or evolvability, as expected if these correlations were associated with stronger antagonistic pleiotropy (**Figs 3,4,S11**, **Tables S1-S3**). This suggests that a general lack of negative pleiotropy among our traits could explain our results. However, the likelihood of this explanation is difficult to assess, because quantitative measures of the pleiotropic costs between plumage traits in birds are rare, and there is no clear predictive framework for which types of plumage traits might be more likely to experience antagonistic pleiotropy with other plumage traits.

A clear link between evolutionary modularity and trait evolvability may also be obscured by the influence of selection. Traits that are more evolvable will only

demonstrate higher evolutionary rates and higher morphological diversification in the absence of selective constraints. Traits may well be highly evolvable due to their modular organization but are less likely to evolve rapidly or occupy more morphospace if they are under a selection regime that constrains diversification. We investigated a range of bird families, with variation in morphological and ecological diversity both within and across families. Included in our analysis were families with plumage under intense sexual selection (Cotingas and icterids, Kirwan and Green 2012, Jaramillo and Burke 1999). These taxa are arguably the most likely to exhibit higher evolutionary rates and an increase in occupied morphospace, and yet, like the other families, there was not a clearer relationship between evolutionary correlation and evolvability in these families.

Although correlated selection can produce patterns of evolutionary correlation that are independent of underlying developmental constraints, the predicted effect of correlated selection on evolvability is not clear. On the one hand, conservation of particular color patterns that provide a selective advantage across multiple species, such as cryptic patterns or repeated elements, could produce blocks of correlated traits that evolve slower than average and have a constrained morphospace. On the other, selection for diversity, such as species recognition patterns or complicated displays under divergent sexual selection, could produce blocks of correlated traits that evolve faster and occupy more of the available morphospace than average. These scenarios may play out over small timescales with a few species, but for selection to be driving the relationships between evolvability and correlation we observed, these patterns of selection would have to influence many plumage elements consistently over deeper evolutionary timescales. Far more likely in most scenarios is that selection varies in which traits are linked over these timescales, making predictions for the relationship between trait correlations, evolutionary rates, and morphological diversification difficult at this phylogenetic scale.

Distinguishing among these hypotheses is beyond the scope of our study. The comparative framework we use here has elucidated patterns of evolutionary correlation across multiple bird families and multiple classes of traits. Such an approach could be useful in guiding future studies by providing cases in particular clades or classes of traits where the relationship between trait integration matches or conflicts with predictions. By focusing on such case studies, more detailed study of trait modularity at multiple levels of

organization can be conducted, including quantification of genetic and developmental modularity within populations as well as details of selection on the traits produced. Such studies will better elucidate the relationship between modularity within development and patterns of evolutionary change.

Acknowledgements

Literature Cited

Andersen, MJ, JM McCullough, WM Mauck III, BT Smith, and RG Moyle (2018) A phylogeny of kingfishers reveals an Indomalayan origin and elevated rates of diversification on oceanic islands. *J Biogeography* **45**:269-281.

Armbruster, WS, C Pelabon, GH Bolstad, and TF Hansen (2014) Integrated phenotypes: understanding trait covariation in plants and animals. *Philosophical Transactions of the Royal Society B* **369**:20130245.

Armbruster, WS, and KE Schwaegerle (1996) Causes of covariation of phenotypic traits among populations. *J Evol Biol* **9**:261-276.

Auber L (1957) The structures producing "non-iridescent" blue colour in bird feathers. *Proceedings of the Zoological Society of London* **129**:455-486

Barrera-Guzman AO, A Aleixo, MD Shawkey, and JT Weir (2018) Hybrid speciation leads to novel male secondary sexual ornamentation of an Amazonian bird. *PNAS* **115**:E218-E225.

Bates D, M Maechler, B Bolker, and S Walker (2015) Fitting linear mixed-effects models using lme4. *Journal of Statistical Software* **67**:1-48.

Berv, JS, and RO Prum (2014) A comprehensive multilocus phylogeny of the Neotropical cotingas (Cotingidae, Aves) with a comparative evolutionary analysis of breeding system and plumage dimorphism and a revised phylogenetic classification. *Molecular Phylogenetics and Evolution* **81**:120-136.

Ciampaglio, CN, M Kemp, and DW McShea (2001) Detecting changes in morphospace occupation patterns in the fossil record: characterization and analysis of measures of disparity. *Paleobiology* **27**:695-715.

Claverie, T, and SN Patek (2013) Modularity and rates of evolutionary change in a power-amplified prey capture system. *Evolution* **67**:3191-3207

Clune, J, J-B Mouret, and H Lipson (2013) The evolutionary origins of modularity. *Proceedings of the Royal Society B* **280**:20122863.

Curson, J, D Quinn, and D Beadle (1994) *Warblers of the Americas: An Identification Guide*. Houghton Mifflin Harcourt.

del Hoyo, J, A Elliot, J Sargatal, DA Christie, E de Juana (eds.) (2016) Handbook of the Birds of the World Alive. Lynx Edicions, Barcelona. (retrieved from http://www.hbw.com/ 2015-2017).

Dray, S, and AB Dufour (2007) The ade4 package: implementing the duality diagram for ecologists. *Journal of Statistical Software* **22**:1-20.

Dufresne ER, H Noh, V Saranathan, SGJ Mochrie, H Cao, and RO Prum (2009) Self-assembly of amorphous biophotonic nanostructures by phase separation. *Soft Matter* **5**:1792-1795.

Eliason, CM, R Maia, and MD Shawkey (2015) Modular color evolution facilitated by a complex nanostructure in birds. *Evolution* **69**:357-367.

Felsenstein, J (2012) A comparative method for both discrete and continuous characters using the threshold model. *The American Naturalist* **179**:145-156.

Fry, CH, and K Fry (1992) *Kingfishers, Bee-eaters, and Rollers*. Princeton University Press.

Grueber, CE, S Nakagawa, RJ Laws, and IG Jamieson (2011) Multimodel inference in ecology and evolution: challenges and solutions. *Journal of Evolutionary Biology* **24**:699-711.

Harrap, S, and D Quinn (1996) *Chickadees, Tits, Nuthatches, and Treecreepers*. Princeton University Press.

Haupaix, N, CCurantz, R Bailleul, S Beck, A Robic, and M Manceau (2018) The periodic coloration in birds forms through a prepattern of somite origin. *Science* **361**:eaar4777.

Hill, GE, and KJ McGraw, Eds. (2006) *Bird Coloration. Volume 1: mechanisms and measurement*. Cambridge, UK: Harvard University Press.

Hlavac, M (2018) stargazer: well-formatted regression and summary statistics tables. R package version 5.2.1. https://CRAN.R-project.org/package=stargazer

Hofmann CM, KJ McGraw, TW Cronin, and KE Omland (2007) Melanin coloration in New World orioles I: carotenoid masking and pigment dichromatism in the orchard oriole complex. *Journal of Avian Biology* **38:**163–171

Jaramillo, A, and P Burke (1999) *New World Blackbirds:The Icterids*. Princeton University Press.

Johansson, US, J Ekman, RCK Bowie, P Halvarsson, JI Ohlson, TD Price, and PGP Ericson (2013) A complete multilocus species phylogeny of the tits and chickadees. *Molecular Phylogenetics and Evolution* **69**:852-860.

Kirwan, GM, G Green (2012) *Cotingas and Manakins*. Princeton University Press.

Klingenberg, CP (2008) Morphological integration and developmental modularity. *Annual Review of Ecology, Evolution, and Systematics* **39**:115-132.

Klingenberg, CP (2014) Studying morphological integration and modularity at multiple levels: concepts and analysis. *Philosophical Transactions of the Royal Society B* **369**:20130249.

Kuznetsova, A, PB Brockhoff, and RHB Christensen (2017) lmerTest package: tests in linear mixed effects models. *Journal of Statistical Software* **82**:1-26.

Lovette, IJ, JL Perez-Eman, JP Sullivan, RC Banks, I Fiorentino, S Cordoba-Cordoba, M Echeverry-Galvis, FK Barker, KJ Burns, J Klicka, SM Lanyon, and E Bermingham (2010) A comprehensive multilocus phylogeny for the wood-warblers and a revised classification of the Parulidae (Aves). *Molecular Phylogenetics and Evolution* **57**:753-770.

Maddison W, RG FitzJohn (2015) The unsolved challenge to phylogenetic correlation tests for categorical characters. *Systematic Biology* **64**:127-136.

Maia R, DR Rubenstein, MD Shawkey (2013) Key ornamental innovations facilitate diversification in an avian radiation. *Proceedings of the National Academy of Science* **110**:10687-10692.

Mazerolle, MJ (2017) AICcmodavg: model selection and multimodel inference based on (Q)AIC(c). R package version 2.1-1. https://cran.r-project.org/package=AICcmodavg

Monteiro, LR, and MR Nogueira (2010) Adaptive radiations, ecological specialization, and the evolutionary integration of complex morphological stuctures. *Evolution* **64**:724-744.

Omland, KE, and SE Lanyon (2000) Reconstructing plumage evolution in orioles (Icterus): repeated convergence and reversal in patterns. *Evolution* **54**:2119-2133.

Pagel, M (1994) Detecting correlated evolution on phylogenies: a general method for the comparative analysis of discrete characters. *Proceedings: Biological Sciences* **255**:37-45.

Peiman, KS, and BW Robinson (2017) Comparative analyses of phenotypic trait covariation within and among populations. The American Naturalist 190:451-468.

Powell, AFLA, FK Barker, SM Lanyon, KJ Burns, J Klicka, and IJ Lovette (2014) A comprehensive species-level molecular phylogeny of the New World Blackbirds (Icteridae). *Molecular Phylogenetics and Evolution* **71**:94-112.

Price, JJ, and MD Eaton (2014) Reconstructing the evolution of sexual dichromatism: current color diversity does not reflect past rates of male and female change. *Evolution* **68**:2026-2037.

Price, T, and M Pavelka (1996) Evolution of a colour pattern: history, development, and selection. *J Evol Biol* **9**:451-470.

Prum, RO (2006) Anatomy, physics, and evolution of structural colors. In: Hill, GE, and KJ McGraw, Eds. *Bird Coloration. Volume 1: mechanisms and measurement*. Cambridge, UK: Harvard University Press.

Prum RO, ER Dufresne, T Quinn, and K Waters (2009) Development of colour-producing beta-keratin nanostructures in avian feather barbs. *Journal of the Royal Society Interface* **6**:S253-S265.

Prum, RO, and J Dyck (2003) A hierarchical model of plumage: morphology, development, and evolution. *Journal of Experimental Zoology (Mol Dev Evol)* **298B**:73-90.

Prum, RO, and S Williamson (2002) Reaction-diffusion models of within-feather pigmentation patterning. *Proc. R. Soc. London B*. **269**:781-792.

Prum RO, AM LaFountain, J Berro, MC Stoddard (2012) Molecular diversity, metabolic transformation, and evolution of carotenoid feather pigments in cotingas (Aves: Cotingidae). *J Comp Physiol B* **182**:1095-1116.

R Core Team (2016). R: A language and environment for statistical computing. R Foundation for Statistical Computing, Vienna, Austria. URL: https://www.R-project.org/.

Revell, LJ (2012) phytools: an R package for phylogenetic comparative biology (and other things). *Methods in Ecology and Evolution* **3**:217-223.

Revell, LJ (2014) Ancestral character estimation under the threshold model from quantitative genetics. *Evolution* **68**:743-759.

Saranathan V, JD Forster, N Noh, S-F Liew, SGJ Mochrie, H Cao, ER Dufresne, and RO Prum (2012) Structure and optical function of amorphous photonic nanostructures from avian feather barbs: a comparative small angle X-ray scattering (SAXS) analysis of 230 bird species. *J R Soc Interface* **9**:2563-2580

Shawkey, MD, and GE Hill (2006) Significance of the basal melanin layer to production of non-iridescent structural plumage color: evidence from an amelanotic Steller's jay (Cyanocitta stelleri). *Journal of Experimental Biology* **209**:1245-1250.

Sokal, RR, and CD Michener (1958) A statistical method for evaluating systematic relationships. *University of Kansas Science Bulletin* **38**:1409-1448.

Stoddard, MC, and RO Prum (2011) How colorful are birds? Evolution of the avian plumage color gamut. *Behavioral Ecology* **22**:1042-1052.

Wagner, GP (1996) Homologues, natural kinds and the evolution of modularity. *American Zoologist* **36**:36-43.

Wagner, GP, and L Altenberg (1996) Perspective: complex adaptations and the evolution of evolvability. *Evolution* **50**:967-976.

Wagner, GP, M Pavlicev, and JM Cheverud (2007) The road to modularity. *Nature Reviews Genetics*. **8**:921-931.
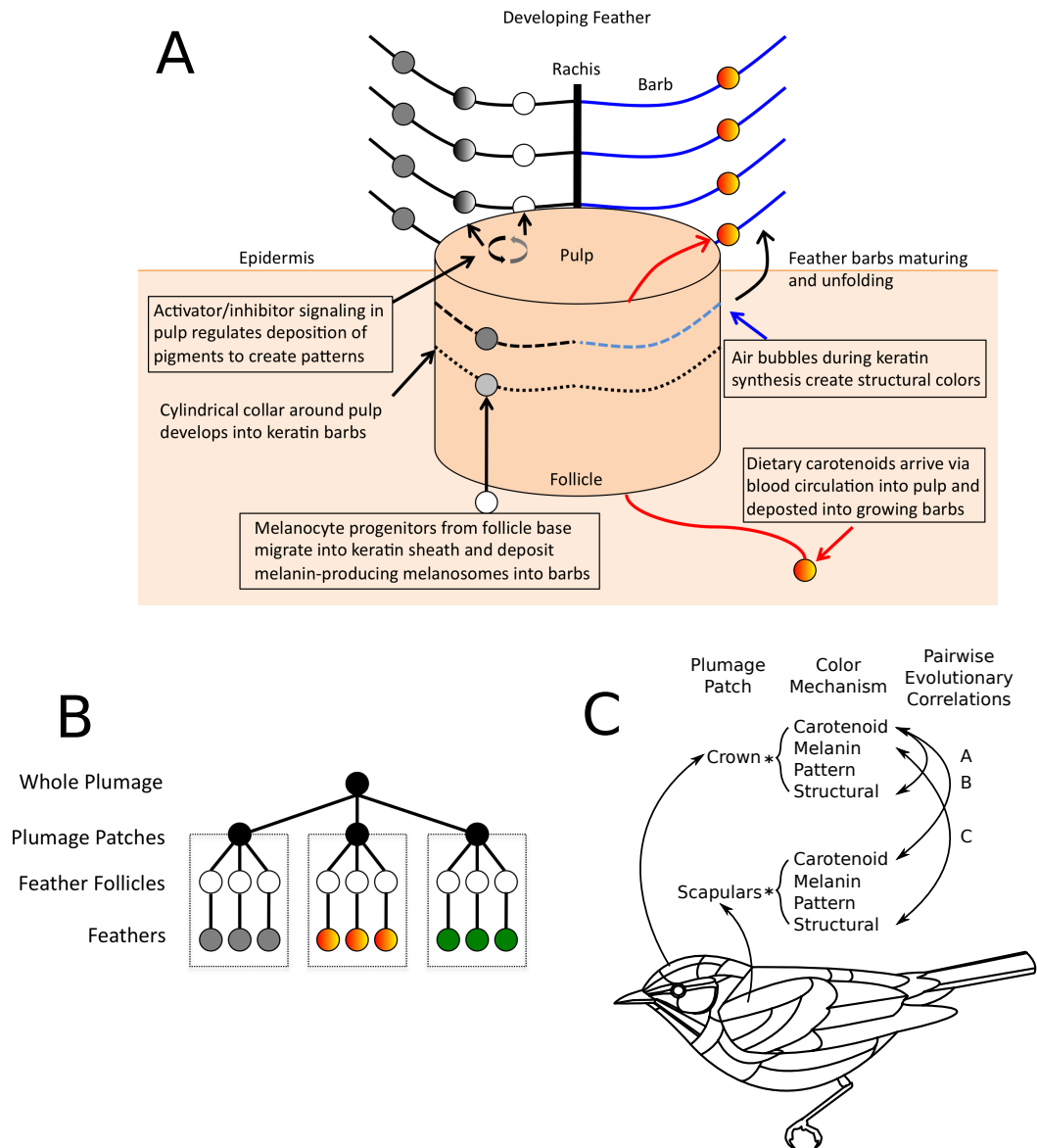
Figure 1: **A**) Simplified model of feather development showing four developmentally modular color production mechanisms (boxes) that produce different aspects of feather color and pattern. **B**) Simplified model for the modular hierarchical organization of plumage. The whole plumage is separated into tracts of feather follicles that are regulated to generate similar feather phenotypes (plumage patches, dotted boxes). Adapted from Prum and Dyck (2003). **C**) We measured the evolutionary independence of color mechanisms and plumage patches by scoring forty-two plumage patches (outlined) for the presence of four color production mechanisms, and testing for evolutionary correlations among all pairwise comparisons of the patch*mechanism traits. Comparisons include: A) correlation of different color mechanisms within the same plumage patch, B) correlation of the same color mechanism across different plumage patches, and C) correlation of different color mechanisms in different plumage patches.
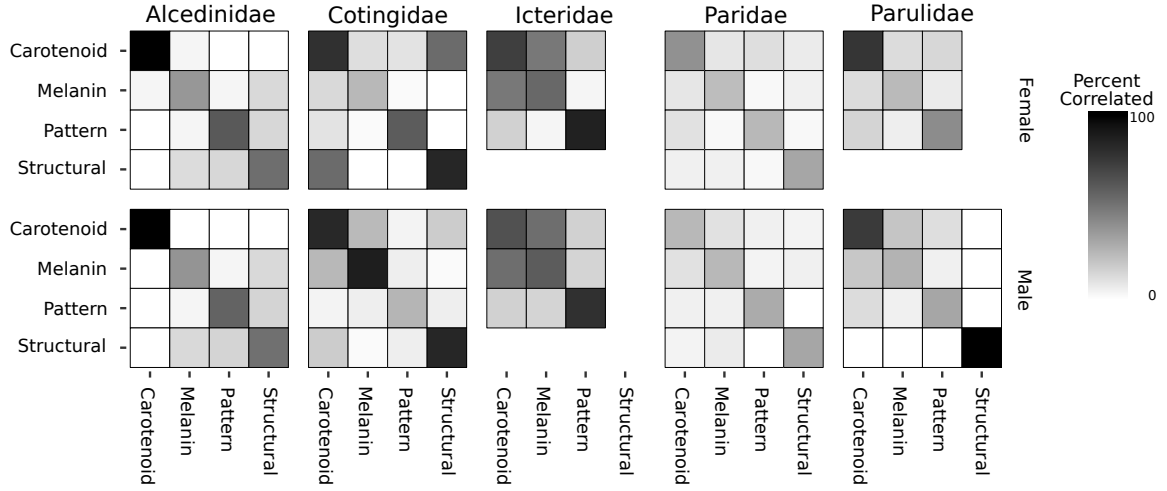
Figure 2: Evolutionary correlation matrices for plumage traits in five families of birds. The color of each box represents the percentage of all pairwise comparisons of plumage patches that have significant evolutionary correlations between the two given color mechanisms. Diagonal boxes represent the correlation of change in one color mechanism across all plumage patches. Off-diagonal boxes represent correlation of change between two different color mechanisms across all plumage patches. Structural color comparisons are omitted for Icteridae (both sexes) and female Parulidae due to a lack sufficient structural color characters for testing after pruning (see Methods, **Table 1**). The full matrices with individual pairwise comparisons among all traits are shown in **Figures S1-S10.**

Figure 3: The relationship between a trait's evolutionary rate and the number of other traits it is correlated with. We compared two metrics of rate: the forward (trait gain, A, B) and reverse (C,D) instantaneous transition rates (log transformed), and two metrics of correlation: the percentage of pairwise comparisons with the same color mechanism that are significantly correlated with the trait (A, C), and the percentage of pairwise comparisons across different color mechanisms that are significantly correlated with the trait (B, D). Color lines represent the best fit simple linear model for each individual family with shading indicating the 95% confidence interval of each fit.
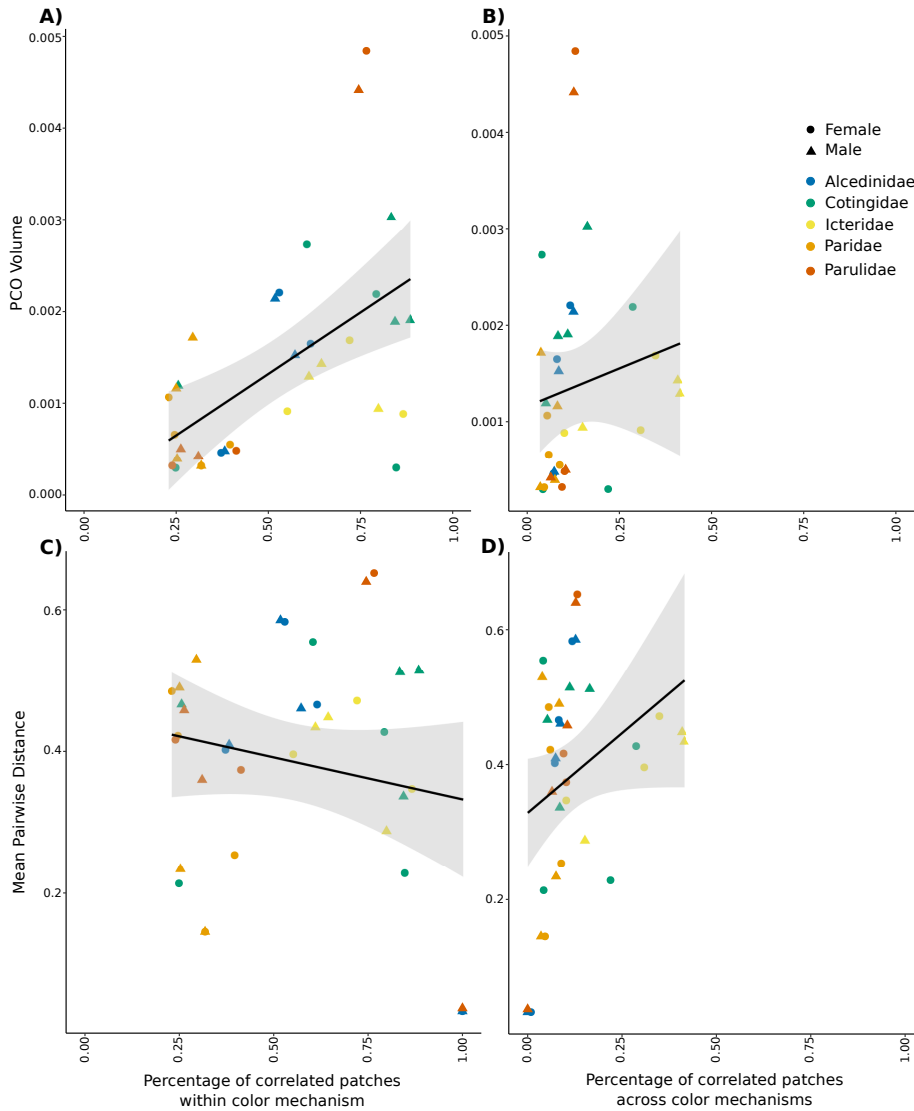
Figure 4: The relationship between morphological disparity and the number of correlated traits for each color mechanism in each family and sex. We compared two metrics of disparity: PCO volume (trait gain, A, B) and mean pairwise distance (C,D), and two metrics of correlation: the percentage of pairwise comparisons within the color mechanism that are significantly correlated (A, C), and the percentage of pairwise comparisons with different color mechanism that are significantly correlated (B, D). Black lines represent the best fit simple linear model with shading indicating the 95% confidence interval of each fit.
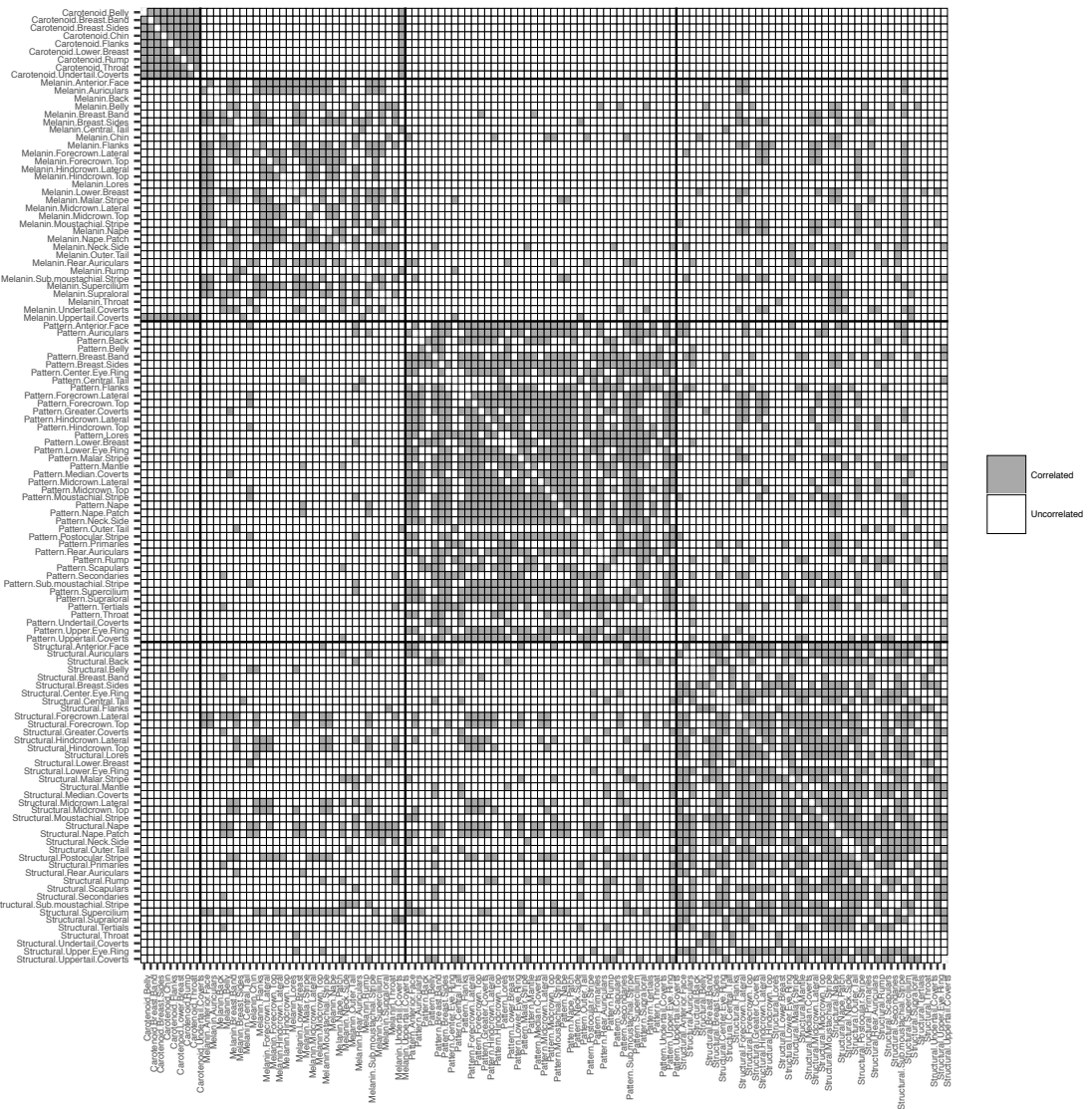
Figure S1: Full evolutionary correlation matrices for individual pairwise comparisons among all plumage traits in female Alcedinidae. Gray-filled boxes indicate significantly evolutionary correlations between the two respective plumage traits (Pagel's test, p < 0.05). Heavy black lines delineate different color mechanisms.
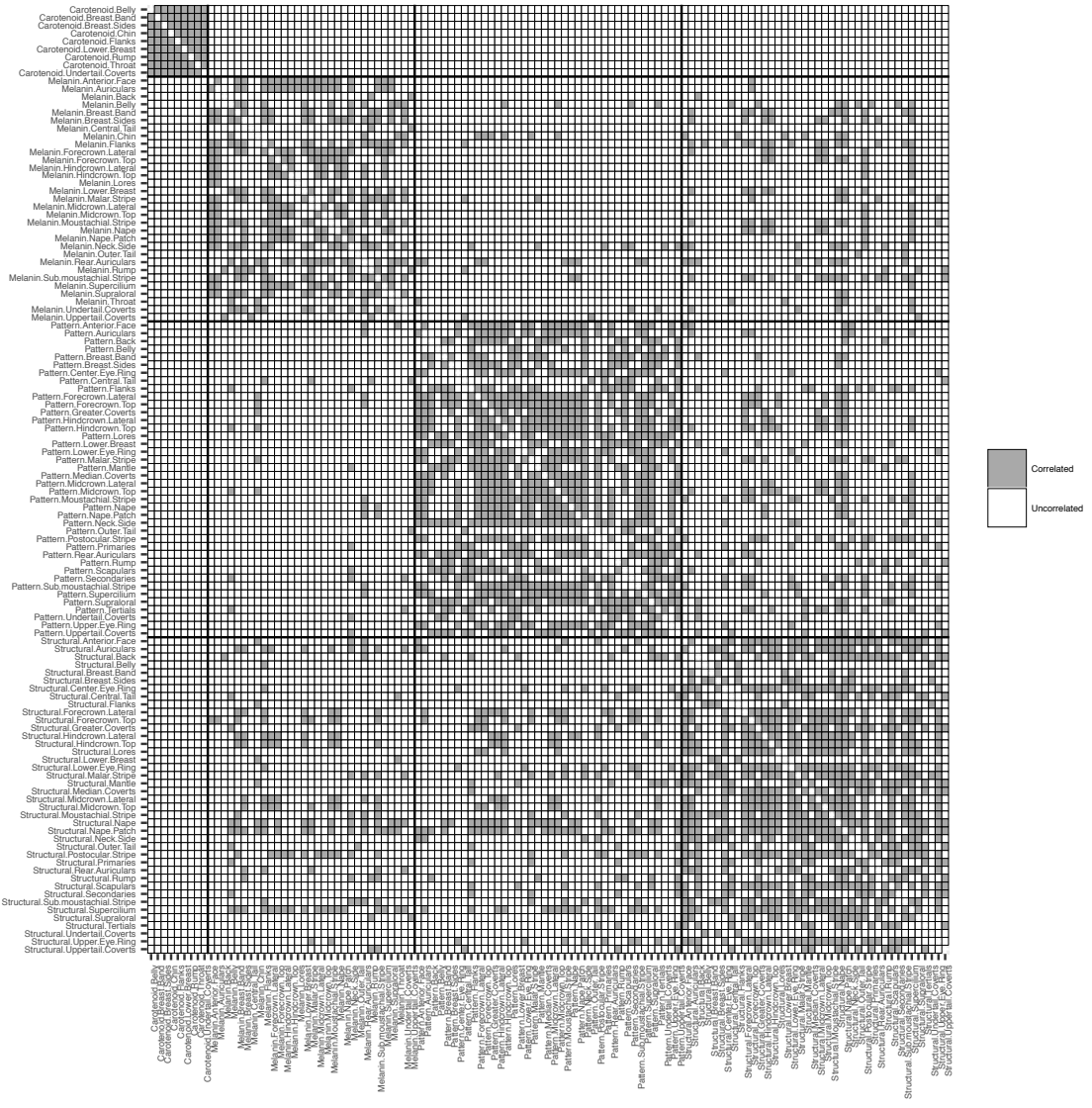
Figure S2: Full evolutionary correlation matrices for individual pairwise comparisons among all plumage traits in male Alcedinidae. Gray-filled boxes indicate significantly evolutionary correlations between the two respective plumage traits (Pagel's test, p < 0.05). Heavy black lines delineate different color mechanisms.
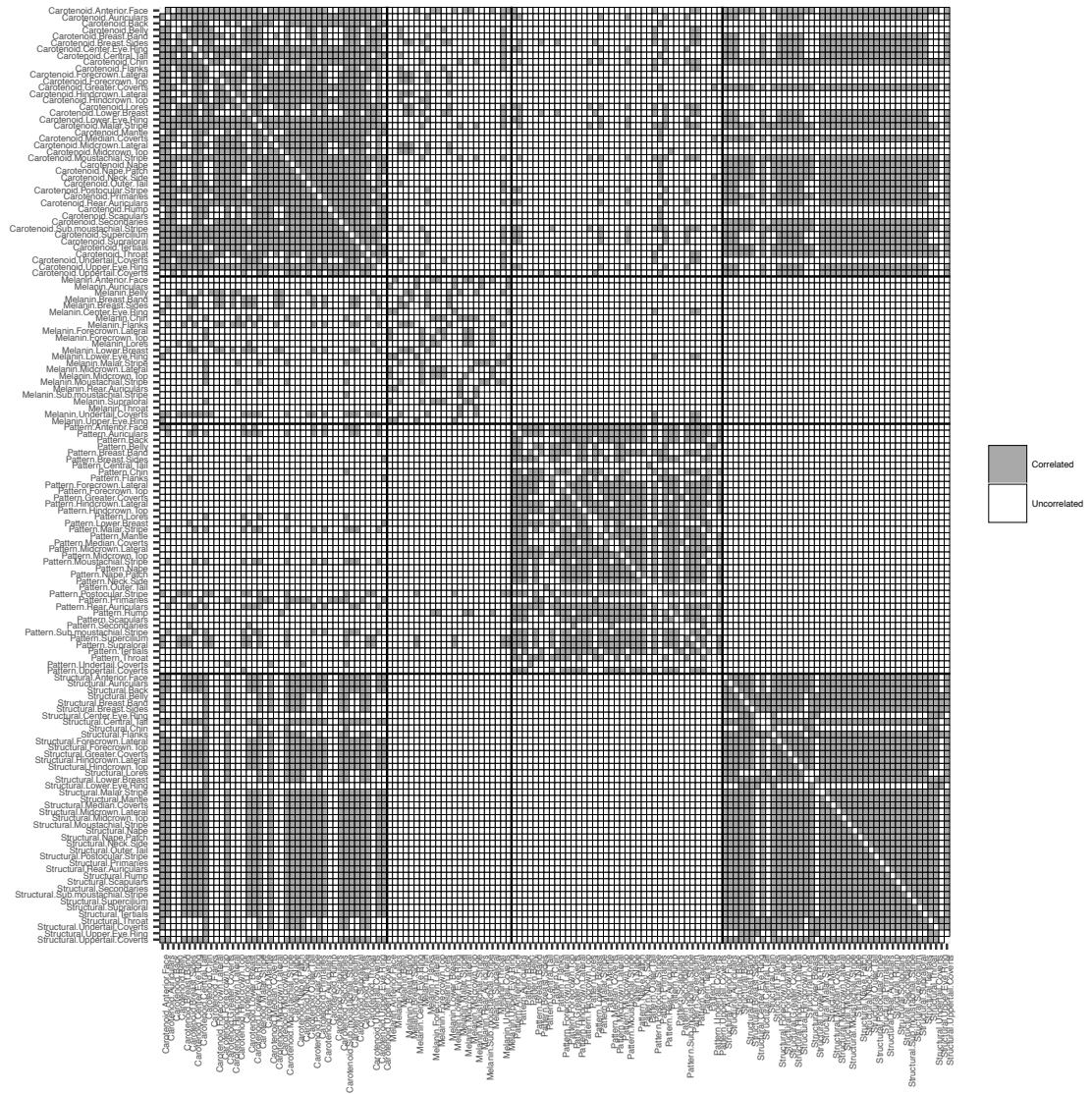
Figure S3: Full evolutionary correlation matrices for individual pairwise comparisons among all plumage traits in female Cotingidae. Gray-filled boxes indicate significantly evolutionary correlations between the two respective plumage traits (Pagel's test, p < 0.05). Heavy black lines delineate different color mechanisms.
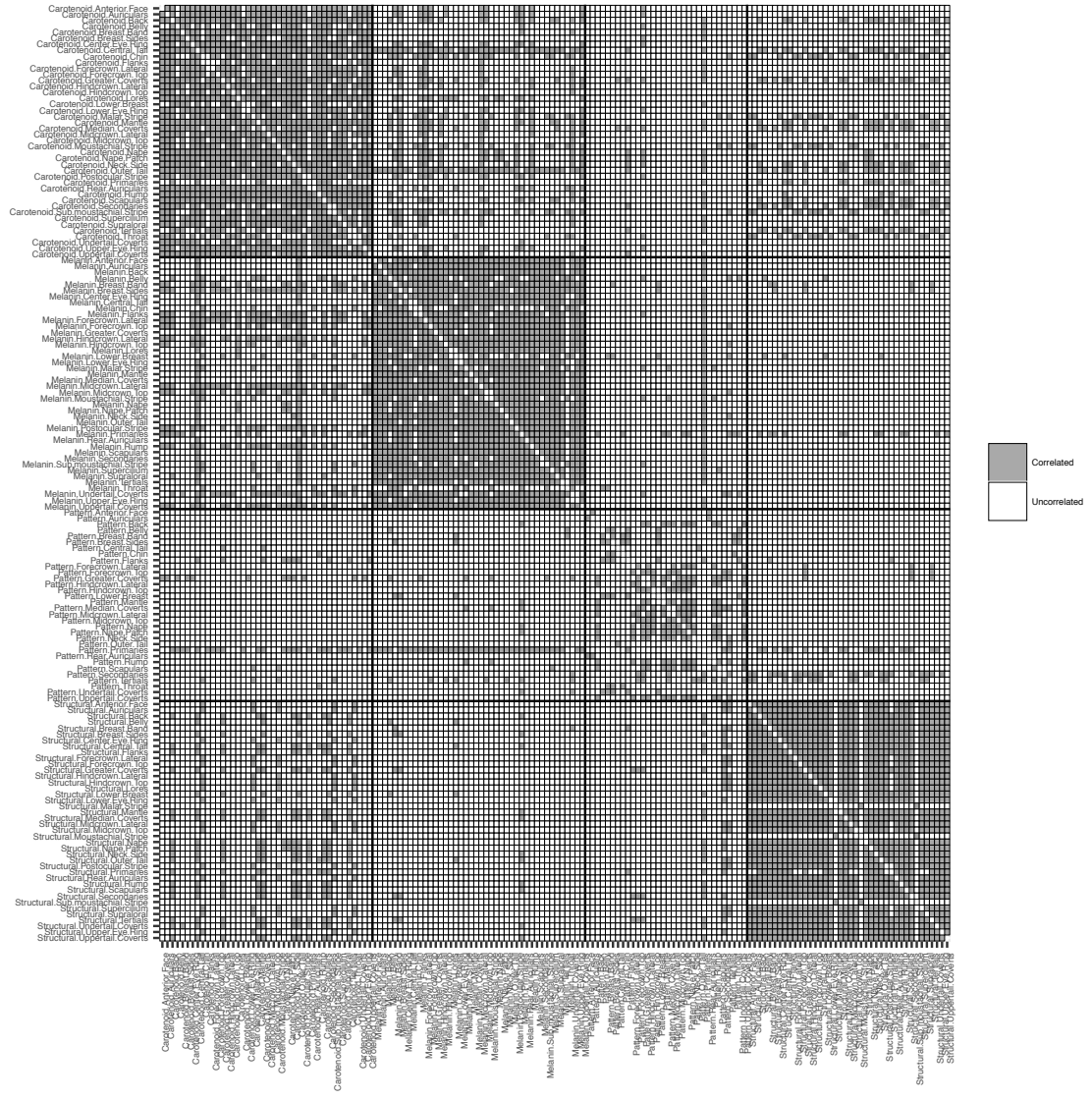
Figure S4: Full evolutionary correlation matrices for individual pairwise comparisons among all plumage traits in male Cotingidae. Gray-filled boxes indicate significantly evolutionary correlations between the two respective plumage traits (Pagel's test, p < 0.05). Heavy black lines delineate different color mechanisms.

Figure S5: Full evolutionary correlation matrices for individual pairwise comparisons among all plumage traits in female Icteridae. Gray-filled boxes indicate significantly evolutionary correlations between the two respective plumage traits (Pagel's test, p < 0.05). Heavy black lines delineate different color mechanisms.
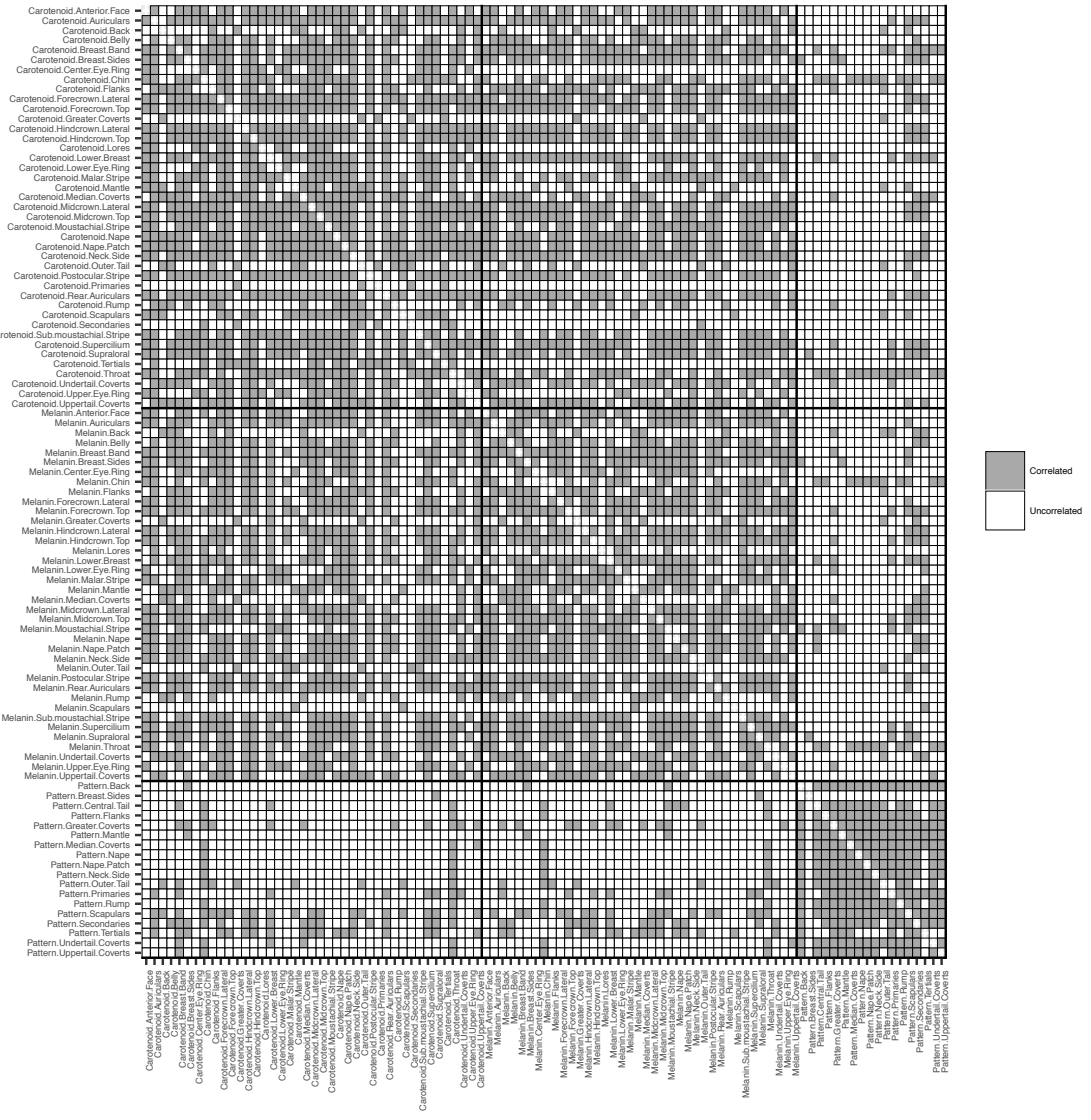
Figure S6: Full evolutionary correlation matrices for individual pairwise comparisons among all plumage traits in male Icteridae. Gray-filled boxes indicate significantly evolutionary correlations between the two respective plumage traits (Pagel's test, $p < 0.05$). Heavy black lines delineate different color mechanisms.
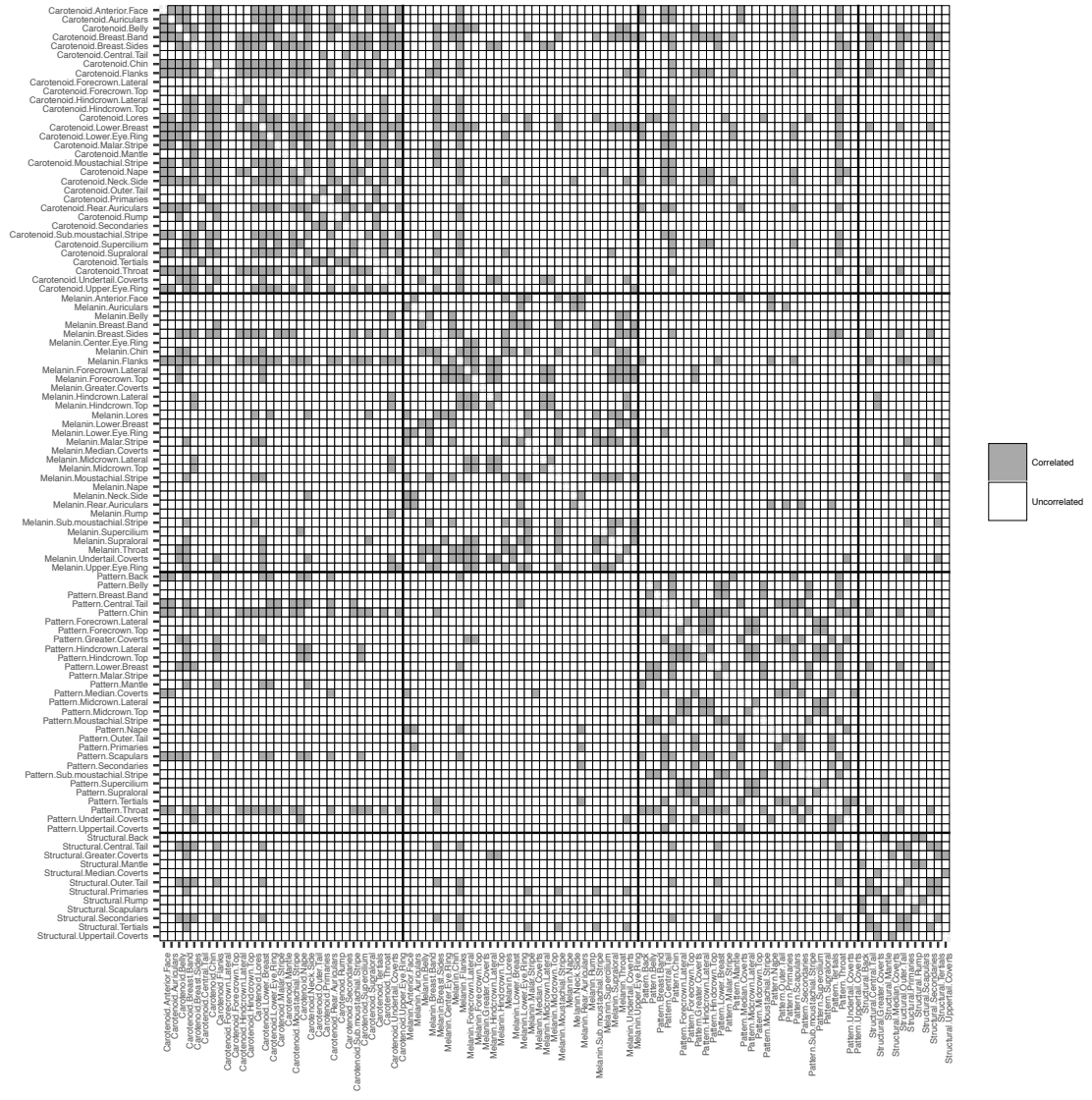
Figure S7: Full evolutionary correlation matrices for individual pairwise comparisons among all plumage traits in female Paridae. Gray-filled boxes indicate significantly evolutionary correlations between the two respective plumage traits (Pagel's test, $p < 0.05$). Heavy black lines delineate different color mechanisms.
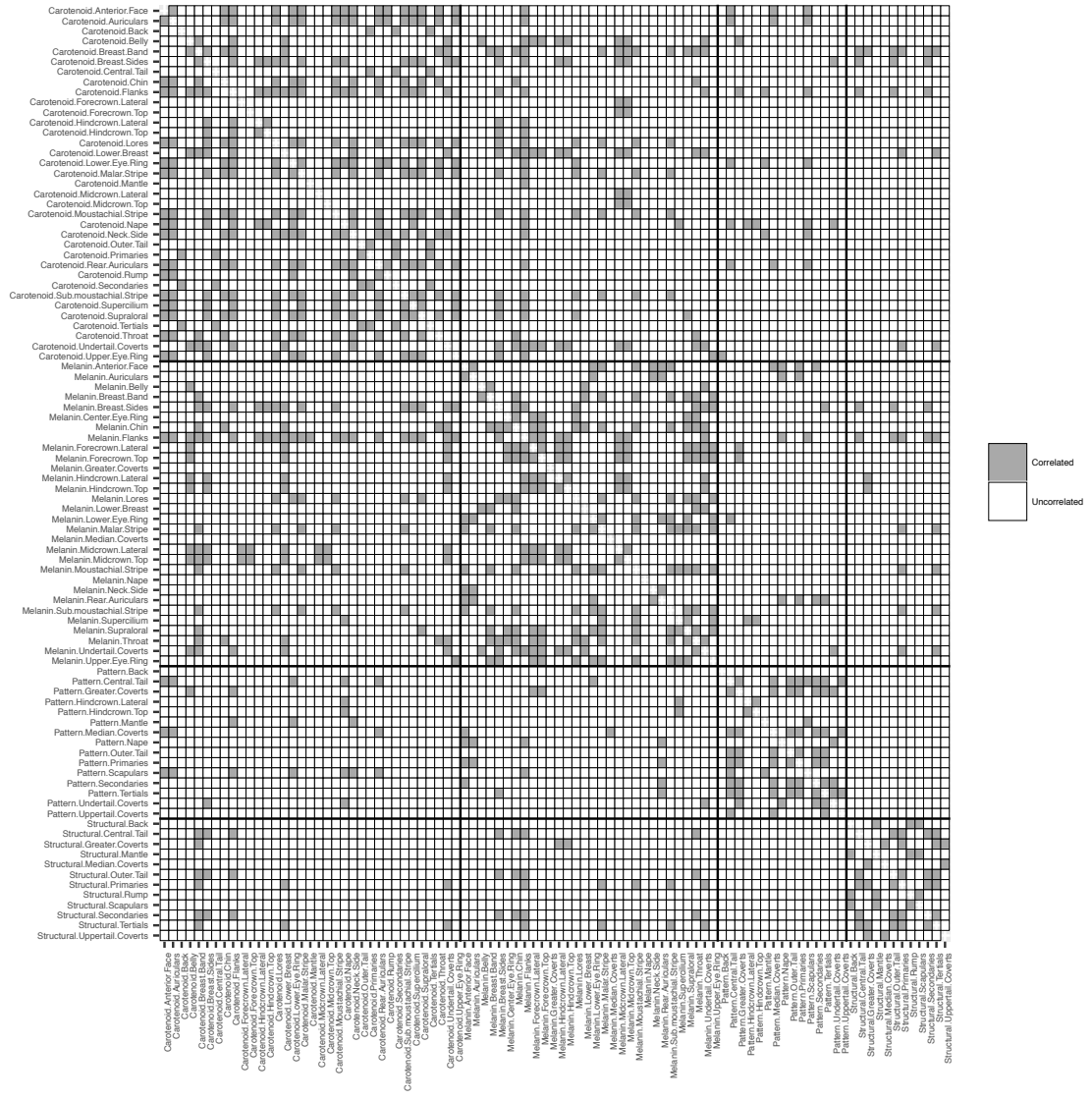
Figure S8: Full evolutionary correlation matrices for individual pairwise comparisons among all plumage traits in male Paridae. Gray-filled boxes indicate significantly evolutionary correlations between the two respective plumage traits (Pagel's test, p < 0.05). Heavy black lines delineate different color mechanisms.
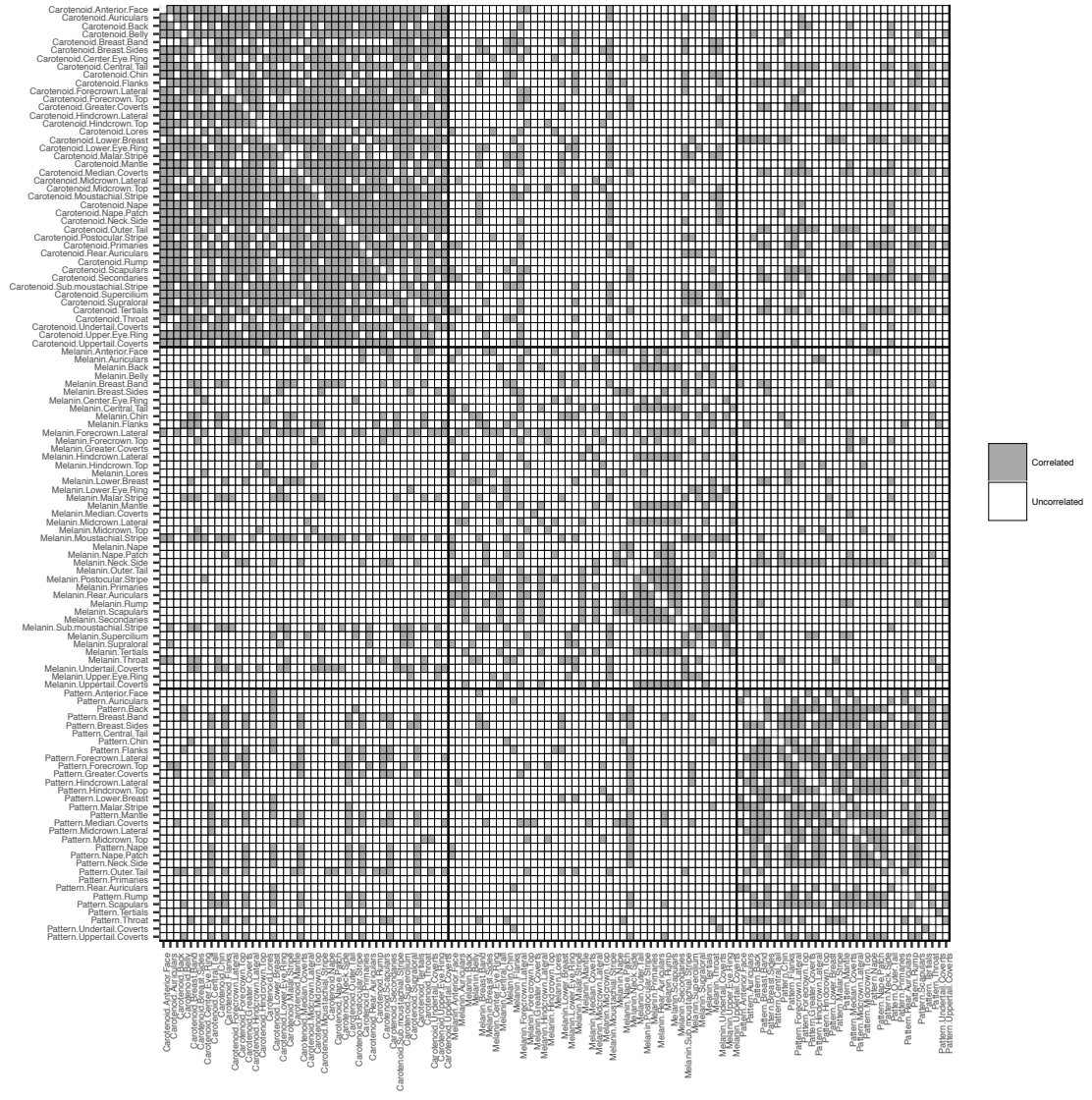
Figure S9: Full evolutionary correlation matrices for individual pairwise comparisons among all plumage traits in female Parulidae. Gray-filled boxes indicate significantly evolutionary correlations between the two respective plumage traits (Pagel's test, p < 0.05). Heavy black lines delineate different color mechanisms.
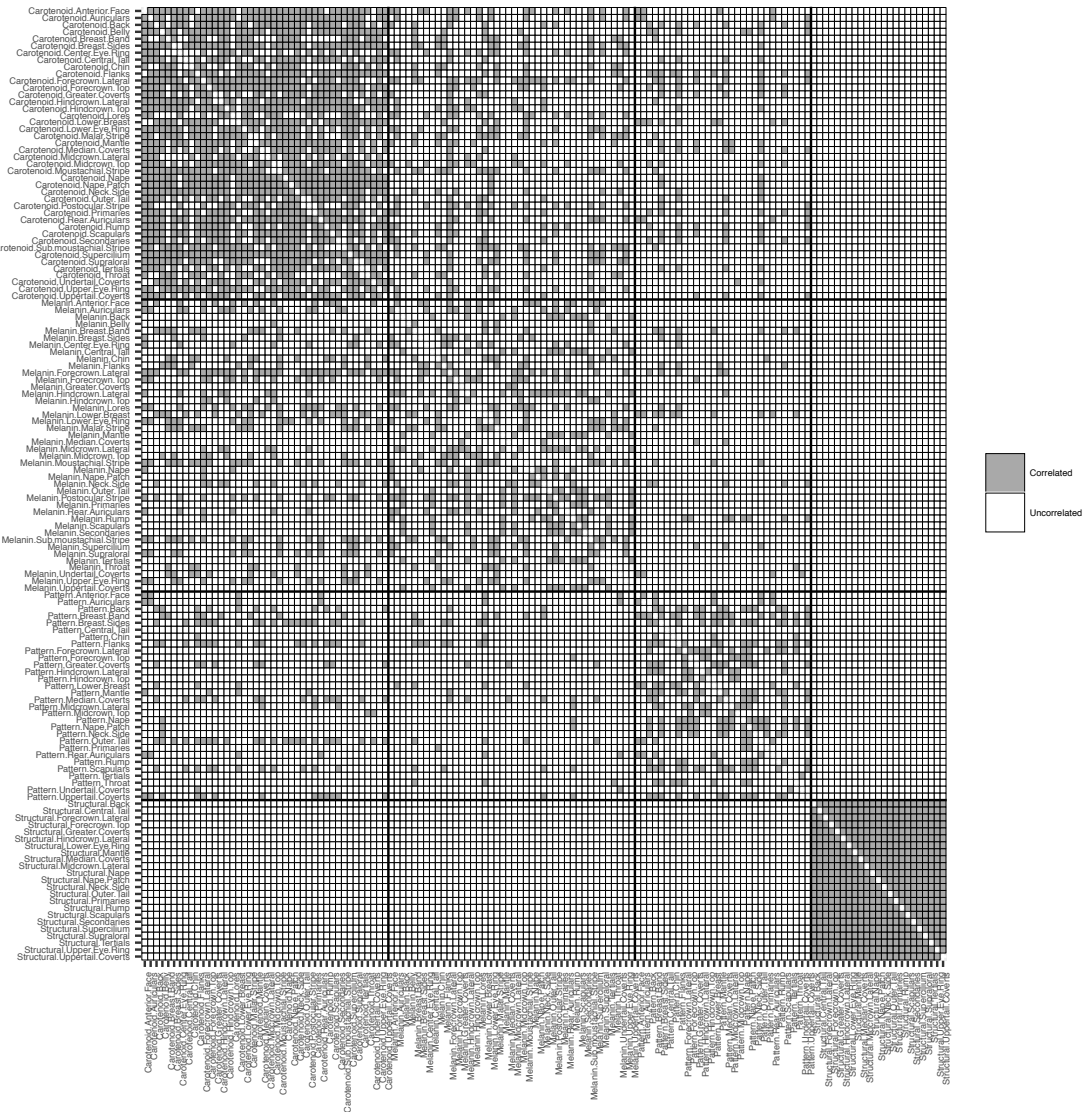
Figure S10: Full evolutionary correlation matrices for individual pairwise comparisons among all plumage traits in male Parulidae. Gray-filled boxes indicate significantly evolutionary correlations between the two respective plumage traits (Pagel's test, p < 0.05). Heavy black lines delineate different color mechanisms.
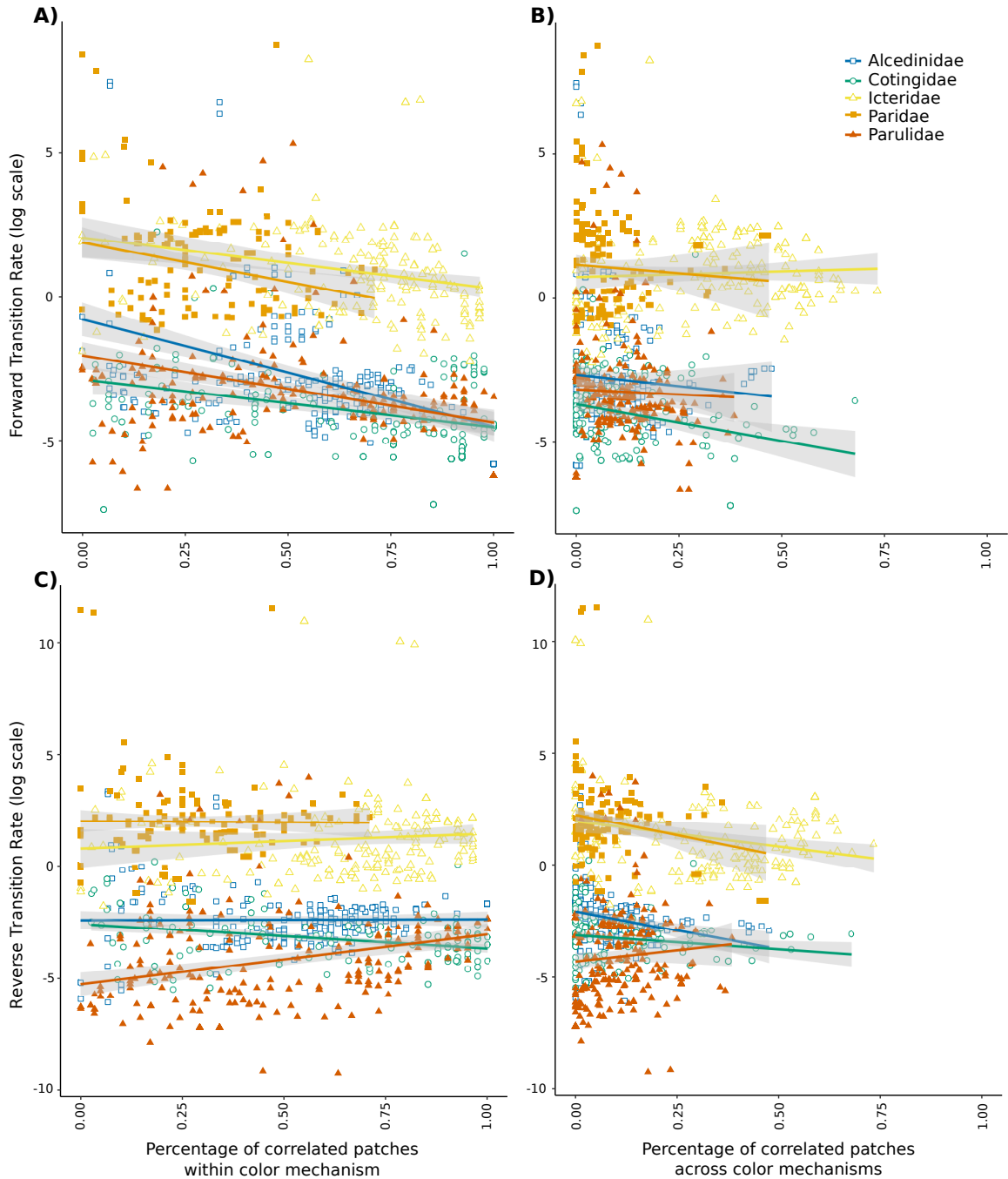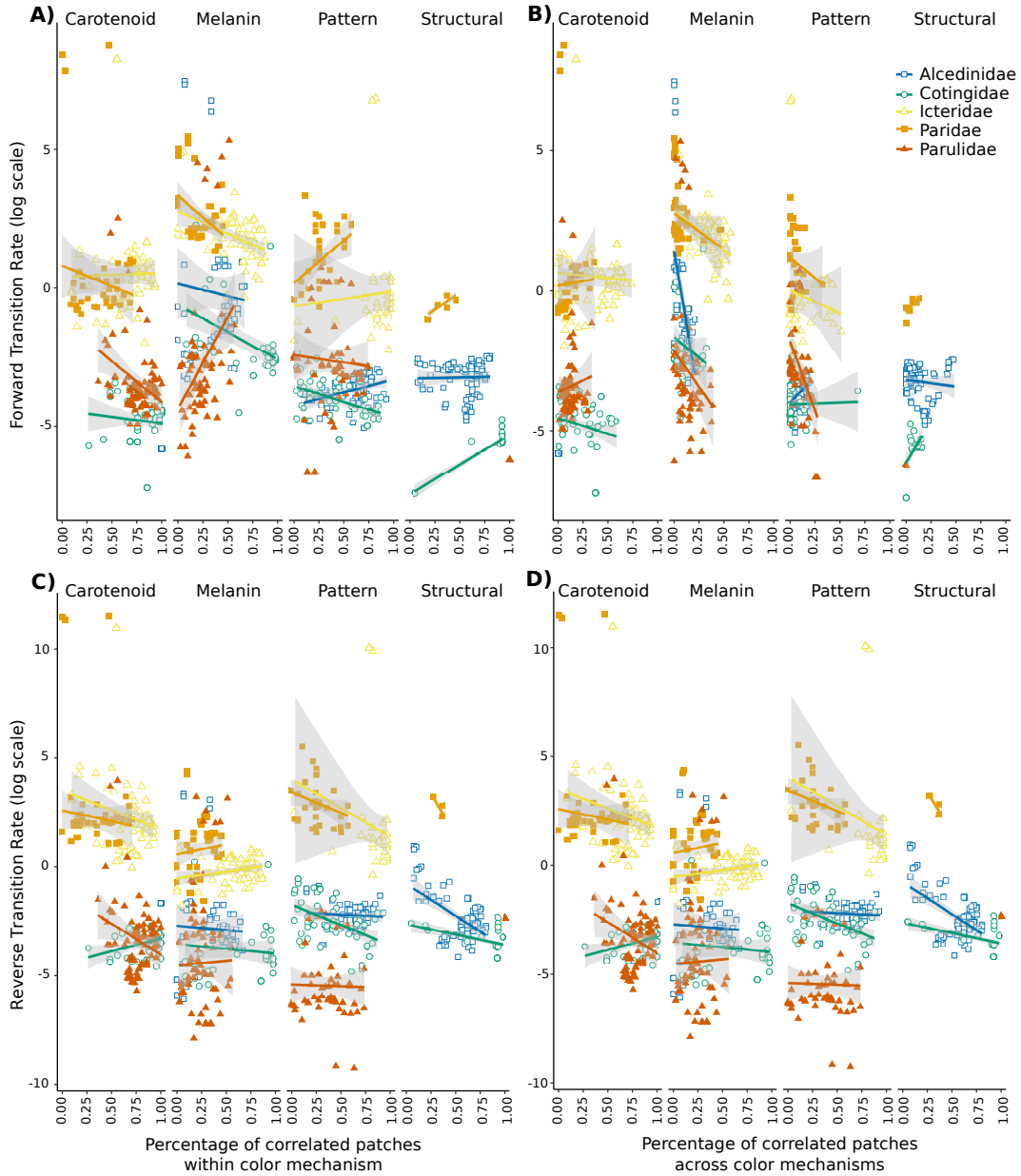
Figure S11: The relationship between a trait's evolutionary rate and the number of other traits it is correlated with, showing the relationships of individual color mechanisms within each family. We compared two metrics of rate: the forward (trait gain, A, B) and reverse (C,D) instantaneous transition rates (log transformed), and two metrics of correlation: the percentage of pairwise comparisons with the same color mechanism that are significantly correlated with the trait (A, C), and the percentage of pairwise comparisons across different color mechanisms that are significantly correlated with the trait (B, D). Color lines represent the best fit simple linear model for each individual family x color module interaction, with shading indicating the 95% confidence interval of each fit.

Tables

Table 1: The number of plumage traits after pruning for each dataset, and Mantel Test results comparing evolutionary correlation matrices to hypotheses of modular structure.

	N traits	Color mechanism independence		Plumage patch independence		100 random matrices	
		r	p-value	r	p-value	Mean r	Proportion of tests significant at $p < 0.05$
Alcedinidae (121 species):							
Female:	122	0.50	< 0.001	-0.02	0.933	0.00	0.04
Carotenoid	9						
Melanin	31						
Pattern	41						
Structural	41						
Male:	120	0.48	< 0.001	0.00	0.418	0.00	0.02
Carotenoid	9						
Melanin	31						
Pattern	40						
Structural	40						
Cotingidae (61 species):							
Female:	146	0.53	< 0.001	-0.03	0.999	0.00	0.02
Carotenoid	42						
Melanin	23						
Pattern	39						
Structural	42						
Male:	156	0.64	< 0.001	-0.02	0.999	0.00	0.05
Carotenoid	42						
Melanin	42						
Pattern	32						
Structural	40						
Icteridae (112 species):							
Female:	108	0.41	< 0.001	0.01	0.141	0.00	0.08
Carotenoid	42						
Melanin	37						
Pattern	29						
Structural	0						
Male:	97	0.28	< 0.001	0.03	0.031	0.00	0.04
Carotenoid	41						
Melanin	38						
Pattern	18						
Structural	0						
Paridae (68 species):							
Female:	107	0.30	< 0.001	-0.01	0.722	0.00	0.03
Carotenoid	31						
Melanin	29						
Pattern	12						
Structural	35						
Male:	92	0.27	< 0.001	0.05	0.001	0.00	0.03
Carotenoid	35						
Melanin	30						
Pattern	15						

Structural	12						
Parulidae (107 species):							
Female:	115	0.42	< 0.001	0.03	0.003	0.00	0.02
Carotenoid	42						
Melanin	42						
Pattern	31						
Structural	0						
Male:	137	0.48	< 0.001	0.02	0.027	0.00	0.06
Carotenoid	42						
Melanin	42						
Pattern	30						
Structural	23						

Table S1: Model coefficients for four comparisons of evolutionary rate and degree of evolutionary correlation

	Dependent variables:			
	Forward transition rate (log transformed)		Reverse transition rate (log transformed)	
	Model 1	Model 2	Model 3	Model 4
	Coefficients	Coefficients	Coefficients	Coefficients
	(Standard Error)	(Standard Error)	(Standard Error)	(Standard Error)
(Intercept)	-5.405***	-5.604***	-0.155	-1.825***
	(0.509)	(0.441)	(0.434)	(0.357)
% Correlation	-0.584*		-1.518***	
Within Mechanism	(0.322)		(0.281)	
% Correlation		-1.448***		-1.859***
Across Mechanism		(0.374)		(0.437)
Color mechanism:				
Melanin	5.539***	5.528***	-2.139***	-1.011***
	(0.497)	(0.500)	(0.391)	(0.381)
Pattern	2.191***	2.050***	-1.149***	-0.336
	(0.469)	(0.485)	(0.367)	(0.374)
Structural	2.604***	2.550***	-1.374***	-0.332
	(0.474)	(0.486)	(0.372)	(0.374)
Sex:				
Male	-0.0001	-0.011	0.123	0.152*
	(0.590)	(0.615)	(0.082)	(0.085)
Family:				
Cotingidae	0.791*	0.910*	-2.167***	-1.318***
	(0.464)	(0.495)	(0.377)	(0.401)
Icteridae	6.189***	6.426***	3.494***	4.834***
	(0.466)	(0.503)	(0.361)	(0.401)
Paridae	5.835***	5.905***	2.912***	4.169***
	(0.497)	(0.505)	(0.391)	(0.379)
Parulidae	2.299***	2.217***	-2.093***	-1.359***
	(0.464)	(0.486)	(0.359)	(0.374)
Sex*Family:				
Male	0.729	0.477		
Cotingidae	(0.651)	(0.680)		
Male Icteridae	0.346	0.492		
	(0.653)	(0.681)		
Male Paridae	0.231	0.222		
	(0.678)	(0.706)		
Male Parulidae	0.337	0.356		
	(0.650)	(0.678)		
Color * Family:				
Melanin	-1.484**	-1.614***	1.325***	0.229
Cotingidae	(0.580)	(0.616)	(0.461)	(0.478)
Pattern	-1.359**	-1.529***	1.717***	1.054**
Cotingidae	(0.544)	(0.582)	(0.439)	(0.469)
Structural	-3.698***	-3.844***	1.459***	0.320
Cotingidae	(0.552)	(0.570)	(0.450)	(0.458)
Melanin	-4.201***	-4.087***	-0.597	-1.557***
Icteridae	(0.565)	(0.583)	(0.440)	(0.442)
Pattern	-2.072***	-2.361***	0.946**	-0.631
Icteridae	(0.565)	(0.594)	(0.458)	(0.481)
Melanin	-3.063***	-3.021***	0.325	-0.659
Paridae	(0.587)	(0.608)	(0.453)	(0.455)
Pattern Paridae	-1.294**	-1.285**	2.088***	1.273***

	Model 1	Model 2	Model 3	Model 4
	(0.574)	(0.599)	(0.451)	(0.461)
Structural Paridae	-3.354***	-3.312***	2.554***	1.475***
	(0.644)	(0.665)	(0.538)	(0.543)
Melanin Parulidae	-4.866***	-4.648***	0.318	-0.065
	(0.553)	(0.578)	(0.422)	(0.439)
Pattern Parulidae	-1.287**	-1.007*	-1.333***	-1.744***
	(0.552)	(0.578)	(0.426)	(0.447)
Structural Parulidae	-5.374***	-5.740***	2.707***	1.281**
	(0.589)	(0.599)	(0.503)	(0.503)
Color * Sex:				
Melanin Male	0.005	0.032		
	(0.673)	(0.701)		
Pattern Male	-0.107	-0.010		
	(0.652)	(0.680)		
Structural Male	-0.043	0.008		
	(0.652)	(0.680)		
Color * Sex * Family:				
Melanin Male Cotingidae	-2.087**	-2.061**		
	(0.811)	(0.833)		
Pattern Male Cotingidae	-0.434	-0.011		
	(0.776)	(0.805)		
Melanin Male Icteridae	-0.281	-0.344		
	(0.785)	(0.817)		
Pattern Male Icteridae	-2.096**	-2.034**		
	(0.825)	(0.860)		
Melanin Male Paridae	-0.572	-0.535		
	(0.819)	(0.853)		
Pattern Male Paridae	0.122	0.110		
	(0.844)	(0.875)		
Structural Male Paridae	-0.188	-0.235		
	(0.893)	(0.930)		
Melanin Male Parulidae	-0.409	-0.441		
	(0.778)	(0.811)		
Pattern Male Parulidae	-0.550	-0.645		
	(0.780)	(0.813)		

*p<0.1; **p<0.05, ***p<0.01

Model 1: log(Forward Rate) ~ % Correlation Within Mechanism + Color Mechanism + Sex + Family + Family*Sex + Color*Family + Sex*Color + Color*Sex*Family + (% Correlation Within Mechanism|Patch)

Model 2: log(Forward Rate) ~ % Correlation Across Mechanism + Color Moule + Sex + Family + Family*Sex + Color*Family + Sex*Color + Color*Sex*Family + (% Correlation Across Mechanism|Patch)

Model 3: log(Reverse Rate) ~ % Correlation Within Mechanism + Color Module + Sex + Family + Color*Family + (% Correlation Within Mechanism|Patch)

Model 4: log(Reverse Rate) ~ % Correlation Across Mechanism + Color Module + Sex + Family + Color*Family + (% Correlation Across Mechanism|Patch)

Reference levels: Alcedinidae, Female, Carotenoid

Table S2: Model coefficients for four comparisons of morphological disparity and degree of evolutionary correlation. Measures are summaries for each sex in each family

	Dependent variables:			
	PCO volume		Mean pairwise distance	
	Model 1 Coefficients (Standard Error)	Model 2 Coefficients (Standard Error)	Model 3 Coefficients (Standard Error)	Model 4 Coefficients (Standard Error)
(Intercept)	-0.0003 (0.0003)	0.0005* (0.0002)	0.297*** (0.066)	0.436*** (0.044)
% Correlation Within-Mechanism	0.001** (0.001)		0.214 (0.113)	
% Correlation Across Mechanism		-0.0001 (0.001)		-0.166 (0.236)
Sex: Male	0.00001 (0.0002)	0.00000 (0.0002)	0.001 (0.036)	0.0003 (0.043)

*p<0.1; **p<0.05, ***p<0.01
Model 1: PCO volume ~ % Correlation Within Mechanism + Sex
Model 2: PCO volume ~ % Correlation Across Mechanism + Sex
Model 3: Mean Pairwise Distance ~ % Correlation Within Mechanism + Sex
Model 4: Mean Pairwise Distance ~ % Correlation Across Mechanism + Sex
Reference level: Female

Table S3: Model coefficients for four comparisons of morphological disparity and degree of evolutionary correlation. Measures are summaries for each color mechanism in each sex in each family

| | Dependent variables: | | | |
| | Mean PCO volume | | Mean Pairwise Distance | |
	Model 1 Coefficients (Standard Error)	Model 2 Coefficients (Standard Error)	Model 3 Coefficients (Standard Error)	Model 4 Coefficients (Standard Error)
(Intercept)	-0.0001 (0.0004)	0.001*** (0.0004)	0.447*** (0.070)	0.324*** (0.049)
% Correlation Within-Mechanism	0.003*** (0.107)		-0.119 (0.001)	
% Correlation Across Mechanism		0.002 (0.002)		0.475* (0.253)
Sex: Male	0.0002 (0.0003)	0.0002 (0.0004)	0.010 (0.054)	0.010 (0.052)

*p<0.1; **p<0.05, ***p<0.01
Model 1: PCO volume ~ % Correlation Within Mechanism + Sex
Model 2: PCO volume ~ % Correlation Across Mechanism + Sex
Model 3: Mean Pairwise Distance ~ % Correlation Within Mechanism + Sex
Model 4: Mean Pairwise Distance ~ % Correlation Across Mechanism + Sex
Reference level: Female

Table S4: Empirical determination of feather color mechanisms in our five focal families.

Family	Taxon	Patch	Color	Mechanism	Method	Reference*
Alcedinidae	Actenoides concretus	Back	Blue	Structural	X-ray scattering	Saranathan et al. 2012
Alcedinidae	Alcedo		Blue	Structural	Microscopy	Auber 1957
Alcedinidae	Alcedo atthis ispida	Rump	Blue	Structural	X-ray scattering	Saranathan et al. 2012
Alcedinidae	Ceryle rudis	Upperparts	Black	Melanin	Microscopy	Auber 1957
Alcedinidae	Ceyx		Blue	Structural	Microscopy	Auber 1957
Alcedinidae	Ceyx erithacus	Scapular	Blue	Structural	Microscopy	Auber 1957
Alcedinidae	Chloroceryle	Upperparts	Green	Iridescence	Microscopy	Auber 1957
Alcedinidae	Cittura		Blue	Structural	Microscopy	Auber 1957
Alcedinidae	Cittura cyanotis sanghisensis	Auriculars	Blue	Structural	X-ray scattering	Saranathan et al. 2012
Alcedinidae	Cittura cyanotis sanghisensis	Throat	Lilac	Structural	X-ray scattering	Saranathan et al. 2012
Alcedinidae	Clytoceyx rex	Rump	Blue	Structural	X-ray scattering	Saranathan et al. 2012
Alcedinidae	Dacelo		Blue	Structural	Microscopy	Auber 1957
Alcedinidae	Dacelo gaudichaud	Coverts	Blue	Structural	X-ray scattering	Saranathan et al. 2012
Alcedinidae	Dacelo novaeguineae	Wing coverts	Blue	Structural	Microscopy	Auber 1957
Alcedinidae	Halcyon		Blue	Structural	Microscopy	Auber 1957
Alcedinidae	Halcyon coromanda	Nape	Purple	Structural	Microscopy	Auber 1957
Alcedinidae	Halcyon leucocephala	Belly	Brown	Not carotenoid	Chromatography	Thomas et al. 2014
Alcedinidae	Halcyon pileata	Back	Blue	Structural	Microscopy	Prum 2006
Alcedinidae	Halcyon pileata	Back	Blue	Structural	X-ray scattering	Saranathan et al. 2012
Alcedinidae	Halcyon smyrnensis	Breast	Brown	Not carotenoid	Chromatography	Thomas et al. 2014
Alcedinidae	Ispidina		Blue	Structural	Microscopy	Auber 1957
Alcedinidae	Ispidina (Ceyx) p. picta	Cheek	Lilac	Structural	X-ray scattering	Saranathan et al. 2012
Alcedinidae	Ispidina picta	Throat	Orange	Not carotenoid	Chromatography	Thomas et al. 2014
Alcedinidae	Ispidina picta	Cheek	Purple	Not carotenoid	Chromatography	Thomas et al. 2014
Alcedinidae	Lacedo		Blue	Structural	Microscopy	Auber 1957
Alcedinidae	Lacedo pulchella	Pileum	Blue	Structural	Microscopy	Auber 1957
Alcedinidae	Megaceryle alcyon	Upperparts	Blue-gray	Structural	Microscopy	Auber 1957
Alcedinidae	Megaceryle alcyon	Upperparts	Blue-gray	Structural	Microscopy	Auber 1957
Alcedinidae	Megaceryle maxima	Upperparts	Gray	Melanin	Microscopy	Auber 1957
Alcedinidae	Melidora macrorrhina	Nape	Blue	Structural	X-ray scattering	Saranathan et al. 2012
Alcedinidae	Melidora macrorrhina	Nape	Pale blue	Structural	X-ray scattering	Saranathan et al. 2012
Alcedinidae	Pelargopsis		Blue	Structural	Microscopy	Auber 1957
Alcedinidae	Pelargopsis capensis	Rump	Blue	Structural	X-ray scattering	Saranathan et al. 2012
Alcedinidae	Syma torotoro	Coverts	Blue	Structural	X-ray scattering	Saranathan et al. 2012
Alcedinidae	Tanysiptera		Blue	Structural	Microscopy	Auber 1957
Alcedinidae	Tanysiptera galatea meyeri	Crown	Blue	Structural	X-ray scattering	Saranathan et al. 2012
Alcedinidae	Tanysiptera nympha	Breast	Pink	Carotenoid	Raman	Thomas et al. 2014
Alcedinidae	Todiramphus chloris chloris	Back	Turquoise	Structural	X-ray scattering	Saranathan et al. 2012
Alcedinidae	[Not stated]		Green	Structural and Pheomelanin	Microscopy	Auber 1957
Alcedinidae	[Not stated]		Purple	Structural and Pheomelanin	Microscopy	Auber 1957
Alcedinidae	[Not stated]		Orange	Not carotenoid	Microscopy	Auber 1957

Cotingidae	Ampelioides tschudii	Undertail coverts	Yellow	Carotenoid	Chromatography	Prum et al. 2012
Cotingidae	Ampelion rufaxilla	Belly	Yellow	Carotenoid	Chromatography	Prum et al. 2012
Cotingidae	Carpornis cucullata				Chromatography	Volker 1952
Cotingidae	Carpornis cucullata	Belly	Yellow	Carotenoid	Chromatography	Prum et al. 2012
Cotingidae	Cotinga amabilis	Breast	Purple	Carotenoid	Chromatography	Prum et al. 2012
Cotingidae	Cotinga amabilis	Back	Blue	Structural	X-ray scattering	Saranathan et al. 2012
Cotingidae	Cotinga cayana	Throat	Purple	Carotenoid	Chromatography and Raman	Thomas et al. 2014
Cotingidae	Cotinga cayana			Structural	Microscopy	Schmidt and Ruska 1962
Cotingidae	Cotinga cayana	Back	Blue	Structural	X-ray scattering	Saranathan et al. 2012
Cotingidae	Cotinga cotinga	Breast	Purple	Carotenoid	Chromatography	Prum et al. 2012
Cotingidae	Cotinga cotinga			Structural	Microscopy	Prum 2006
Cotingidae	Cotinga cotinga	Back	Blue	Structural	X-ray scattering	Saranathan et al. 2012
Cotingidae	Cotinga maculata	Breast	Purple	Carotenoid	Chromatography	Prum et al. 2012
Cotingidae	Cotinga maculata	Back	Blue	Structural	X-ray scattering	Saranathan et al. 2012
Cotingidae	Cotinga maynana			Structural	Microscopy	Dyck 1971, Prum et al. 1998
Cotingidae	Cotinga maynana	Back	Blue	Carotenoid	?	Dyck 1971
Cotingidae	Cotinga maynana	Back	Blue	Structural	Microscopy	Dyck 1971
Cotingidae	Cotinga maynana	Throat	Purple	Not structural	X-ray scattering	Saranathan et al. 2012
Cotingidae	Cotinga maynana	Back	Blue	Structural	X-ray scattering	Saranathan et al. 2012
Cotingidae	Cotinga nattereri	Back	Blue	Structural	X-ray scattering	Saranathan et al. 2012
Cotingidae	Cotinga ridgwayi	Back	Blue	Structural	X-ray scattering	Saranathan et al. 2012
Cotingidae	Haematoderus militaris	Back, Belly	Crimson	Carotenoid	Chromatography	Prum et al. 2012
Cotingidae	Iodopleura isabellae	tuft	Purple	Not structural	X-ray scattering	Saranathan et al. 2012
Cotingidae	Lipaugus streptophorus	Undertail coverts	Pink	Carotenoid	Chromatography	Prum et al. 2012
Cotingidae	Phibalura flavirostris	Belly	Yellow	Carotenoid	Chromatography	Prum et al. 2012
Cotingidae	Phoenicircus carnifex	Belly	Red	Carotenoid	Chromatography	Prum et al. 2012
Cotingidae	Phoenicircus carnifex				Chromatography	Volker 1961
Cotingidae	Phoenicircus nigricollis				Chromatography	Volker 1951
Cotingidae	Pipreola arcuata	Breast	Yellow	Carotenoid	Chromatography	Thomas et al. 2014
Cotingidae	Pipreola aureopectus	Belly	Yellow	Carotenoid	Chromatography	Prum et al. 2012
Cotingidae	Pipreola chlorolepidota	Throat	Orange	Carotenoid	Chromatography	Prum et al. 2012
Cotingidae	Pipreola formosa	Belly	Yellow	Carotenoid	Chromatography	Prum et al. 2012
Cotingidae	Pipreola formosa	Throat	Orange	Carotenoid	Chromatography	Prum et al. 2012
Cotingidae	Pipreola r. riefferii	Back	Green	Structural	X-ray scattering	Saranathan et al. 2012
Cotingidae	Pipreola whitelyi	Breast	Orange	Carotenoid	Chromatography	Prum et al. 2012
Cotingidae	Porphyrolaema porphyrolaema	Throat	Purple	Carotenoid	Chromatography	Prum et al. 2012
Cotingidae	Procnias	Belly	Yellow	Carotenoid	Chromatography	Prum et al.

	tricarunculatus					2012
Cotingidae	Pyroderus s. occidentalis	Throat	Orange	Carotenoid	Chromatography	Prum et al. 2012
Cotingidae	Pyroderus s. scutatus	Throat	Orange	Carotenoid	Chromatography	Prum et al. 2012
Cotingidae	Pyroderus scutatus	Breast	Red	Carotenoid	Chromatography	Thomas et al. 2014
Cotingidae	Pyroderus scutatus				Chromatography	Volker 1952
Cotingidae	Querula purpurata	Throat	Crimson	Carotenoid	Chromatography	Prum et al. 2012
Cotingidae	Rupicola peruvianus	Breast	Red	Carotenoid	Chromatography	Thomas et al. 2014
Cotingidae	Rupicola peruvianus				Chromatography	Volker 1951
Cotingidae	Rupicola peruvianus sanguinolenta	Back, Belly	Red	Carotenoid	Chromatography	Prum et al. 2012
Cotingidae	Rupicola peruvianus saturata	Belly	Orange	Carotenoid	Chromatography	Prum et al. 2012
Cotingidae	Rupicola rupicola	Belly	Orange	Carotenoid	Chromatography	Prum et al. 2012
Cotingidae	Snowornis subalaris	Underwing	Yellow	Carotenoid	Chromatography	Prum et al. 2012
Cotingidae	Tijuca atra	Secondaries	Yellow	Carotenoid	Chromatography	Prum et al. 2012
Cotingidae	Xipholena atropurpurea	Back	Dark purple	Carotenoid	Chromatography	Prum et al. 2012
Cotingidae	Xipholena lamellipennis	Back	Dark purple	Carotenoid	Chromatography	Prum et al. 2012
Cotingidae	Xipholena punicea	Back, Belly	Purple	Carotenoid	Chromatography	Prum et al. 2012
Cotingidae	Xipholena punicea		Purple	Carotenoid (Not melanin or structural)	Chromatography	LaFountain et al. 2010
Cotingidae	Xipholena punicea	Back	Purple	Not structural	X-ray scattering	Saranathan et al. 2012
Icteridae	Agelaius assimilis	Lesser coverts	Red	Carotenoid	Spectrometry	Friedman et al. 2011
Icteridae	Agelaius humeralis	Lesser coverts	Tawny	Not carotenoid	Spectrometry	Friedman et al. 2011
Icteridae	Agelaius phoeniceus	Epaulet	Yellow	Melanin	Chromatography	McGraw et al. 2004
Icteridae	Agelaius phoeniceus	Lesser coverts	Red	Carotenoid	Spectrometry	Friedman et al. 2011
Icteridae	Agelaius phoeniceus		Black	Melanin	Chromatography	McGraw et al. 2004
Icteridae	Agelaius phoeniceus	Belly	Black	Melanin	Spectrometry, Microscopy	Shawkey et al. 2006
Icteridae	Agelaius tricolor	Lesser coverts	Red	Carotenoid	Spectrometry	Friedman et al. 2011
Icteridae	Agelaius xanthomus	Epaulet	Yellow	Carotenoid	Raman	Thomas et al. 2014
Icteridae	Agelaius xanthomus	Lesser coverts	Yellow	Carotenoid	Spectrometry	Friedman et al. 2011
Icteridae	Agelasticus thilius	Epaulet	Yellow	Carotenoid	Raman	Thomas et al. 2014
Icteridae	Agelasticus thilius	Lesser coverts	Yellow	Carotenoid	Spectrometry	Friedman et al. 2011
Icteridae	Amblyramphus holosericeus	Breast	Red	Carotenoid	Spectrometry	Friedman et al. 2011
Icteridae	Cacicus cela		Yellow	Carotenoid	Chromatography	Friedman et al. 2014
Icteridae	Cacicus cela cela	Rump	Yellow	Carotenoid	Spectrometry	Friedman et al. 2011
Icteridae	Cacicus chrysonotus chrysonotus	Rump	Yellow	Carotenoid	Spectrometry	Friedman et al. 2011
Icteridae	Cacicus chrysopterus	Rump	Yellow	Carotenoid	Raman	Thomas et al. 2014
Icteridae	Cacicus	Rump	Yellow	Carotenoid	Spectrometry	Friedman et

	chrysopterus					al. 2011
Icteridae	Cacicus haemorrhous		Red	Carotenoid	Chromatography	Friedman et al. 2014
Icteridae	Cacicus haemorrhous	Rump	Red	Carotenoid	Spectrometry	Friedman et al. 2011
Icteridae	Cacicus leucoramphus		Yellow	Carotenoid	Chromatography	Friedman et al. 2014
Icteridae	Cacicus melanicterus	Rump	Yellow	Carotenoid	Raman	Thomas et al. 2014
Icteridae	Cacicus melanicterus		Yellow	Carotenoid	Chromatography	Friedman et al. 2014
Icteridae	Cacicus melanicterus	Rump	Yellow	Carotenoid	Spectrometry	Friedman et al. 2011
Icteridae	Cacicus solitarius		Black	Not carotenoid	Chromatography	Friedman et al. 2014
Icteridae	Cacicus uropygialis		Red	Carotenoid	Chromatography	Friedman et al. 2014
Icteridae	Cacicus uropygialis uropygialis	Rump	Red	Carotenoid	Spectrometry	Friedman et al. 2011
Icteridae	Chrysomus icterocephalus	Breast	Yellow	Carotenoid	Spectrometry	Friedman et al. 2011
Icteridae	Chrysomus ruficapillus	Chin	Yellow	Carotenoid	Raman	Thomas et al. 2014
Icteridae	Chrysomus ruficapillus	Breast	Chestnut	Not carotenoid	Spectrometry	Friedman et al. 2011
Icteridae	Clypicterus oseryi	Retrices	Yellow	Carotenoid	Spectrometry	Friedman et al. 2011
Icteridae	Dives warszewiczi	Belly	Black	Melanin	Spectrometry, Microscopy	Shawkey et al. 2006
Icteridae	Dolichonyx oryzivorus		Black	Not carotenoid	Chromatography	Friedman et al. 2014
Icteridae	Dolichonyx oryzivorus	Nape	Buff	Not carotenoid	Spectrometry	Friedman et al. 2011
Icteridae	Dolychonyx oryzivorus	Belly	Black	Melanin	Spectrometry, Microscopy	Shawkey et al. 2006
Icteridae	Gymnomystax mexicanus	Breast	Yellow	Carotenoid	Spectrometry	Friedman et al. 2011
Icteridae	Hypopyrrhus pyrohypogaster	Belly	Red	Carotenoid	Spectrometry	Friedman et al. 2011
Icteridae	Icterus abeillei	Breast, Belly	Orange	Carotenoid	Spectrometry	Hofmann et al. 2007b
Icteridae	Icterus abeillei	Breast	Yellow	Carotenoid	Spectrometry	Friedman et al. 2011
Icteridae	Icterus auratus	Breast	Orange	Carotenoid	Spectrometry	Hofmann et al. 2007b
Icteridae	Icterus auratus	Breast	Orange	Carotenoid	Spectrometry	Friedman et al. 2011
Icteridae	Icterus auricapillus	Epaulet, Rump, Breast, Belly, Crown	Orange	Carotenoid	Spectrometry	Hofmann et al. 2007b
Icteridae	Icterus auricapillus	Breast	Yellow	Carotenoid	Spectrometry	Friedman et al. 2011
Icteridae	Icterus bonana	Epaulet, Rump, Breast, Belly	Tawny	Melanin	Spectrometry	Hofmann et al. 2007b
Icteridae	Icterus bonana	Breast	Tawny	Not carotenoid	Spectrometry	Friedman et al. 2011
Icteridae	Icterus bullockii	Breast	Orange	Carotenoid	Spectrometry	Friedman et al. 2011
Icteridae	Icterus bullockii	Rump, Breast, Belly	Orange	Carotenoid	Spectrometry	Hofmann et al. 2007b
Icteridae	Icterus cayanensis	Lesser coverts	Yellow	Carotenoid	Spectrometry	Friedman et al. 2011
Icteridae	Icterus cayanensis cayanensis	Epaulet	Yellow	Carotenoid	Spectrometry	Hofmann et al. 2007b
Icteridae	Icterus cayanensis periporphyrus	Epaulet	Tawny	Carotenoid and Melanin	Spectrometry	Hofmann et al. 2007b
Icteridae	Icterus cayanensis pyrrhopterus	Epaulet	Chestnut	Melanin	Spectrometry	Hofmann et al. 2007b
Icteridae	Icterus chrysater	Breast	Yellow	Carotenoid	Spectrometry	Friedman et

al. 2011

Icteridae	Icterus chrysater chrysater	Back, Rump, Breast, Belly, Crown	Yellow	Carotenoid	Spectrometry	Hofmann et al. 2007b
Icteridae	Icterus chrysater hondae	Back, Rump, Breast, Belly, Crown	Yellow	Carotenoid	Spectrometry	Hofmann et al. 2007b
Icteridae	Icterus chrysocephalus	Epaulet, Rump, Crown	Yellow	Carotenoid	Spectrometry	Hofmann et al. 2007b
Icteridae	Icterus chrysocephalus	Lesser coverts	Yellow	Carotenoid	Spectrometry	Friedman et al. 2011
Icteridae	Icterus croconotus	Breast	Orange	Carotenoid	Spectrometry	Friedman et al. 2011
Icteridae	Icterus cucullatus	Breast	Orange	Carotenoid	Spectrometry	Friedman et al. 2011
Icteridae	Icterus cucullatus igneus	Rump, Breast, Belly, Crown	Yellow-orange	Carotenoid	Spectrometry	Hofmann et al. 2007b
Icteridae	Icterus cucullatus nelsoni	Rump, Breast, Belly, Crown	Yellow-orange	Carotenoid	Spectrometry	Hofmann et al. 2007b
Icteridae	Icterus dominicensis	Lesser coverts	Yellow	Carotenoid	Spectrometry	Friedman et al. 2011
Icteridae	Icterus dominicensis dominicensis	Epaulets, Rump, Belly	Yellow	Carotenoid	Spectrometry	Hofmann et al. 2007b
Icteridae	Icterus dominicensis melanopsis	Epaulets, Rump	Yellow	Carotenoid	Spectrometry	Hofmann et al. 2007b
Icteridae	Icterus dominicensis northropi	Epaulets, Rump, Belly, Breast	Yellow	Carotenoid	Spectrometry	Hofmann et al. 2007b
Icteridae	Icterus dominicensis portoricensis	Epaulets, Rump	Yellow	Carotenoid	Spectrometry	Hofmann et al. 2007b
Icteridae	Icterus dominicensis prosthemelas	Epaulets, Rump, Belly, Breast	Yellow	Carotenoid	Spectrometry	Hofmann et al. 2007b
Icteridae	Icterus dominicensis prosthemelas	Breast	Chestnut	Melanin	Spectrometry	Hofmann et al. 2007b
Icteridae	Icterus fuertesi	Underparts	Tawny	Melanin and Carotenoid	Chromatography	Hofmann et al. 2007a
Icteridae	Icterus fuertesi	Epaulets, Rump, Belly, Breast	Tawny	Melanin and Carotenoid	Spectrometry	Hofmann et al. 2007b
Icteridae	Icterus fuertesi	Belly	Tawny	Not carotenoid	Spectrometry	Friedman et al. 2011
Icteridae	Icterus galbula		Orange	Carotenoid	Chromatography	Hudon 1991
Icteridae	Icterus galbula	Breast	Orange	Carotenoid	Spectrometry	Friedman et al. 2011
Icteridae	Icterus galbula galbula	Epaulets, Rump, Belly, Breast	Orange	Carotenoid	Spectrometry	Hofmann et al. 2007b
Icteridae	Icterus graceannae	Epaulets, Rump, Belly, Breast, Crown	Yellow-orange	Carotenoid	Spectrometry	Hofmann et al. 2007b
Icteridae	Icterus graceannae	Breast	Yellow	Carotenoid	Spectrometry	Friedman et al. 2011
Icteridae	Icterus graduacauda	Breast	Yellow	Carotenoid	Spectrometry	Friedman et al. 2011
Icteridae	Icterus graduacauda audubonii	Epaulets, Belly, Breast	Yellow	Carotenoid	Spectrometry	Hofmann et al. 2007b
Icteridae	Icterus graduacauda audubonii	Back, Rump	Yellow-olive	Carotenoid (reduced reflectance)	Spectrometry	Hofmann et al. 2007b
Icteridae	Icterus gularis	Breast	Yellow	Carotenoid	Spectrometry	Friedman et al. 2011
Icteridae	Icterus gularis gularis	Epaulets, Rump, Belly, Breast, Crown	Orange	Carotenoid	Spectrometry	Hofmann et al. 2007b

52

Icteridae	Icterus icterus	Belly	Orange	Carotenoid	Raman	Thomas et al. 2014
Icteridae	Icterus icterus	Breast	Orange	Carotenoid	Spectrometry	Friedman et al. 2011
Icteridae	Icterus icterus ridgwayi	Epaulets, Rump, Belly, Breast	Orange	Carotenoid	Spectrometry	Hofmann et al. 2007b
Icteridae	Icterus jamacaii	Breast	Orange	Carotenoid	Spectrometry	Friedman et al. 2011
Icteridae	Icterus jamacaii croconotus	Epaulets, Back, Rump, Belly, Breast, Crown	Orange	Carotenoid	Spectrometry	Hofmann et al. 2007b
Icteridae	Icterus jamacaii strictifrons	Epaulets, Rump, Belly, Breast, Crown	Orange	Carotenoid	Spectrometry	Hofmann et al. 2007b
Icteridae	Icterus laudabilis	Epaulet, Rump, Belly	Tawny-orange	Carotenoid	Spectrometry	Hofmann et al. 2007b
Icteridae	Icterus laudabilis	Belly	Chestnut	Melanin	Spectrometry	Hofmann et al. 2007b
Icteridae	Icterus laudabilis	Lesser Coverts	Orange	Carotenoid	Spectrometry	Friedman et al. 2011
Icteridae	Icterus leucopteryx	Breast	Yellow	Carotenoid	Spectrometry	Friedman et al. 2011
Icteridae	Icterus leucopteryx leucopteryx	Back, Rump, Belly, Breast, Crown	Yellow-olive	Carotenoid (reduced reflectance)	Spectrometry	Hofmann et al. 2007b
Icteridae	Icterus maculialatus	Epaulets, Rump, Belly, Breast	Yellow	Carotenoid	Spectrometry	Hofmann et al. 2007b
Icteridae	Icterus maculialatus	Breast	Yellow	Carotenoid	Spectrometry	Friedman et al. 2011
Icteridae	Icterus melanopsis	Lesser coverts	Yellow	Carotenoid	Spectrometry	Friedman et al. 2011
Icteridae	Icterus mesomelas	Breast	Yellow	Carotenoid	Spectrometry	Friedman et al. 2011
Icteridae	Icterus mesomelas mesomelas	Epaulets, Rump, Belly, Breast, Crown	Yellow-orange	Carotenoid	Spectrometry	Hofmann et al. 2007b
Icteridae	Icterus nigrogularis	Breast	Yellow	Carotenoid	Spectrometry	Friedman et al. 2011
Icteridae	Icterus nigrogularis nigrogularis	Epaulets, Back, Rump, Breast, Belly, Crown	Yellow	Carotenoid	Spectrometry	Hofmann et al. 2007b
Icteridae	Icterus northropi	Lesser coverts	Yellow	Carotenoid	Spectrometry	Friedman et al. 2011
Icteridae	Icterus oberi	Rump, Belly, Breast	Tawny	Carotenoid	Spectrometry	Hofmann et al. 2007b
Icteridae	Icterus oberi	Breast	Tawny	Not carotenoid	Spectrometry	Friedman et al. 2011
Icteridae	Icterus parisorum	Epaulets, Rump, Belly, Breast	Yellow	Carotenoid	Spectrometry	Hofmann et al. 2007b
Icteridae	Icterus parisorum	Breast	Yellow	Carotenoid	Spectrometry	Friedman et al. 2011
Icteridae	Icterus pectoralis	Epaulets, Rump, Belly, Breast, Crown	Orange	Carotenoid	Spectrometry	Hofmann et al. 2007b
Icteridae	Icterus pectoralis	Breast	Yellow	Carotenoid	Spectrometry	Friedman et al. 2011
Icteridae	Icterus portoricensis	Lesser coverts	Yellow	Carotenoid	Spectrometry	Friedman et al. 2011
Icteridae	Icterus prosthemelas	Lesser coverts	Yellow	Carotenoid	Spectrometry	Friedman et al. 2011
Icteridae	Icterus pustulatus	Breast	Yellow	Carotenoid	Spectrometry	Friedman et al. 2011
Icteridae	Icterus pustulatus formosus	Back	Orange	Carotenoid (reduced reflectance)	Spectrometry	Hofmann et al. 2007b

Icteridae	Icterus pustulatus formosus	Rump, Belly, Breast, Crown	Orange	Carotenoid	Spectrometry	Hofmann et al. 2007b
Icteridae	Icterus pyrrhopterus	Lesser coverts	Chestnut	Not carotenoid	Spectrometry	Friedman et al. 2011
Icteridae	Icterus spurius	Underparts	Chestnut	Melanin	Chromatography	Hofmann et al. 2007a
Icteridae	Icterus spurius	Epaulets, Rump, Belly, Breast	Chestnut	Melanin	Spectrometry	Hofmann et al. 2007b
Icteridae	Icterus spurius	Belly	Chestnut	Not carotenoid	Spectrometry	Friedman et al. 2011
Icteridae	Icterus wagleri	Breast	Yellow	Carotenoid	Spectrometry	Friedman et al. 2011
Icteridae	Icterus wagleri wagleri	Epaulets, Rump, Belly, Breast	Yellow-orange	Carotenoid	Spectrometry	Hofmann et al. 2007b
Icteridae	Icterus wagleri wagleri	Breast	Chestnut	Melanin	Spectrometry	Hofmann et al. 2007b
Icteridae	Macroagelaius imthurni	Axillaries	Yellow	Carotenoid	Spectrometry	Friedman et al. 2011
Icteridae	Macroagelaius subalaris	Axillaries	Chestnut	Not carotenoid	Spectrometry	Friedman et al. 2011
Icteridae	Molothrus aeneus	Belly	Black	Melanin	Spectrometry, Microscopy	Shawkey et al. 2006
Icteridae	Molothrus ater	Belly	Black	Melanin	Spectrometry, Microscopy	Shawkey et al. 2006
Icteridae	Molothrus bonariensis	Belly	Black	Melanin	Spectrometry, Microscopy	Shawkey et al. 2006
Icteridae	Molothrus rufoaxillaris	Belly	Black	Melanin	Spectrometry, Microscopy	Shawkey et al. 2006
Icteridae	Ocyalus latirostris	Retrices	Yellow	Carotenoid	Spectrometry	Friedman et al. 2011
Icteridae	Psarocolius angustifrons	Retrices	Yellow	Carotenoid	Spectrometry	Friedman et al. 2011
Icteridae	Psarocolius atrovirens	Retrices	Yellow	Carotenoid	Spectrometry	Friedman et al. 2011
Icteridae	Psarocolius decumanus	Retrices	Yellow	Carotenoid	Spectrometry	Friedman et al. 2011
Icteridae	Psarocolius guatimozinus	Retrices	Yellow	Carotenoid	Spectrometry	Friedman et al. 2011
Icteridae	Psarocolius montezuma		Yellow	Carotenoid	Chromatography	Friedman et al. 2014
Icteridae	Psarocolius montezuma	Retrices	Yellow	Carotenoid	Spectrometry	Friedman et al. 2011
Icteridae	Psarocolius viridis	Retrices	Yellow	Carotenoid	Spectrometry	Friedman et al. 2011
Icteridae	Psarocolius wagleri		Yellow	Carotenoid	Chromatography	Friedman et al. 2014
Icteridae	Psarocolius wagleri	Retrices	Yellow	Carotenoid	Spectrometry	Friedman et al. 2011
Icteridae	Pseudoleistes guirahuro	Lesser coverts	Yellow	Carotenoid	Spectrometry	Friedman et al. 2011
Icteridae	Pseudoleistes virescens	Lesser coverts	Yellow	Carotenoid	Spectrometry	Friedman et al. 2011
Icteridae	Quiscalus major	Belly	Black	Melanin	Spectrometry, Microscopy	Shawkey et al. 2006
Icteridae	Quiscalus mexicanus	Belly	Black	Melanin	Spectrometry, Microscopy	Shawkey et al. 2006
Icteridae	Scaphidura oryzivora	Belly	Black	Melanin	Spectrometry, Microscopy	Shawkey et al. 2006
Icteridae	Sturnella bellicosa		Red	Carotenoid	Chromatography	Friedman et al. 2014
Icteridae	Sturnella bellicosa	Breast	Red	Carotenoid	Spectrometry	Friedman et al. 2011
Icteridae	Sturnella defilippii	Breast	Red	Carotenoid	Spectrometry	Friedman et al. 2011
Icteridae	Sturnella lilianae	Breast	Yellow	Carotenoid	Spectrometry	Friedman et al. 2011
Icteridae	Sturnella loyca	Breast	Red	Carotenoid	Spectrometry	Friedman et al. 2011

Icteridae	Sturnella magna		Yellow	Carotenoid	Chromatography	Friedman et al. 2014
Icteridae	Sturnella magna	Breast	Yellow	Carotenoid	Spectrometry	Friedman et al. 2011
Icteridae	Sturnella militaris	Belly	Red	Carotenoid	Raman	Thomas et al. 2014
Icteridae	Sturnella militaris		Red	Carotenoid	Chromatography	Friedman et al. 2014
Icteridae	Sturnella militaris	Breast	Red	Carotenoid	Spectrometry	Friedman et al. 2011
Icteridae	Sturnella neglecta		Yellow	Carotenoid	Chromatography	Friedman et al. 2014
Icteridae	Sturnella neglecta	Breast	Yellow	Carotenoid	Spectrometry	Friedman et al. 2011
Icteridae	Sturnella neglecta	Belly	Black	Melanin	Spectrometry, Microscopy	Shawkey et al. 2006
Icteridae	Sturnella superciliaris		Red	Carotenoid	Chromatography	Friedman et al. 2014
Icteridae	Sturnella superciliaris	Breast	Red	Carotenoid	Spectrometry	Friedman et al. 2011
Icteridae	Xanthocephalus xanthocephalus		Yellow	Carotenoid	Chromatography	Friedman et al. 2014
Icteridae	Xanthocephalus xanthocephalus	Breast	Yellow	Carotenoid	Spectrometry	Friedman et al. 2011
Icteridae	Xanthopsar flavus	Breast	Yellow	Carotenoid	Spectrometry	Friedman et al. 2011
Paridae	Cyanistes c. cyanus	Rump	Blue	Structural	X-ray scattering	Saranathan et al. 2012
Paridae	Cyanistes caeruleus	Crown	Blue	Structural	X-ray scattering	Saranathan et al. 2012
Paridae	Cyanistes caeruleus		Yellow	Carotenoid	Chromatography	Stradi 1998
Paridae	Cyanistes caeruleus			Carotenoid	Chromatography	Partali et al. 1987
Paridae	Cyanistes cyanus	Pileum	Blue	Structural	Microscopy	Auber 1957
Paridae	Parus ater			Carotenoid	Chromatography	Partali et al. 1987
Paridae	Parus major		Yellow	Carotenoid	Chromatography	Partali et al. 1987
Paridae	Parus major	Breast	Yellow	Carotenoid	Chromatography	Senar et al. 2008
Paridae	Parus spilonotus		Yellow	Carotenoid	Chromatography	Stradi 1999
Parulidae	Basileuterus lachrymosus	Belly	Yellow	Carotenoid	Raman	Thomas et al. 2014
Parulidae	Cardellina rubra	Belly	Red	Carotenoid	Raman	Thomas et al. 2014
Parulidae	Cardellina rubrifrons	Chin	Red	Carotenoid	Raman	Thomas et al. 2014
Parulidae	Geothlypis tolmiei	Belly	Yellow	Carotenoid	Raman	Thomas et al. 2014
Parulidae	Geothlypis trichas		Yellow	Carotenoid	Chromatography	McGraw et al. 2003
Parulidae	Leiothlypis ruficapilla		Yellow	Carotenoid	Chromatography	Brush and Johnson 1976
Parulidae	Leiothlypis virginiae		Yellow	Carotenoid	Chromatography	Brush and Johnson 1976
Parulidae	Myioborus pictus	Belly	Red	Carotenoid	Raman	Thomas et al. 2014
Parulidae	Myiothlypis bivittata	Belly	Yellow	Carotenoid	Raman	Thomas et al. 2014
Parulidae	Setophaga caerulescens	Back	Blue	Structural	X-ray scattering	Saranathan et al. 2012
Parulidae	Setophaga cerulea	Back	Blue	Structural	X-ray scattering	Saranathan et al. 2012
Parulidae	Setophaga coronata		Yellow	Carotenoid	Chromatography	McGraw 2006
Parulidae	Setophaga fusca	Belly	Orange	Carotenoid	Raman	Thomas et al. 2014
Parulidae	Setophaga palmarum		Yellow	Carotenoid	Chromatography	McGraw 2006
Parulidae	Setophaga petechia		Yellow	Carotenoid	Chromatography	McGraw et al. 2003

| Parulidae | Setophaga ruticilla | Yellow-orange | Carotenoid | Chromatography | McGraw 2006 |

* Literature Cited:

Auber L (1957) The structures producing "non-iridescent" blue colour in bird feathers. *Proceedings of the Zoological Society of London* **129**:455-486

Brush AH, and NK Johnson (1976) The evolution of color differences between Nashville and Virginia's warbler. *Condor* **78**:412-414.

Dyck J (1971) Structure and colour-production of the blue barbs of Agapornis roseicollis and Cotinga maynana. *Zeitschrift Zellforsch* **115**:17-29.

Friedman NR, KJ McGraw, and KE Omland (2014) Evolution of carotenoid pigmentation in caciques and meadowlarks (Icteridae): repeated gains of red plumage coloration by carotenoid C4-Oxygenation. *Evolution* **68**:791-801.

Friedman NR, LM Kiere, and KE Omland (2011) Convergent gains of red carotenoid-based coloration in the New World Blackbirds. *The Auk* **128**:678-687.

Hofmann CM, KJ McGraw, TW Cronin, and KE Omland (2007a) Melanin coloration in New World orioles I: carotenoid masking and pigment dichromatism in the orchard oriole complex. *Journal of Avian Biology* **38**:163–171

Hofmann CM, TW Cronin, and KE Omland (2007b) Melanin coloration in New World orioles II: ancestral state reconstruction reveals lability in the use of carotenoids and phaeomelanins. *J Avian Biol* **38**:172-181

Hudon J (1991) Unusual carotenoid use by the western tanager (Piranga ludoviciana) and its evolutionary implications. *Can J Zool* **69**:2311-230.

Lafountain AM, S Kaligotla, S Cawley, KM Riedl, SJ Schwartz, HA Frank, and RO Prum (2010) Novel methoxy-carotenoids from the burgundy-colored plumage of the Pompadour Cotinga Xipholena punicea. *Archives of Biochemistry and Biophysics* **504**:142-153.

McGraw KJ (2006) Mechanics of carotenoid-based coloration. In: *Bird Coloration Volume 1: Mechanisms and Measurements* (Eds. GE Hill and KJ McGraw). Cambridge: Harvard University Press

McGraw KJ, K Wakamatsu, AB Clark, and K Yasukawa (2004) Red-winged blackbirds use carotenoid and melanin pigments to color their epaulets. *Journal of Avian Biology* **35**:543–550

McGraw KJ, MD Beebee, GE Hill, RS Parker (2003) Lutein-based plumage coloration in songbirds is a consequence of selective pigment incorporation into feathers. *Comp Biochem Physiol B* **135**:689-696

Partali V, S Liaaen-Jensen, T Slagsvold, JT Lifjeld (1987) Carotenoids in food chain studies-II. The food chain of Parus spp. monitored by carotenoid analysis. *Comp Biochem Physiol* **87**:885-888.

Prum RO (2006) Anatomy, physics, and evolution of structural colors. In: *Bird Coloration Vol. 1: Mechanisms and Measurements*. Eds: GE Hill and KJ McGraw. Harvaryd University Press, Cambridge, MA

Prum RO, AM LaFountain, J Berro, MC Stoddard (2012) Molecular diversity, metabolic transformation, and evolution of carotenoid feather pigments in cotingas (Aves: Cotingidae). *J Comp Physiol B* **182**:1095-1116.

Prum RO, RH Torres, S Williamson, and J Dyck (1998) Coherent light scattering by blue feather barbs. *Nature* **396**:28-29.

Saranathan V, JD Forster, N Noh, S-F Liew, SGJ Mochrie, H Cao, ER Dufresne, and RO Prum (2012) Structure and optical function of amorphous photonic nanostructures from avian feather barbs: a comparative small angle X-ray scattering (SAXS) analysis of 230 bird species. *J R Soc Interface* **9**:2563-2580

Schmidt WJ and H Ruska (1962) Tyndallblau-struktur von federn im elektronenmikroskop. *Zeitschrift fur Zellforschung* **56**:693-708

Senar JC, JJ Negro, J Quesada, I Ruiz, and J Garrido (2008) Two pieces of information in a single trait? The yellow breast of the great tit (Parus major) reflects both pigment acquisition and body condition. *Behaviour* **145**:1195-1210.

Shawkey MD, ME Hauber, LK Estep, and GE Hill (2006) Evolutionary transitions and mechanisms of matte and iridescent plumage coloration in grackles and allies (Icteridae) *J R Soc Interface* **3**:777-786

Stavenga, DG, J Tinbergen, HL Leertouwer, and BD Wilts (2011) Kingfisher feathers - colouration by pigments, spongy nanostructures and thin films. *Journal of Experimental Biology* **214**:3960-3967.

Stradi R (1998) *The colour of flight: carotenoids in bird plumage*. Milan: Solei Gruppo Editoriale Informatico

Stradi R (1999) Pigmenti e sistematica degli uccelli. In: *Colori in volo: il piumaggio degli uccelli* (Eds: L Brambilla, G Canali, E Mannucci, R Massa, N Saino, R Stradi, G Zerbi). Milan: Univ devli Studi di Milano.

Thomas, DB, KJ McGraw, MW Butler, MT Carrano, O Madden, and HF James (2014) Ancient origins and multiple appearances of carotenoid-pigmented feathers in birds. *Proceedings of the Royal Society B* **281**:20140806

Volker O (1951) Rhodoxanthin un zeaxanthin als pigmente in den federn von Cotingiden. *Naturwissen* **24**:565.

Volker O (1952) Die lipochrome in der federn der Cotingiden. *J Ornithol* **93**:122-129.

Volker O (1961) The chemical characteristic of red lipochrome in bird feathers. *J Ornithol* **102**:430-438.

Chapter 2: Patterns of gene expression underlying melanin pigmentation in the Zebra Finch (*Taeniopygia guttata*)

Abstract

Melanin pigmentation is ubiquitous in the animal world, but we still lack a strong mechanistic understanding of how melanin production is regulated to produce variation across the integument. Here, we describe patterns of gene expression relating to melanin-based pigmentation in bird plumage. We take advantage of domestic pigment variation in a model species of bird, the Zebra Finch, to control for confounding expression variation relating to sex, body position, and population structure, in order to isolate gene expression changes relating to melanin production. We found several melanogenesis pathway genes that show consistent sex-biased expression across multiple patches and colors, likely indicating that their expression levels are not important for driving phenotypic differences. Overall, we found that differences in melanin production in feathers are associated with expression changes in relatively few genes of functional importance in melanogenesis, as well as relatively few changes in expression in the signaling pathways governing melanogenesis. Notably, expression in multiple signaling pathways in addition to the well-characterized Agouti/MC1R-activated signaling pathway are important in regulating phenotypic differences in melanin production.

Introduction

Identifying the mechanisms that give rise to phenotypic variation is necessary for understanding the processes that underlie the evolution of novel traits. Color patterns are excellent models of complex phenotypes that offer exciting opportunities to link genotype to phenotype (Hoekstra 2006). Integumentary pigmentation has a long history of ecological, behavioral, and biochemical study (Hill and McGraw 2006a,b), yet knowledge of the developmental and genetic mechanisms that produce color and shape it into patterns across the body remains incomplete. These gaps in our mechanistic understanding of pigment production and patterning in turn limit our understanding of how adaptive color variation is generated, and how that variation is distributed among sexes, age classes, and seasons to produce variation within species (Prum and Dyck 2003, Hoekstra 2006, Hubbard et al. 2010).

Of the various classes of integumentary pigments, work on evolutionary genetics is most advanced in melanins, which produce most earth-tone colors (including black, gray, brown, and yellowish-brown to reddish-brown). Melanins are the most common and well-studied pigment in birds and mammals, being present in nearly all species, and the core melanogenesis pathways seem conserved across deep evolutionary timescales (Hill and McGraw 2006a, Hoekstra 2006, Schiaffino 2010, D'Alba and Shawkey 2019). Previous work on the genetic basis for color variation has focused on identifying mutations in key pigmentation genes that are conserved in birds and mammals (Mundy 2005, Hoekstra 2006, Hubbard et al. 2010); these mutations generally have the effect of producing broad changes in melanin pigment levels across the integument. Functional coding mutations are known in a variety of relatively well-characterized melanogenesis pathway genes to produce variation in skin or coat color (Hoekstra 2006). Most notably, coding and regulatory mutations in melanocortin-1 receptor (MC1R) and its agonist, agouti signaling protein (ASIP), which induce a signaling cascade that controls regulation of melanogenesis, are now known from a variety of domestic and wild systems (Mundy 2005, Hoekstra 2006, Manceau et al. 2011, Lin et al. 2013, Jones et al. 2018). The activation of MC1R induces the production of eumelanin, a predominately black pigment, while inactivation of MC1R by ASIP induces the production of pheomelanin, a predominately reddish-brown pigment. Coding mutations in these genes are associated with large-scale changes in melanin expression across the integument in a variety of vertebrate species (Mundy 2005, Hoekstra 2006, Jones et al. 2018). However, coding mutations at candidate loci like MC1R and ASIP seem unrelated to pigmentation changes in specific plumage patches or plumage dichromatism (Cheviron et al. 2006, Hoffman et al. 2014, MacDougall-Shackleton et al. 2003).

Integumentary color is often not a discrete, static phenotype, and pigmentation varies at multiple scales within a species. For example, individual hairs or feathers can exhibit complex banding patterns. Colors of specific integumentary patches vary across the body to produce different patterns. Seasonal molts allow individual follicles to successively produce hairs or feathers of different colors. The sexes are often dimorphic in their coloration. Rather than coding mutations that alter the function of key melanogenesis genes, this variation seems to require spatial and/or temporal differences

in the regulation of pigment production. Within feathers, for example, regulatory control produces fine-scale variation in pigment production and deposition within feather follicles (Prum and Dyck 2003, Lin et al. 2013), while higher levels of signaling and developmental pattern formation produce variation in pigmentation across the body, molts, and sexes (Prum and Dyck 2003, Kimball 2006, Haupaix et al. 2018). Thus, coding-region mutations that affect pigmentation across the whole plumage are unlikely to account for much of the natural variation in pigmentation, and an additional focus on gene expression and other regulatory mechanisms is warranted. Gene expression has been associated with melanin variation in the integument (Ferreira et al. 2017, Dick et al. 2018), including in plumage (Emaresi et al. 2013, Poelstra et al. 2015, Abolins-Abols et al. 2018). Such comprehensive transcriptomic studies have so far been limited in phenotypic and taxonomic scope, making general predictions about the role of gene expression in the production of pigmentation variation unclear.

Here, we use Zebra Finches (Estrildidae: *Taeniopygia guttata*) as a model system to investigate pigmentation-related gene expression with two objectives: 1) to describe gene expression changes associated with a range of melanin-based plumage colors, and 2) to describe differences between the sexes in pigmentation-related gene expression. Zebra Finches are an extensively studied avian model species (Griffith and Buchanan 2010) with a well-annotated genome (Warren et al. 2010) whose plumage is well suited for study of pigmentation. Zebra Finch plumage is composed of several discrete melanin-based colors (McGraw and Wakamatsu 2004) – an orange cheek patch and brown flanks in males, and black, gray, and white plumage present in both sexes. In addition to the variation in melanin-based colors that are present in the Wild-type Zebra Finch, a number of pigment mutations in domestic Zebra Finches have been produced and selectively bred (Landry 1997). Of particular interest are Mendelian mutations that exhibit discrete variation in color, in the expression of specific plumage patches, and in the expression of sexual dimorphism in plumage color (**Figure 1**).

These color mutations represent a powerful system for identifying the mechanisms of plumage variation because they allow us to control for important confounding factors that are potentially correlated with differences in pigmentation. Comparisons of different plumage patches within an individual confounds pigmentation

60

variation with variation in feather shape and position across the body. The domestic color mutants allow for a comparison of colors across Wild-type and mutant lines expressed in the same plumage patch (cheek – **Figure 1**), however, this comparison potentially confounds pigmentation variation with population structure among different inbred captive lines (Hoffman et al. 2014). In this study, we used a sampling design that controls for these confounding variables by combining the two types of comparison. We test for differential expression between two colors within Wild-type Finches, and across different finch mutations that express those two colors in the same plumage patch. The union of these two sets of differentially expressed genes represents a candidate set of genes whose expression is related to pigmentation alone, and is not confounded by expression differences relating to body position or population structure (**Figure 1**). For our first objective, we compare patterns of gene expression among two plumage colors expressed in male Zebra Finches – orange and black - and three plumage colors expressed in females – black, gray, and white.

For our second objective, we characterize sex-biased gene expression in multiple plumage patches and colors. Sex-biased gene expression is pervasive (Ellegren and Parsch 2007), and could potentially confound attempts to relate gene expression to pigmentation variation when comparing across the sexes (sensu Dick et al. 2018). A direct comparison of gene expression in sexually dichromatic plumage cannot necessarily distinguish between gene expression differences relating to pigmentation and sex-biased expression in those tissues that is unrelated to pigmentation. Previous transcriptomic studies of feather coloration have focused on male plumage (Emaresi et al. 2013, Poelstra et al. 2015, Abolins-Abols et al. 2018), so the extent to which sex-biased expression could affect comparisons of pigmentation is relatively unexplored. We attempt to separate the effects of sex-biased expression from pigmentation-related expression by testing for differential expression between the sexes in several plumage patches (white face feathers, buff belly feathers, black rump feathers, and black cheek feathers) that are phenotypically similar between the sexes. These tests should reveal sex-biased expression in genes that do not directly contribute to pigmentation variation. We evaluate whether such differences occur in known melanogenesis genes, and then account for that expression variation while comparing orange male plumage to gray female plumage.

Additionally, we compare how the sexes differ in regulating orange vs gray with how orange vs gray plumage is regulated within the male plumage. Taken altogether, our analyses here will present a descriptive look at the gene regulation of melanin pigmentation in Zebra Finch in different contexts.

Methods

We obtained Zebra Finches from commercial wholesalers. Birds were group housed and maintained by animal care staff at UIUC (IACUC Protocol #14134) and UMT (AUP Protocol #039-15) light/dark cycle. After at least 48hrs recovery from transport stress, we stimulated molt by manually plucked ten feathers from a small contiguous area in the relevant plumage patches of each individual. We determined through preliminary experiments that an optimal time for feather regrowth was eleven days, at which point the tip of the growing feather was just visible in the sheath, but the pigmented part of the feather was still growing and thus pigment production is still occurring. At the eleven day mark, birds were anesthetized with isoflurane and euthanized by cervical dislocation. The regrowing feather tissues were immediately removed as a contiguous patch, including the developing feathers, feather follicles, and skin surrounding them, but excluding mature feathers. Pectoral muscle tissue samples were also removed, and both feather and muscle tissues were snap frozen in liquid nitrogen. All tissues were subsequently stored at -80°C until extraction.

We extracted total RNA from frozen developing feather tissues using TRI Reagent (Sigma-Aldrich, St. Louis, MO, USA) following manufacturer protocols. We generated Illumina sequencing libraries following the Lohman et al. (2016) Tagseq protocol. We modified this protocol by including a custom oligo with a longer degenerate sequence for detecting PCR duplicates (sequence: ACC CCA TGG GGC TAC ACG ACG CTC TTC CGA TCT NNMWNN GGG). TagSeq libraries were multiplexed with Illumina index adapters and randomly divided into two normalized pools containing 29 individual libraries each. Each pool was sequenced on one lane of 100 nucleotide single-read Illumina HiSeq 2500 at the Genomic Sequencing and Analysis Facility at University of Texas at Austin.

After demultiplexing, we used custom perl scripts (Matz 2017) and the FASTX-Toolkit (http://hannonlab.cshl.edu/fastx_toolkit/index.html) to remove PCR duplicates, trim adapter sequences, discard reads shorter than 20 nucleotides, trim poly-A tails, and set a minimum quality score of 20. We aligned reads to the Zebra Finch reference genome (assembly taeGut3.2.4, Warren et al. 2010) using bwa-mem v0.7.15-r1140 (Li and Durbin 2009, Li 2013). We used featureCounts v.1.5.2 (Liao et al. 2014) to generate read count tables for each library. We then normalized counts by library size for analysis in R with the R package edgeR v.3.12.1 (Robinson et al. 2010, McCarthy et al. 2012) functions *calcNormFactors* and *cpm*.

We tested for differential gene expression in normalized read counts between thirteen different pairs of tissues (**Table 1**), using the edgeR function *exactTest* and a False Discovery Rate of 0.05. First, we tested for differential expression among three plumage colors, comparing gray vs. white, gray vs. black, and orange vs. black. For each of these color comparisons, we tested for differential gene expression separately in multiple pairs of plumage patches that express those colors (**Table 1**, **Figure 1**). We then summarized gene expression for these three color comparisons by identifying the genes that were a) significantly differentially expressed in each individual paired comparison, and b) had a $\log_2$ fold change in the same direction for each significant individual test. These genes represent those that are differentially expressed in relation to color, but not plumage patch or morph (**Figure 1**). Second, we tested for differential gene expression between the sexes in four plumage patches that are phenotypically similar in each sex (**Table 1**). We tested these four sets of differentially expressed genes for gene ontology (GO) enrichment by converting Gene IDs to Ensembl Gene IDs with the db2db function on the biological Database network (Mudunuri et al. 2009), and using testing for enrichment with g:Profiler (Reimand et al. 2016) with *Taeniopygia guttata* as the organism. Third, we tested for differential gene expression between orange and gray plumage both within male plumage and between the sexes (**Table 1**).

We mapped patterns of differential gene expression onto the melanogenesis pathway. To identify melanogenesis genes and interactions, we used the KEGG melanogenesis network for *Taeniopygia guttata* (Kanehisa and Goto 2000, Kanehisa et al. 2016) with the addition of several candidate genes and interactions identified from the

literature (**Table 2**). We calculated log$_2$ fold change and differential gene expression in melanogenesis genes for each of the paired comparisons as above, conditioning the False Discovery Rate correction on the number of genes in the melanogenesis network alone rather than the whole transcriptome.

Results

After controlling for the potentially confounding factors of body position and population structure, we were able to relate the expression of a few key genes to differences in plumage color. The number and identity of differentially expressed genes implicated in color differences varied according to the specific colors that were compared. Four genes were differentially expressed across all orange vs. black patch comparisons, and two were differentially expressed across gray vs. black patch comparisons. We did not detect any differentially expressed genes that were shared among all gray and white patch comparisons and the genome-wide significance threshold (FDR < 0.05, **Table 3**). The two genes differentially expressed in each gray vs. black comparison were melanogenesis-related genes tyrosinase related protein 1 (TYRP1) and oculocutaneous albinism II (OCA2). These genes were similarly upregulated in black relative to orange feathers. Two additional genes were significantly upregulated in black relative to orange feathers: hematopoietic prostaglandin D synthase (HPGDS) and glycerol-3-phosphate dehydrogenase 1-like protein (GPD1L). We summarized differential expression between plumage colors for melanogenesis pathway genes in **Table 4** and **Figure 2**. In addition to the two melanogenesis genes significant at FDR < 0.05, we added genes significant at uncorrected $p < 0.05$ to **Figure 2**.

Sexes differed significantly in the expression of 17 to 141 genes in four patches that are phenotypically similar in each sex (FDR < 0.05, **Table 3**). Significantly enriched GO terms in each of these sets of differentially expressed genes are summarized in **Table 5**. There were no GO terms that were significantly overrepresented among the genes that were differentially expressed between the sexes in black rump feathers. Similarly, there was little consistency among significantly enriched GO terms across plumage patch comparisons: no term was significantly enriched in more than one comparison. Overlap between the four differentially expressed gene sets is shown in **Figure 3**. Consistent with

the GO enrichment analysis, the specific genes that differed in expression between the sexes were largely idiosyncratic across plumage patches. No single gene differed in expression across all four comparisons, and the majority of differentially expressed genes (204/257, 79.4%) were unique to a single patch. We summarized differential expression between the sexes in these four patches for melanogenesis pathway genes in **Table 6** and **Figure 4**. In addition, we highlighted genes that had the same direction of $\log_2$ fold change across all four comparisons, regardless of significance of expression differences, in **Figure 4**. In genes with that were significantly differentially expressed in two or more patch comparisons, the fold change had the same direction. Several genes also had consistent fold change directions across all four comparisons, but the magnitude of fold changes were small and expression did not significantly differ in any patch.

Gene expression differences between orange and gray plumage within and between the sexes is summarized in **Figure 5** and **Table 7**. At a FDR of 0.05, two genes were differentially expressed between orange male cheeks and gray female cheeks: the signaling ligand KIT, and GNAQ, a member of the Gα protein family. Both are downregulated in female gray cheeks relative to orange male cheeks. Similarly, at a FDR of 0.05 just two genes were differentially expressed between orange male cheeks and gray male crown feathers: OCA2 and TYRP1, with both upregulated in gray relative to orange plumage. Additional genes significantly differentially expressed between orange and gray plumage are noted in **Figure 5** and **Table 7**.

Discussion

Pigmentation-related gene expression

We explored patterns of gene expression relating to pigmentation in Zebra Finches using a sampling design that isolates gene expression patterns associated with pigmentation differences from those due to the confounding factors of body position and population structure (**Figure 1**). These strict comparisons yielded just four significantly differentially expressed genes among three color comparisons (TYRP1, OCA2, HPGDS, and GPD1L; FDR < 0.05). In addition to the four genes significant at FDR < 0.05, we examined patterns of gene expression in known melanogenesis genes that were significant at the uncorrected significance threshold ($p < 0.05$; **Figure 2**, **Table 4**). This

more liberal approach does not control for multiple testing, so the potential for false positives is increased. However, we restricted this approach to the subset of genes associated with melanogenesis, and found several additional candidates with strong functional hypotheses for effecting pigmentation.

All three of our color comparisons involve upregulation of black eumelanin content, whether relative to no pigment (gray vs. white), relative to less eumelanin (black vs. gray), or relative to reddish-brown pheomelanin (black vs. orange). Both types of melanin are constructed from tyrosine as a precursor through a series of enzymatic steps in the melanosome organelle (D'Alba and Shawkey 2019). An initial rate-limiting step converts tyrosine to the intermediate dopaquinone with the enzyme tyrosinase (TYR). Dopaquinone is further converted into either eumelanin, through the actions of the enzymes tyrosinase-related protein 1 (TYRP1) and dopachrome tautomerase (DCT), or into pheomelanin in the presence of cysteine. Of these three enzymes, only TYRP1 shows significant differential expression in our color comparisons. TYRP1 is significantly upregulated (FDR < 0.05) in black plumage relative to both orange and gray pigmentation, consistent with the production of more eumelanin in those patches (McGraw and Wakamatsu 2004). However, the enzyme actions of TYR, not TYRP1, are thought to be rate-limiting step in melanogenesis. Moreover, TYRP1 is not known to be a regulator of switching from pheomelanin production to eumelanin production.

Regulation of which melanin type is produced is largely a function of the melanosome concentrations of TYR and cysteine (which is essential for pheomelanin but not eumelanin): higher TYR or lower cysteine concentrations lead to higher production of eumelanin (Smit et al. 1997). Expression differences in two membrane-bound transporters may explain pigmentation differences despite no differential regulation of TYR. The gene oculocutaneous albinism II (OCA2) is a membrane-bound protein localized to the melanosome that has been implicated in regulating melanin synthesis through post-translational modification of melanogenesis enzymes, enzyme transport into the melanosome, and regulation of melanosome pH for optimal enzyme function (Potterf et al. 1998, Manga et al. 2001, Chen et al. 2002, Toyofuku et al. 2002, Visser et al. 2014). OCA2 is significantly upregulated (FDR < 0.05) in black plumage relative to both orange and gray plumage. Upregulation of OCA2 may thus increase the concentration of TYR in

the melanosome and alter melanosome physiological conditions, preferentially shifting production of pheomelanin to eumelanin in feathers with black plumage. The upregulation of OCA2 in black feathers may in turn be driven by a downregulation in black feathers of the gene CTCF, which inhibits OCA2. Cysteine concentrations in the melanosome may be regulated in part by the gene SLC7A11, a membrane-bound cysteine transporter in melanocytes (Chintala et al. 2005). SLC7A11 is downregulated in black plumage relative to orange feathers (uncorrected $p < 0.05$), putatively reducing cysteine concentrations and favoring eumelanogenesis over phaeomelanogenesis (Smit et al. 1997). Since gray feathers contain reduced concentrations of eumelanin but no pheomelanin, it is therefore not surprising that SLC7A11 does not show differential expression in comparisons of gray plumage.

Transcription of melanogenesis enzymes, as well as OCA2, is regulated by the gene microphthalmia-associated transcription factor (MITF; Cheli et al. 2009). MITF is additionally known to target dozens of other genes, and is itself regulated by multiple signaling cascades (Cheli et al. 2009). MITF was not differentially expressed in any of our color comparisons, which might not be surprising for a highly connected hub gene (Poelstra et al. 2015). However, we did see expression differences in the start of the signaling cascades that regulate MITF. MITF is regulated by at least three signaling cascades in the melanocyte: Wnt/β-catenin signaling, c-AMP dependent signaling initiated by MC1R, and MAPK signaling initiated by the receptor KIT. We saw upregulation of the KIT receptor in black feathers, which could amplify the MAPK signaling pathway that regulates MITF expression. We did not see any significant differential regulation in MC1R-activated signaling pathway. The ligand NDP, which is an activator of Wnt/β-catenin signaling (Hendrickx and Leyns 2008), was downregulated in black relative to orange feathers. FZD4, one of the frizzled class of receptors that activates Wnt/β-catenin signaling, is upregulated in black feathers relative to gray, but also upregulated in white relative to gray. Another Wnt receptor, FZD9, is downregulated in black feathers relative to gray. Unfortunately, we lack concrete hypotheses for how these expression differences in signaling cascades may act through the complicated hub of MITF expression regulation to influence the production of melanin.

Two additional genes were significantly upregulated (FDR < 0.05) in black relative to orange feathers: hematopoietic prostaglandin D synthase (HPGDS) and glycerol-3-phosphate dehydrogenase 1-like protein (GPD1L). HPGDS is a synthase that produces prostaglandin D_2 (PGD2). It is a transcriptional target of MITF, and has been linked to inflammatory responses generated by mast cells (Morii and Oboki 2004). HPGDS-produced PGD2 also regulates expression of SOX9 (Moniot et al. 2011), which in turn is another regulator of MITF transcription (Passeron et al. 2007). HPGDS may thus be expressed in Zebra Finch feathers as either a pleiotropic by-product of the regulation of MITF, or as a part of a regulatory feedback loop governing MITF expression. While HPGDS expression has been associated with pigmentation variation before (Poelstra et al. 2015), we are unaware of a direct mechanistic connection to the production of melanin, nor a functional hypothesis for why HPGDS would be linked to production of black relative to orange feathers. GPD1L is a poorly characterized protein with homology to phosphorylating enzymes. It has been linked to cardiac arrhythmia and to hypoxia-induced gene regulation (London et al. 2007, Valdivia et al. 2009, He et al. 2017), but we are unaware of any previous link to pigmentation.

In summary, we found that discrete variation in melanin pigmentation is associated with gene expression changes in several known melanogenesis-related genes. Support for differential gene expression is strongest in the enzymes that synthesize melanin, and the membrane-bound transporters that regulate melanosome contents and function. We found few expression differences at the top of signaling pathways that regulate expression of those genes, and no expression differences in the intermediate steps of those pathways. We found fewer melanogenesis genes were differentially expressed than in previous whole transcriptome studies. For example, Poelstra et al. (2015) compared gene expression in gray and black plumage of crows and found differential expression at all levels of the melanogenesis pathway, notably in most of the transcriptional targets of MITF (but not MITF itself). Our results suggest that pigmentation variation can be regulated in a more fine-scale fashion, with fewer regulatory inputs and fewer regulatory targets of MITF showing differential expression. It is also plausible that the divergence between crow species is much older than the population structure generated by recent domestication in Zebra Finches, resulting in

elevated divergence in gene expression that is not strictly necessary to generate the pigmentation differences observed. Additional study of expression in the whole melanogenesis pathway across more species will be necessary to understand what common patterns of gene expression may be driving pigmentation.

Our results stand in contrast to previous work in two additional ways. First, we found that, of 58 genes differentially expressed between white and gray plumage (uncorrected $p < 0.05$), only one is associated with melanogenesis. Previous studies comparing white to black integumentary expression found numerous melanogenesis genes are downregulated in white, consistent with a lack of production of melanin (Fan et al. 2013, Zhang et al. 2015, Song et al. 2017). White feathers, which lack pigment, can be produced by either downregulating melanin production, or by a failure of melanocytes to migrate from the feather follicle into the developing feather (Lin et al. 2013). ASIP has been identified in multiple systems as a suppressor of melanin production (Lin et al. 2013, Jones et al. 2018), but we did not detect any differential regulation of ASIP in any of our color comparisons. Thus, a plausible alternative biological explanation for our results is that melanin-producing melanocytes are present in our white feather tissues, thus displaying no significant differences from pigmented feathers in melanin gene expression, but these melanocytes fail to migrate into the developing feather. This hypothesis can be directly tested by identifying the location of melanocyte progenitors in these feather follicles, and quantifying pigment content in the follicles outside of the developing feather. If confirmed, future work could identify genes associated with melanocyte differentiation and migration, and test whether those genes are differentially expressed in our transcriptomic data.

A final difference from past studies is, as noted above, the lack of differential expression of MC1R and its antagonist ASIP. These genes have been implemented in many systems as controlling the general production of melanin, or controlling the production of eumelanin vs. pheomelanin (Mundy 2005, Hoekstra 2006, Manceau et al. 2011, Lin et al. 2013, Jones et al. 2018). Our failure to find differential expression in MC1R and ASIP is possibly explained by those genes acting through pulses of expression during feather development, or fine-scale differences in localized expression, that are difficult to detect in our samples. However, we note that previous studies with

similar methods have found detectable expression differences in these genes associated with pigmentation (*sensu* Poelstra et al. 2015). While the frequent importance of MC1R and ASIP to pigmentation variation is not in doubt, their ubiquity is perhaps surprising, given the complex regulation of MITF. Multiple signaling cascades and feedback loops operate on MITF, which itself regulates dozens of targets including those related to pigment production (Cheli et al. 2009). Our finding that regulation of the MAPK and Wnt signaling pathways is associated with pigmentation, but not MC1R, suggests that the complicated regulation of melanin-producing genes potentially gives the system flexibility to regulate its pigmentation output through different signaling inputs. Indeed, several additional recent studies have identified variation in these other signaling pathways as producing melanin variation (Vickrey et al. 2018, **Chapter 3**). However, additional study will be needed to untangle the complicated web of MITF interactions.

Sex-biased expression in pigmentation pathways

We further explored patterns of pigment gene expression by examining whether Zebra Finch sexes differ in their regulation of pigmentation. However, any comparison between sexually dimorphic phenotypes confounds phenotypic expression with general sex differences in gene expression that are expected to be pervasive (Ellegren and Parsch 2007). Here, we initially characterized sex-biased gene expression in plumage that is phenotypically similar between the sexes, in order to identify any genes that may show general sex-bias across the plumage and whether they occupy potentially functionally significant roles in generating pigmentation. Then we characterized gene expression changes in a sexually dimorphic patch, and compared it with the same color variation within a sex to determine if there is significant sex-bias in the melanogenesis network.

We examined sex-biased gene expression in four plumage patches of three different colors that are phenotypically similar between the sexes (**Table 1**), and found little overlap in the genes that were differentially expressed across comparisons. Instead, the majority of differentially expressed genes were unique to each patch (**Figure 3**). In addition, the differentially expressed gene sets for each patch did not share any enrichment of GO terms with other patches (**Table 5**). These results indicate that sex-biased expression is largely patch- or color-specific, and evaluating any functional

significance of these expression differences between the sexes is difficult. However, when sex-biased expression was mapped onto the melanogenesis network (**Figure 4**), interesting patterns emerge.

Notably, we found no significant sex bias (FDR < 0.05) in the expression of the melanin-synthesizing enzymes (TYR, TRYP1, DCT), nor in the membrane-bound transporters that regulate the physiological conditions within the melanosome (OCA2, SLC7A11). These results suggest that there is not sexual dimorphism in the direct synthesis of melanin. However, we do find sex-biased expression differences in the regulatory pathways controlling expression of those genes. For example, we found significant sex-biased gene expression in some of the ligand/receptor pairs at the top of the MITF-regulating signal transduction cascades. However, the specifics of these sex-biased expression patterns varied among patches in several ways. First, sex-biased expression in these ligand/receptor pairs is limited to one or two patches out of the four compared (**Figure 4**), limiting the generality of these findings. Second, some of the expression differences between ligand and receptor act in counterintuitive directions. For example, the ligand NDP was significantly downregulated in male black rump feathers, but its receptor FZD4 was upregulated in males in that same patch, which does not lead to a clear prediction for how that pathway may be activated in a sex-biased fashion. Thus, while we found sex-biased expression in a number of melanogenesis genes, we have little evidence for most of those expression patterns having any functional significance on pigmentation in these patches. None of the melanogenesis genes that were significantly differentiated among plumage colors (**Figure 2**) are sex-biased in their expression in more than two patches (**Figure 4**). These results indicate that most of the sex-biased expression patterns found here may have little consistent and confounding effect on comparisons of pigmentation variation across the sexes.

More revealing, however, are the small number of genes differentially expressed between the sexes in multiple patches. Notably, these sex-biased genes shared across multiple plumage colors are concentrated at intermediate steps in the signaling pathways regulating MITF. We found that GNAQ, a member of the Gα protein family, was significantly upregulated in males in white face, black cheek, and black rump feathers, and marginally upregulated in males in buff belly feathers (log$_2$ fold change = 0.771,

uncorrected $p = 0.089$). GNAQ and other Gα proteins function are not necessary for Wnt-induced signaling, but enhance those signals, and regulation of multiple targets of Wnt signaling may be mediated by inclusion of different Gα proteins in the signal cascade (Liu et al. 2005, Regard et al. 2011). Gα proteins thus are functionally significant as a potential branching point in Wnt-induced signaling. Differential regulation of Gα proteins has been previously implicated in inducing sexual dimorphism in downstream signaling pathway targets (Murphy et al. 2001), highlighting the potential importance of this signal branching point. This makes Wnt/β-catenin signaling a good candidate pathway for future investigation of sexual dimorphism in pigmentation. While sex-bias in GNAQ expression is not associated with sexual dimorphism in color in the patches examined here, constitutive upregulation of GNAQ in males could potentially produce sexually dimorphism in the response to different Wnt or NDP signals in other patch- or color-specific contexts.

We observed similar patterns in the other MITF-regulating signaling pathways. An intermediate gene in the MAPK signaling pathway, HRAS, is significantly downregulated in males in buff belly and black rump patches. Notably, differentially expressed genes in buff belly feathers show enrichment for the GO term 'negative regulation of MAPK', which could potentially act by targeting this step in the cascade. However, HRAS does not show significant sex-biased expression in white face or black cheek feathers. Additionally, it is not known whether HRAS can induce differential regulation of MAPK downstream targets, as in GNAQ. Likewise, we observed consistent upregulation of CREB3, an intermediate in the c-AMP signaling pathway, in males in all four patch comparisons. CREB3 is a transcription factor activated by this path, but whether its role in regulating MITF and other CREB-family steps could serve as a branch-point in the signaling pathway (as in GNAQ) is not clear.

These intermediate pathway genes, because they are sex biased across the range of patches examined here, may represent genes that are generally sex-biased across the plumage, independent of color phenotype. However, pigmentation genes that are sex-biased in these undifferentiated patches could drive sexual dimorphism in different patch- or color-specific signaling contexts, especially when these genes occupy pathway positions of functional significance such as branch points or rate-limiting steps (Flowers

72

et al. 2007, Alvarez-Ponce et al. 2009). Sexual dimorphism has evolved repeatedly in the Estrildid finches, with many close relatives of Zebra Finch being sexually monomorphic (Clement 1993, Forshaw and Shephard 2012, Gomes et al. 2016). While sex differences in plumage color are regulated by circulating hormones in many avian species (Kimball 2006), this is not the case for Zebra Finches (Adkins-Regan et al. 1990; E Adkins-Regan, pers. comm.). Mechanisms of hormonal regulation of sexual dimorphism evolve substantially across birds and other taxa (Kimball 2006, Hayes 1997). One hypothesis for how sexual dichromatism can be regulated in species without hormone-mediated pigmentation is via sex-specific transcriptomic responses in feather follicles during pigment deposition. In these cases, the signals that induce pigmentation are not dimorphic, but melanocytes differ between the sexes in their response to those signals. The sex-biased genes identified here could serve as candidate loci for such sex-specific response in future research.

In addition to sex-biased expression in phenotypically monomorphic patches, we examined expression differences between wild-type Zebra Finch cheeks (orange in males, gray in females) and between orange and gray patches within wild-type males (**Table 1**). Like our previous color comparisons, these within- and across-sex comparisons involve upregulation of eumelanin content, where the gray cheek and crown feathers pigmented with black eumelanin are compared to orange cheeks pigmented with reddish-brown pheomelanin. In the comparison of orange vs gray within male plumage, there are clear functional hypotheses for many of melanogenesis gene expression differences found, even with the confounding variation of comparing across different positions on the body. OCA2 and TYRP1 are upregulated in gray relative to orange plumage (FDR < 0.05), as expected if they are contributing to an increased production of eumelanin (see previous discussion). The signaling ligands NDP and ASIP are downregulated in gray ($p < 0.05$), as expected for ASIP as a known antagonist to eumelanin production (Lin et al. 2013). LEF1, a transcription factor affecting MITF and OCA2, is also downregulated in gray ($p < 0.05$).

The contrast between the within-sex and between sex comparison of orange vs gray is notable. At a FDR of < 0.05, there was no overlap in significantly differentially expressed melanogenesis genes between these two comparisons (**Table 7**). Between the

73

sexes, the KIT signaling receptor was associated with the difference in cheek color but no other signaling ligand or receptor (**Table 7**, FDR < 0.05). TYR is the only melanogenesis enzyme significantly differentially expressed (p < 0.05, **Figure 5**), and no transport proteins differed. Oddly, we found TYR was downregulated in gray female cheeks, counterintuitive to its known function of regulating eumelanin production over pheomelanin production through higher concentrations (Smit et al. 1997). It is possible that other expression changes occur in females relative to males that compensate for this while maintaining TYR's function. More investigation is needed. Several of the remaining differences in expression between the sexes - GNAQ, HRAS, and CREB3 (p < 0.05, **Table 7**) – are the same genes that had sex-biased expression in many of the monomorphic patches examined. Thus, they are unlikely to have functional significance in producing the phenotypic differences in gray vs orange plumage, unless as noted above they induce significant branch points in the signaling cascade (as is plausible at least for GNAQ).

We make two notable conclusions from the comparison of orange vs gray within and between the sexes. First, in agreement with the other color comparisons made in the previous section, it seems that the complex signaling that regulates MITF and other melanin-producing genes offers considerable flexibility. The sets of signaling inputs that are differentially expressed are not only different between orange vs gray and the other color comparisons, but are also different when comparing orange vs gray within males vs between the sexes. This suggests that signal inputs that drive melanogenesis differ between the sexes to produce the same phenotypic results. Additionally, it is noteworthy that only one melanogenesis enzyme or transporter protein is regulated differently in males vs female cheeks, despite their color differences, and this difference in TYR expression does not align with its known function in other contexts to produce more eumelanin. This suggests additional mechanisms are needed to explain the phenotypic differences in male vs female cheek color than those examined here.

Conclusions

Here, we have described how patterns of gene expression in the melanogenesis pathway differ among different feather colors and between the sexes. We found that

differences in pigment production in feathers are likely driven by expression changes in relatively few genes of functional importance, and that those differences are associated with relatively few changes in the signaling pathways governing melanin production. The multiple signaling pathways that regulate key melanogenesis genes seems to offer the system some flexibility in regulation, in that different pathways are important for different types of color production and the pathways used differ between the sexes as well. Our work here provides an overview of how gene expression may regulate pigmentation variation in one bird species, but may also guide future studies in elucidating the function of key genes in melanin regulation.

Literature Cited

Abolins-Abols, M, E Kornobis, P Ribeca, K Wakamatsu, MP Peterson, ED Ketterson, and B Mila (2018) Differential gene regulation underlies variation in melanic plumage coloration in the dark-eyed junco (Junco hyemalis). *Molecular Ecology* **27**:4501-4515.

Adkins-Regan, E, M Abdelnabi, M Mobarak, and MA Ottinger (1990) Sex steroid levels in developing and adult male and female zebra finches (Poephila guttata). *General and Comparative Endocrinology* **78**:93-109.

Alvarez-Ponce, D, M Aguade, and J Rozas (2009) Network-level molecular evolutionary analysis of the insulin/TOR signal transduction pathway across 12 Drosophila genomes. *Genome Research* **19**:234-242.

Cheli, Y, M Ohanna, R Ballotti, and C Bertolotto (2009) Fifteen-year quest for microphthalmia-associated transcription factor target genes. *Pigment Cell Melanoma Research* **23**:27-40.

Chen, K., Manga, P., and Orlow, S.J. (2002). Pink-eyed dilution protein controls the processing of tyrosinase. *Molecular Biology of the Cell* **13**:1953–1964.

Cheviron, ZA, SJ Hackett, and RT Brumfield (2006) Sequence variation in the coding region of the melanocortin-1 receptor gene (mc1r) is not associated with plumage variation in the blue-crowned manakin (Lepidothrix coronata). *Proc R Soc B* **273**:1613-1618.

Chintala, S, W Li, ML Lamoreux, S Ito, K Wakamatsu, EV Sviderskaya, DC Bennett, Y-M Park, WA Gahl, M Huizing, RA Spritz, S Ben, EK Novak, J Tan, and RT Swank (2005) Slc7a11 gene controls production of pheomelanin pigment and proliferation of cultured cells. *PNAS* **102**:10964-10969.

Clement, P (1993) *Finches & Sparrows: An Identification Guide*. Princeton University Press,

D'Alba, L, and MD Shawkey (2019) Melanosomes: biogenesis, properties, and evolution of an ancient organelle. *Physiological Reviews* **99**:1-19.

Dick, C, DN Reznick, and CY Hayashi (2018) Sex-biased expression between guppies varying in the presence of ornamental coloration. *PeerJ* **6**:e5782.

Ellegren, H, and J Parsch (2007) The evolution of sex-biased genes and sex-biased gene expression. *Nature Reviews Genetics* **8**:689-698.

Fan, R, J Xie, H Wang, X Tian, R Bai, X jia, L Yang, Y Song, M Herrid, W Gao, X He, J Yao, GW Smith, and C Dong (2013) Skin transcriptome profiles associated with coat color in sheep. *BMC Genomics* **14**:389.

Ferreira, MS, PC Alves, CM Callahan, JP Marques, LS Mills, JM Good, and J Melo-Ferreira (2017) The transcriptional landscape of seasonal coat colour moult in snowshoe hare. *Molecular Ecology* **26**:4173-4185.

Flowers, JM, E Sezgin, S Kumagai, DD Duvernell, LM Matzkin, PS Schmidt, and WF Eanes (2007) Adaptive evolution of metabolic pathways in Drosophila. *Molecular Biology and Evolution* **24**:1347-1354

Forshaw, JM, and M Shephard (2012) *Grassfinches in Australia*. CSIRO Publishing.

Gomes, ACR, MD Sorenson, and GC Cardoso (2016) Speciation is associated with changing ornamentation rather than stronger sexual selection. *Evolution* **70**:2823-2838.

Griffith, SC, and KL Buchanan (2010) The Zebra Finch: the ultimate Australian supermodel. *Emu* **110**:v-xii.

Haupaix, N, C Curantz, R Bailleul, S Beck, A Robic, and M Manceau (2018) The periodic coloration in birds forms through a prepattern of somite origin. *Science* **361**:1216

Hayes, TB (1997) Hormonal mechanisms as potential constraints on evolution: examples from the Anura. *Integrative and Comparative Biology* **37**:482-490.

He, H, D Sun, Y Zeng, R Wang, W Zhu, S Cao, GA Bray, W Chen, H Shen, FM Sacks, L Qi, and H-w Deng (2017) A systems genetics approach identified GPD1L and its molecular mechanism for obesity in human adipose tissue. *Scientific Reports* **1799**

Hendrickx, M, and L Leyns (2008) Non-conventional Frizzled ligands and Wnt receptors. *Development, Growth, and Differentiation* **50**:229-243.

Hill, GE, and KJ McGraw (2006a) *Bird Coloration Volume I: Mechanisms and Measurement*. Harvard University Press, Cambridge, MA, USA.

Hill, GE, and KJ McGraw (2006b) *Bird Coloration Volume II: Function and Evolution*. Harvard University Press, Cambridge, MA, USA.

Hoekstra, HE (2006) Genetics, development and evolution of adaptive pigmentation in vertebrates. *Heredity* **97**:222-234.

Hoffman, JI, ET Krause, K Lehmann, and O Kruger (2014) MC1R genotype and plumage colouration in the Zebra Finch (Taeniopygia guttata): population structure generates artefactual associations. *PLoS ONE* **9**:e86519

Hubbard, JK, JAC Uy, ME Hauber, HE Hoekstra, and RJ Safran (2010) Vertebrate pigmentation: from underlying genes to adaptive function. *Trends in Genetics* **26**:231-239.

Jones, MR, LS Mills, PC Alves, CM Callahan, JM Alves, DJR Lafferty, FM Jiggins, JD Jensen, J Melo-Ferreira, and JM Good (2018) Adaptive introgression underlies polymorphic seasonal camouflage in snowshoe hares. *Science* **360**:1355-1358.

Junge, HJ, S Yang, JB Burton, K Paes, X Shu, DM French, M Costa, DS Rice, and W Ye (2009) TSPAN12 regulates retinal vascular development by promoting Norrin- but not Wnt-induced FZD4/B-Catenin signaling. *Cell* **139**:299-311.

Kanehisa, M, and S Goto (2000) KEGG: Kyoto Encyclopedia of Genes and Genomes. *Nucleic Acids Research* **28**:27-30.

Kanehisa, M, Y Sato, M Kawashima, M Furumichi, and M Tanabe (2016) KEGG as a reference resource for gene and protein annotation. *Nucleic Acids Research* **44**:D457-D462.

Kimball, RT (2006) Hormonal control of coloration. In: Hill, GE, and KJ McGraw (2006a) *Bird Coloration Volume I: Mechanisms and Measurement*. Harvard University Press, Cambridge, MA, USA.

Landry, G (1997) *An Almost complete Guide to: The Varieties and Genetics of the Zebra Finch*. 3rd Edition: 2017. Poule d'eau Publishing, Franklin, Louisiana, USA.

Li, H (2013) Aligning sequence reads, clone sequences and assembly contigs with BWA-MEM. *arXiv*:1303.3997v2 [q-bio.GN]

Li, H, and R Durbin (2009) Fast and accurate short read alignment with Burrows-Wheeler transform. *Bioinformatics* **25**:1754-1760.

Liao, Y, GK Smyth, and W Shi (2014) featureCounts: an efficient general purpose program for assigning sequence reads to genomic features. *Bioinformatics* **30**:923-930.

Lin, SJ, J Foley, TX Jiang, CY Yeh, P Wu, A Foley, CM Yen, YC Huang, HC Cheng, CF Chen, B Reeder, SH Jee, RB Widelitz, and CM Chuong (2013) Topology of feather melanocyte progenitor niche allows complex pigment patterns to emerge. *Science* **340**:1442-1445.

Liu, X, JS Rubin, and AR Kimmel (2005) Rapid, Wnt-Induced changes in GSK3β associations that regulate β-catenin stabilization are mediated by Gα proteins. *Current Biology* **15**:1989-1997.

Lohman, BK, JN Weber, and DI Bolnick (2016) Evaluation of TagSeq, a reliable low-cost alternative for RNAseq. *Molecular Ecology Resources* **16**:1315-1321.

London, B, M Michalec, H Mehdi, X Zhu, L Kerchner, S Sanyal, PC Viswanathan, AE Pfahnl, LL Shang, M Madhusudanan, CJ Baty, S Lagana, R Aleong, R Gutmann, MJ Ackerman, DM McNamara, R Weiss, and SC Dudley (2007) Mutation in glycerol-3-phosphate dehydrogenase 1-like gene (GPD1-L) decreases cardiac Na+ current and causes inherited arrhythmias. *Circulation* **116**:2260-2268.

MacDougall-Shackleton, EA, L Blanchard, and HL Gibbs (2003) Unmelanized plumage patterns in Old World leaf warblers do not correspond to sequence variation at the melanocortin-1 receptor locus (mc1r). *Mol Biol Evol* **20**:1675-1681.

Manga, P., Boissy, R.E., Pifko-Hirst, S., Zhou, B.K., and Orlow, S.J. (2001). Mislocalization of melanosomal proteins in melanocytes from mice with oculocutaneous albinism type 2. *Experimental Eye Research* **72**:695–710.

Matz, M (2017) Genome-wide gene expression profiling with tag-based RNA-seq (TagSeq). Github repository: https://github.com/z0on/tag-based_RNAseq

McCarthy, DJ, Y Chen, and GK Smyth (2012) Differential expression analysis of multifactor RNA-Seq experiments with respect to biological variation. *Nucleic Acids Research* **40**:4288-4297.

McGraw, KJ, and K Wakamatsu (2004) Melanin basis of ornamental feather colors in male Zebra Finches. *The Condor* **106**:686-690.

Moniot B, A Farhat, K Aritake, F Declosmenii, S Nef, N Eguchi, Y Urade, F Poulat, and B Boizet-Bonhoure (2011) Hematopoetic prostaglandin D synthase (H-Pgds) is expressed in the early embryonic gonad and participates to the initial nuclear translocation of the SOX9 protein. *Developmental Dynamics* **240**:2335-2343.

Morii,E, and K Oboki (2004) MITF is necessary for generation of prostaglandin D2 in mouse mast cells. *Journal of Biological Chemistry* **279**:48923-48929.

Mudunuri, U, A Che, M Yi, and RM Stephens (2009) bioDBnet: the biological database network. *Bioinformatics* **25**:555-556.

Mundy, NI (2005) A window on the genetics of evolution: MC1R and plumage colouration in birds. *Proc. R Soc. London B.* **272**:1633-1640;

Murphy, FA, K Tucker, and DA Fadool (2001) Sexual dimorphism and developmental expression of signal-transduction machinery in the vomeronasal organ. *The Journal of Comparative Neurology* **432**:61-74.

Passeron, T, JC Valencia, C Bertolotto, T Hoashi, E Le Pape, K Takahashi, R Ballotti, and VJ Hearing (2007) SOX9 is a key player in ultraviolet B-induced melanocyte differentiation and pigmentation. *PNAS* **104**:13984-13989.

Poelstra, JW, N Vijay, MP Hoeppner, and JBW Wolf (2015) Transcriptomics of colour patterning and coloration shifts in crows. *Molecular Ecology* **24**:4617-4628.

Potterf, S.B., Furumura, M., Sviderskaya, E.V., Santis, C., Bennett, D.C., and Hearing, V. (1998). Normal tyrosine transport and abnormal tyrosinase routing in pink-eyed dilution melanocytes. *Experimental Cell Research* **244**:319–326.

Prum, RO, and J Dyck (2003) A hierarchical model of plumage: morphology, development, and evolution. *Journal of Experimental Zoology (Mol Dev Evol)* **298B**:73-90.

Regard, JB, N Cherman, D Palmer, SA Kuznetsov, FS Celi, J-M Guettier, M Chen,N Bhattacharyya, J Wess, SR Coughlin, LS Weinstein, MT Collins, PG Robey, and Y Yang (2011) Wnt/β-catenin signaling is differentially regulated by Gα proteins and contributes to fibrous dysplasia. *PNAS* **108**:20101-20106.

Reimand, J, T Arak, P Adler, L Kolberg, S Reisberg, H Peterson, J Vilo (2016) g:Profiler – a web server for functional interpretation of gene lists (2016 update). *Nucleic Acids Research* **44**:W83-W89.

Robinson, MD, DJ McCarthy, GK Smyth (2010) edger: a Bioconductor package for differential expression analysis of digital gene expression data. *Bioinformatics* **26**:139-140.

Schiaffino, MV (2010) Signaling pathways in melanosome biogenesis and pathology. *The International Journal of Biochemistry & Cell Biology* **42**:1094-1104.

Smit, NP, HVan der Meulen, HK Koerten, RM Kolb, AM Mommaas, EG Lentjes, and S Pavel (1997) Melanogenesis in cultured melanocytes can be substantially influenced by L-tyronsine and L-cysteine. *The Journal of Investigative Dermatology* **109**:796-800

Song, X, C Xu, Z Liu, Z Yue, L Liu, T Yang, B Cong, and F Yang (2017) Comparative transcriptome analysis of Mink (Neovison vison) skin reveals the key genes involved in the melanogenesis of black and white coat colour. *Scientific Reports* **7**:12461.

Toyofuku, K., Valencia, J.C., Kushimoto, T., Costin, G.E., Virador, V.M., Vieira, W.D., Ferrans, V.J., and Hearing, V.J. (2002). The etiology of oculocutaneous albinism (OCA) type II: the pink protein modulates the processing and transport of tyrosinase. *Pigment Cell Research* **15**:217–224.

Valdivia, CR, K Ueda, MJ Ackerman, and JC Makielski (2009) GPD1L links redox state to cardiac excitability by PKC_dependent phosphorylation of the sodium channel SCN5A. *American Journal of Physiology: Heart and Circulatory Physiology* **297**:H1446-H1452.

Vickrey, AI, R Bruders, Z Kronenberg, E Mackay, RJ Bohlender, ET Maclary, R Maynez, EJ Osborne, KP Johnson, CD Huff, M Yandell, and MD Shapiro (2018) Introgression of regulatory alleles and a missense coding mutation drive plumage pattern diversity in the rock pigeon. *eLife* **7**:e34803

Visser, M, M Kayser, F Grosveld, and R-J Palstra (2014) Genetic variation in regulatory DNA elements: the case of OCA2 transcriptional regulation. *Pigment Cell Melanoma Research* **27**:169-177.

Warren, WC, DF Clayton, H Ellegren, AP Arnold, LW Hillier, A Künstner, S Searle, S White, AJ Vilella, S Fairley, A Heger, L Kong, CP Ponting, ED Jarvis, CV Mello, P Minx, P Lovell, TAF Velho, M Ferris, CN Balakrishnan, S Sinha, C Blatti, SE London, Y Li, Y-C Lin, J George, J Sweedler, B Southey, P Gunaratne, M Watson, K Nam, N Backström, L Smeds, B Nabholz, Y Itoh, O Whitney, AR Pfenning, J Howard, M Völker, BM Skinner, DK Griffin, L Ye, WM McLaren, P Flicek, V Quesada, G Velasco, C Lopez-Otin, XS Puente, T Olender, D Lancet, AFA Smit, R Hubley, MK Konkel, JA Walker, MA Batzer, W Gu, DD Pollock, L Chen, Z Cheng, EE Eichler, J Stapley, J Slate, R Ekblom, T Birkhead, T Burke, D Burt, C Scharff, I Adam, H Richard, M Sultan, A Soldatov, H Lehrach, SV Edwards, S-P Yang, X Li, T Graves, L Fulton, J Nelson, A Chinwalla, S Hou, ER Mardis, and RK Wilson (2010) The genome of a songbird. *Nature* **464**:757-762.

Xu, Q, Y Wang, A Dabdoub, PM Smallwood, J Williams, C Woods, MW Kelley, L Jiang, W Tasman, K Zhang, and J Nathans (2004) Vascular development in the retina and inner ear: control by Norrin and Frizzled-4, a high-affinity ligand-receptor pair. *Cell* **116**:883-895

Zhang, J, F Liu, J Cao, and X Liu (2015) Skin transcriptome profiles associated with skin color in chickens. *PLoS ONE* **10**:e0127301
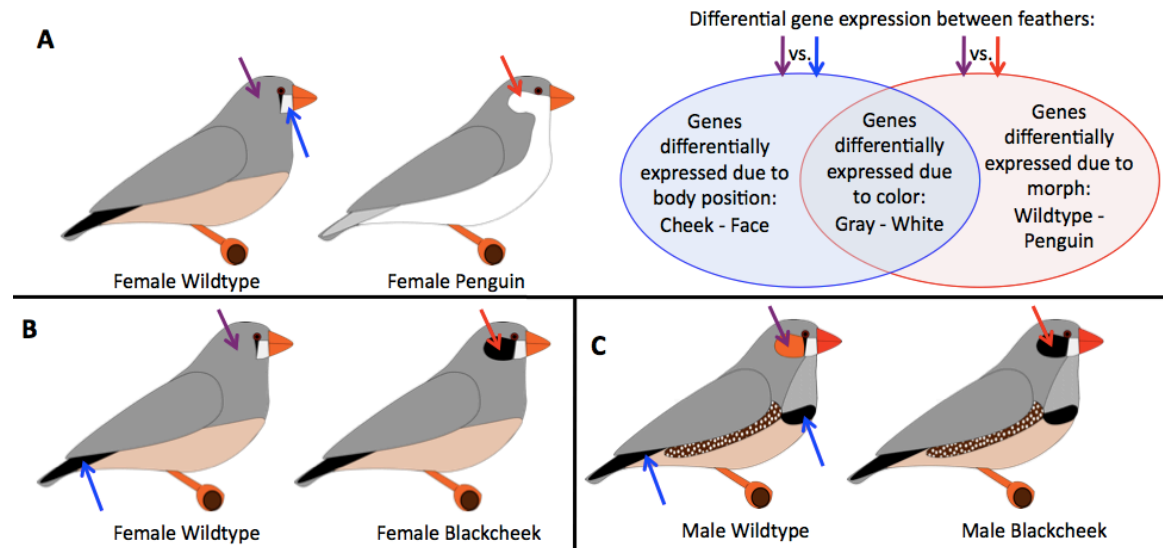
Figure 1: Testing for differential expression in developing feathers in Wild-type Zebra Finches and two color mutations: Penguin and Blackcheek. We make three comparisons of feather color: A) Gray vs. white, B) Gray vs. black, and C) Orange vs. black. In each comparison, we test for differential expression between these colors across plumage within the Wild-type (blue and purple arrows) and for differential expression between those colors in the Wild-type and mutant (purple and red arrows; see also **Table 1**). The differentially expressed genes common to both comparisons are those most likely tied to pigment production, excluding those genes differentially expressed relating to population structure across morphs or body position variation across different plumage patches.
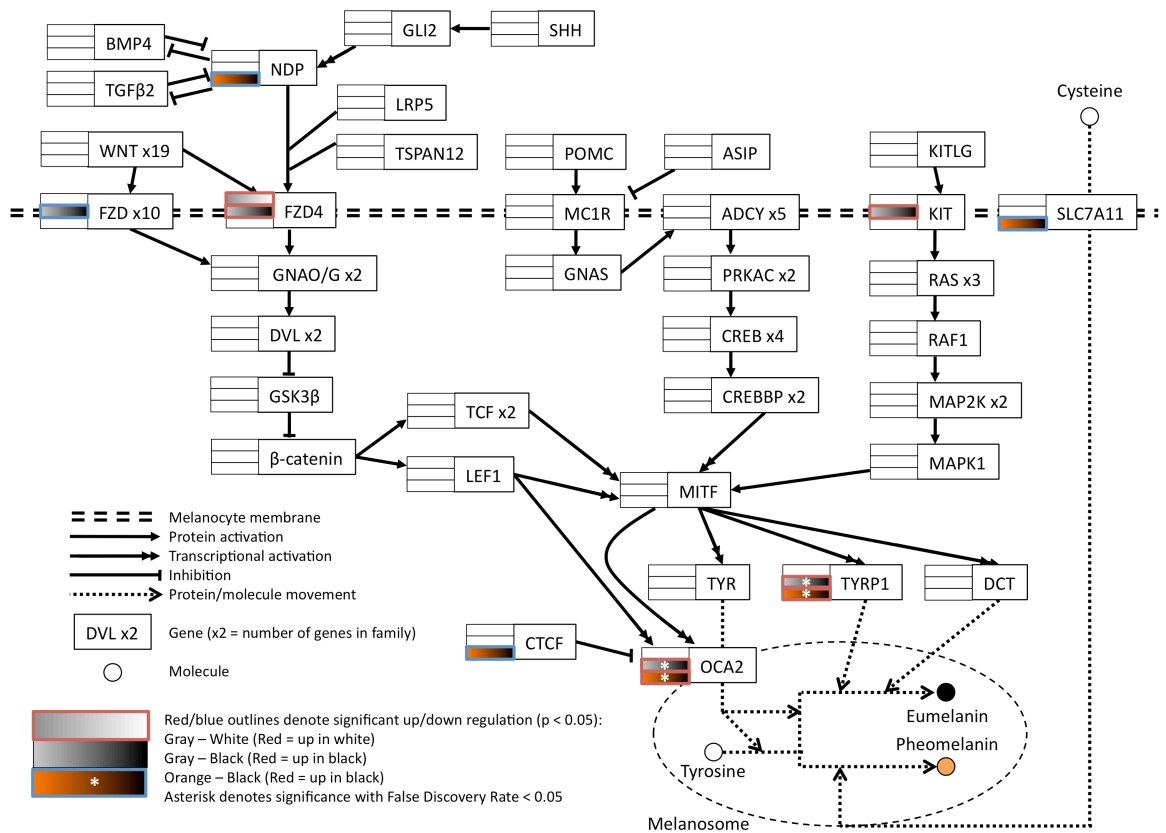
Figure 2: Variation in melanogenesis network gene expression between Zebra Finch plumage colors. The network is based on the KEGG melanogenesis pathway for Zebra Finch, with additional candidate genes and interactions added (**Table 2**). The endothelin signaling pathway has been omitted as it is not involved in MITF or OCA2 regulation. Highlighted rectangles denote the significantly differentially expressed genes in three color comparisons: Gray vs. White, Gray vs. Black, and Orange vs. Black.
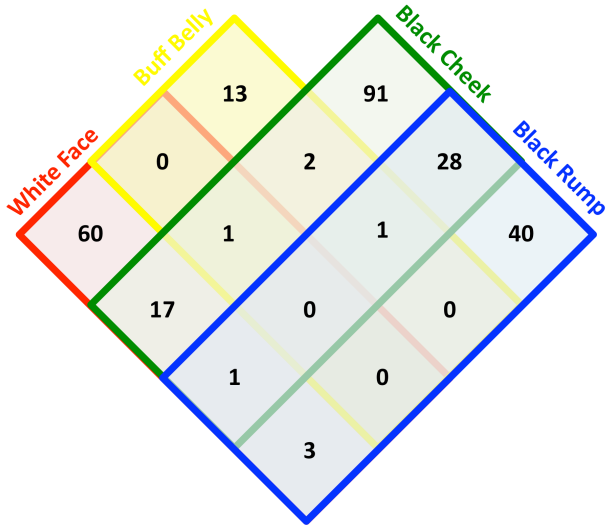
Figure 3: Venn diagram of the overlap in genes that are significantly differentially expressed between the sexes in each of four plumage patches: white face, buff belly, black cheek, and black rump. Values are the number of significant genes in each category.
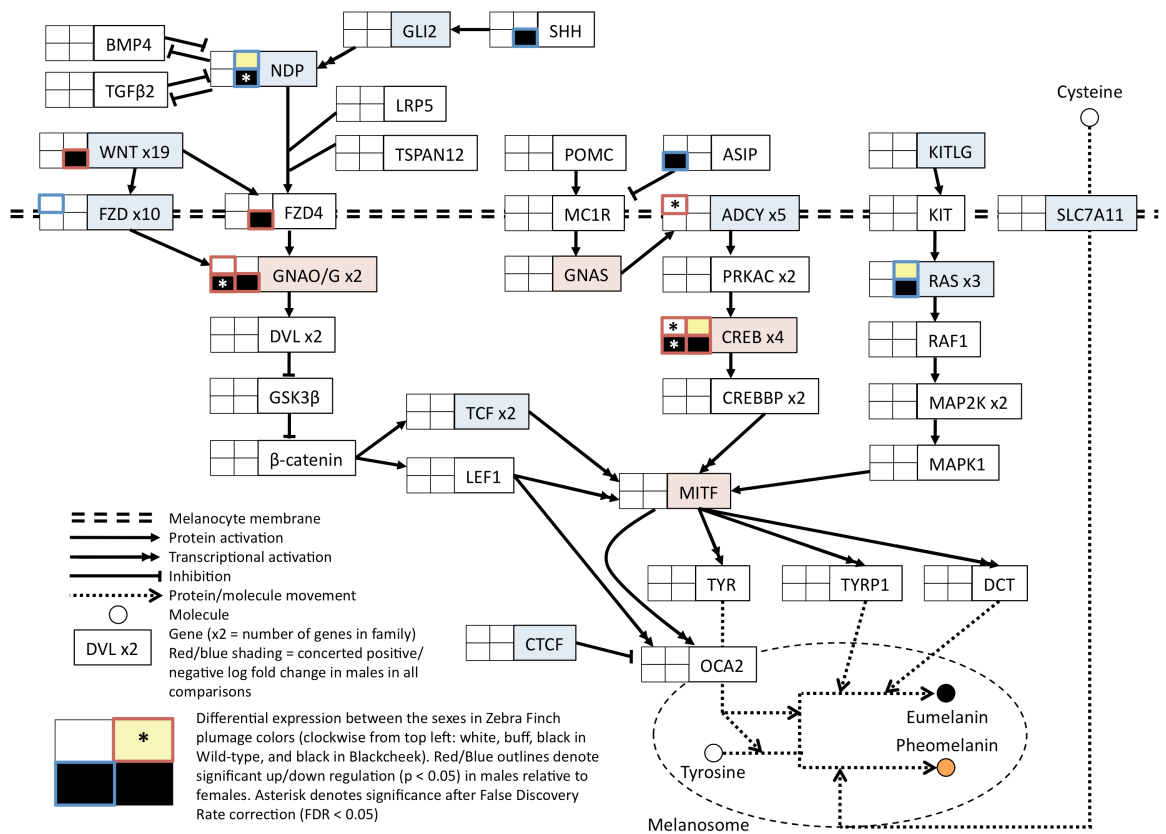
Figure 4: Sex-biased gene expression in the melanogenesis network for Zebra Finch plumage colors. The network is based on the KEGG melanogenesis pathway for Zebra Finch, with additional candidate genes and interactions added (**Table 2**). The endothelin signaling pathway has been omitted as it is not involved in MITF or OCA2 regulation. Highlighted squares denote significant differential expression between the sexes in four patches (legend).
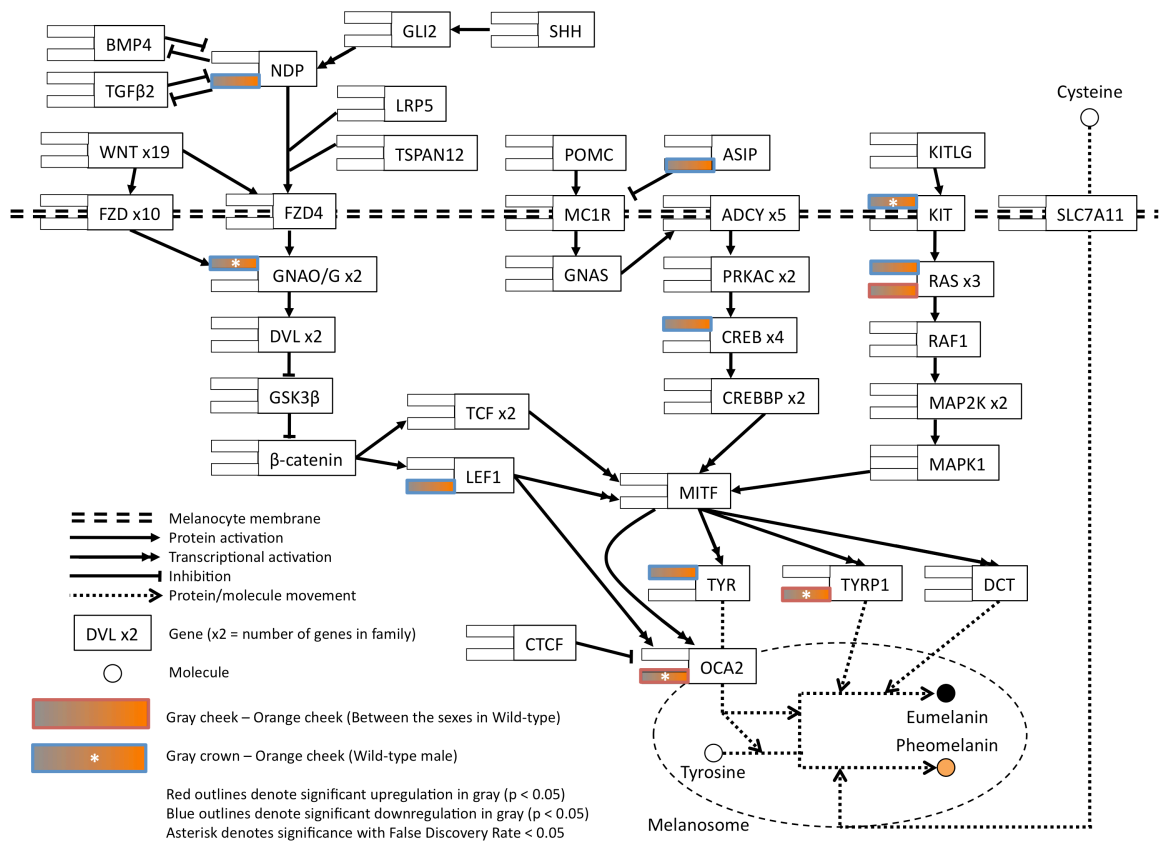
Figure 5: Differential gene expression in the melanogenesis network between orange and gray plumage colors in wild-type Zebra Finch. Highlighted rectangles (see legend) denote significant differential expression between orange male cheeks and gray female cheeks (top rectangle) and between orange male cheeks and gray male crown feathers (bottom rectangle). The network is based on the KEGG melanogenesis pathway for Zebra Finch, with additional candidate genes and interactions added (**Table 2**). The endothelin signaling pathway has been omitted as it is not involved in MITF or OCA2 regulation.

Tables

Table 1: Sample sizes and tissue comparisons for testing differentially expressed genes relating to color and sex in Zebra Finches

	Comparison	Sample 1	*n*	Sample 2	*n*
Color	Black-Gray	Gray Wild-type female cheek	5	Black Blackcheek female cheek	4
		Gray Wild-type female cheek	5	Black Wild-type female rump	4
	Gray-White	Gray Wild-type female cheek	5	White Penguin female cheek	4
		Gray Wild-type female cheek	5	White Wild-type female face	4
	Orange-Black	Orange Wild-type male cheek	5	Black Blackcheek male cheek	5
		Orange Wild-type male cheek	5	Black Wild-type male breast	5
		Orange Wild-type male cheek	5	Black Wild-type male rump	3
Sex	Male - Female	White Wild-type male face	5	White Wild-type female face	4
		Buff Wild-type male belly	2	Buff Wild-type female belly	4
		Black Wild-type male rump	3	Black Wild-type female rump	4
		Black Blackcheek male cheek	5	Black Blackcheek female cheek	4
Sex and color	Male – Female	Orange Wild-type male cheek	5	Gray Wild-type female cheek	5
	Male - Male	Orange Wild-type male cheek	5	Gray Wild-type male crown	5

Table 2: Candidate genes and interactions added to KEGG Zebra Finch melanogenesis pathway

Gene name	Gene description	Gene ID	Function	Citation
BMP4	Bone morphogenetic protein 4	100221891	Mutual inhibitor of NDP through direct binding	Xu et al. (2012)
CTCF	CCCTC-binding factor	100224119	Suppresses the enhancer region of OCA2	Visser et al. (2014)
FZD4	Frizzled class receptor 4	100231781	Receptor for NDP and WNT; triggers canonical WNT signaling	Hendrickx and Leyns (2008)
Gli2	GLI family zinc finger 2	100221648	Induced by Shh signaling to bind to NDP promoter and initiate transcription	McNeill et al. (2013)
LEF1	Lymphoid enhancer binding factor 1	100228376	Transcription factor of OCA2 and MITF activated by NDP/FZD4 signaling	Visser et al. (2014)
LRP5	LDL receptor related protein 5	100220027	Co-receptor required for NDP/FZD4 signaling activation	Xu et al. (2004)
MITF	Melanocyte inducing transcription factor	100232286	Target of NDP/FZD4 signaling; Enhances OCA2 expression	Visser et al. (2014)
NDP	Norrie disease protein	100224175	Fzd4 ligand	Hendrickx and Leyns (2008)
OCA2	Oculocutaneous albinism type 2	100228502	Regulates Tyrosinase transportation and function	Visser et al. (2014)
Shh	Sonic hedgehog signaling molecule	100222391	Induces signaling cascade to activate NDP transcription	McNeill et al. (2013)
Slc7a11	Solute carrier family 7 member 11	100223276	Regulates pheomelanin production by transporting cysteine into melanocyte	Chintala et al. (2005)
TGFB2	Transforming growth factor beta 2	100231617	Mutual inhibitor of NDP through direct binding	Xu et al. (2012)
TSPAN12	Tetraspanin 12	100220256	Co-receptor required for NDP/FZD4 signaling activation	Junge et al. (2009)

Table 3: Numbers of differentially expressed genes for each comparison of plumage color (see **Table 1**, **Figure 1**) and for each comparison between the sexes for phenotypically similar patches.

	Comparison	$p < 0.05$	FDR < 0.05	Combined	$p < 0.05$	FDR < 0.05
				Number of differentially expressed genes		
Color	Cheek - Cheek	11	5	Black-Gray	9	2
	Cheek - Rump	697	32			
	Cheek - Cheek	424	0	Gray-White	58	0
	Cheek - Face	1224	39			
	Cheek - Cheek	1284	40	Orange-Black	16	4
	Cheek - Breast	1291	74			
	Cheek - Rump	536	38			
Sex	White Face	985	82			
	Buff Belly	788	17			
	Black Rump	850	73			
	Black Cheek	661	141			

Table 4: Melanogenesis pathway genes that are significantly differentially expressed among color comparisons. Positive fold change represents overexpression in white relative to gray, black relative to gray, and black relative to orange, respectively, and negative fold change represents the opposite. P-values and false discovery rate corrections are bolded when significant (< 0.05).

Gene	GeneID	Color: Gray – Black				Color: Gray – White				Color: Orange - Black					
		Cheek – Face		Cheek – Cheek		Cheek – Rump		Cheek – Cheek		Cheek – Rump		Cheek – Breast		Cheek – Cheek	
		Log Fold Change	p-value (FDR)	Log Fold Change	p-value (FDR)	Log Fold Change	p-value (FDR)	Log Fold Change	p-value (FDR)	Log Fold Change	p-value (FDR)	Log Fold Change	p-value (FDR)	Log Fold Change	p-value (FDR)
ASIP	100218186	0.991	**0.027** (0.229)	-2.303	**0.013** (0.772)	-0.332	0.666 (1.000)	-0.083	0.882 (1.000)	0.897	0.054 (0.702)	-1.269	0.113 (1.000)	-2.721	0.304 (1.000)
CTCF	100223276	-0.054	0.951 (1.000)	-0.524	0.185 (1.000)	-0.677	0.351 (1.000)	0.546	0.146 (0.989)	-1.439	**0.002** (0.243)	-1.475	**0.024** (1.000)	-1.942	**0.004** (0.240)
FZD4	100231781	1.028	**0.004** (0.060)	1.131	**0.005** (0.538)	1.046	**0.024** (1.000)	1.115	**0.005** (0.311)	0.414	0.159 (0.896)	1.575	**0.000** (0.017)	1.281	**0.000** (0.019)
FZD9	100217519	-0.852	**0.006** (0.081)	-0.975	**0.006** (0.545)	0.567	0.286 (1.000)	-0.964	**0.006** (0.341)	-0.171	0.672 (1.000)	-0.289	0.532 (1.000)	1.045	0.055 (0.711)
KIT	100221238	0.750	**0.014** (0.141)	1.663	**0.000** (0.058)	-0.084	0.861 (1.000)	1.578	**0.000** (0.053)	-0.744	0.077 (0.778)	-0.085	0.898 (1.000)	-1.453	**0.003** (0.220)
NDP	100224175	-2.956	**0.000** (**0.000**)	-0.477	0.273 (1.000)	0.214	0.668 (1.000)	-1.251	**0.015** (0.475)	-3.237	**0.000** (**0.000**)	-2.892	**0.000** (**0.004**)	-1.221	**0.007** (0.316)
OCA2	100228502	1.995	**0.000** (**0.008**)	3.757	**0.000** (**0.000**)	-0.615	0.558 (1.000)	-2.127	**0.046** (0.704)	4.335	**0.000** (**0.000**)	4.985	**0.000** (**0.000**)	3.486	**0.000** (**0.015**)
SLC7A11	100223276	-0.054	0.951 (1.000)	-0.524	0.185 (1.000)	-0.677	0.351 (1.000)	0.546	0.146 (0.989)	-1.439	**0.002** (0.243)	-1.475	**0.024** (1.000)	-1.942	**0.004** (0.240)
TYRP1	100218715	2.718	**0.000** (**0.000**)	4.100	**0.000** (**0.000**)	0.010	0.979 (1.000)	-1.149	**0.044** (0.694)	4.238	**0.000** (**0.000**)	4.999	**0.000** (**0.000**)	3.608	**0.000** (**0.000**)

Table 5: Gene Ontology (GO) terms that are significantly enriched in the significantly differentially expressed genes in each comparison between the sexes.

DE Gene List	GO term ID	GO term description	*P* value	term genes (*n*)	query genes (*n*)	common genes (*n*)
Sex: White	REAC:R-TGU-917977	Transferrin endocytosis and recycling	0.037	28	27	3
Sex: Buff	GO:0043409	negative regulation of MAPK cascade	0.025	80	10	3
	GO:1903747	regulation of establishment of protein localization to mitochondrion	0.043	13	10	2
	GO:1903748	negative regulation of establishment of protein localization to mitochondrion	0.006	5	10	2
Sex: Black Cheek	GO:0005730	nucleolus	0.004	432	88	13
	GO:0043226	organelle	0.005	6192	88	60
	GO:0043227	membrane-bounded organelle	0.042	5289	88	52
	GO:0005622	intracellular	0.006	7424	88	67
	GO:0044424	intracellular part	0.012	7011	88	64
	GO:0005737	cytoplasm	0.007	4711	88	50
	GO:0044444	cytoplasmic part	0.000	3846	88	48
	GO:0043229	intracellular organelle	0.007	6081	88	59
	GO:0043231	intracellular membrane-bounded organelle	0.045	4997	88	50

Table 6: Melanogenesis pathway genes that are significantly differentially expressed between the sexes in four plumage patches of similar phenotype between the sexes. Positive fold change represents overexpression in males relative to females, and negative fold change the opposite. Fold change values are bolded when their direction is consistent in all four comparisons. P-values and false discovery rate corrections are bolded when significant (< 0.05).

| Gene | GeneID | Morph: Wild-type | | | | | | Blackcheek | |
| | | White face | | Buff belly | | Black rump | | Black cheek | |
		Log Fold Change	p-value (FDR)	Log Fold Change	p-value (FDR)	Log Fold Change	p-value (FDR)	Log Fold Change	p-value (FDR)
ADCY7	100225700	**-0.578**	0.075 (1.000)	**-0.149**	0.676 (1.000)	**-0.236**	0.390 (1.000)	**-0.214**	0.339 (1.000)
ADCY8	100230277	5.137	**0.000 (0.005)**	1.551	0.200 (1.000)	-0.709	0.492 (1.000)	1.468	0.123 (1.000)
CAMK2B	100228031	**-0.744**	1.000 (1.000)	**-0.650**	1.000 (1.000)	**-2.825**	0.407 (1.000)	**-0.367**	0.880 (1.000)
CAMK2D	100219415	**0.431**	0.132 (1.000)	**0.068**	0.860 (1.000)	**0.055**	0.921 (1.000)	**0.025**	0.936 (1.000)
CREB3	100222350	**1.603**	**0.000 (0.023)**	**1.311**	**0.001** (0.208)	**0.947**	**0.004** (0.301)	**0.924**	**0.000 (0.027)**
CREB3L1	100220102	0.227	0.945 (1.000)	-0.039	1.000 (1.000)	1.921	**0.002** (0.207)	0.282	0.795 (1.000)
CREB3L2	100219636	**0.231**	0.460 (1.000)	**0.217**	0.526 (1.000)	**0.370**	0.138 (1.000)	**0.025**	0.959 (1.000)
CTCF	100223276	**-0.693**	0.102 (1.000)	**-0.228**	0.610 (1.000)	**-0.137**	0.840 (1.000)	**-0.467**	0.189 (1.000)
FZD4	100231781	0.195	0.646 (1.000)	0.044	1.000 (1.000)	0.793	**0.031** (0.857)	-0.246	0.352 (1.000)
FZD6	100222044	**-0.775**	**0.010** (0.431)	**-0.005**	1.000 (1.000)	**-0.093**	0.773 (1.000)	**-0.257**	0.223 (1.000)
FZD9	100217519	1.357	**0.007** (0.369)	-0.114	0.963 (1.000)	0.135	0.819 (1.000)	0.108	0.651 (1.000)
GLI2	100221648	**-0.341**	0.268 (1.000)	**-0.151**	0.694 (1.000)	**-0.214**	0.449 (1.000)	**-0.048**	0.813 (1.000)
GNAQ	100230245	**1.061**	**0.003** (0.224)	**0.771**	0.089 (1.000)	**0.726**	**0.010** (0.521)	**1.070**	**0.000 (0.008)**
GNAS	100232476	**0.109**	0.674 (1.000)	**0.426**	0.170 (1.000)	**0.050**	0.862 (1.00)	**0.010**	0.954 (1.000)
HRAS	100190361	-0.208	0.507 (1.000)	-0.919	**0.027** (0.946)	-0.971	**0.033** (0.874)	0.000	0.997 (1.000)
KITLG	100225713	**-0.191**	0.699 (1.000)	**-0.070**	0.863 (1.000)	**-0.142**	0.749 (1.000)	**-0.359**	0.241 (1.000)
KRAS	100227892	**-0.052**	0.834 (1.000)	**-0.373**	0.280 (1.000)	**-0.178**	0.522 (1.000)	**-0.209**	0.314 (1.000)
MITF	100232286	**0.003**	0.992 (1.000)	**0.062**	0.841 (1.000)	**0.023**	0.891 (1.000)	**0.135**	0.537 (1.000)
NDP	100224175	**-1.397**	0.075 (1.000)	**-2.137**	0.020 (0.845)	**-2.557**	**0.000 (0.018)**	**-0.422**	0.688 (1.000)
PLCB1	100219122	**0.513**	0.114 (1.000)	**0.060**	0.844 (1.000)	**0.056**	0.802 (1.000)	**0.082**	0.671 (1.000)
PLCB4	100221959	0.752	**0.035** (0.776)	-0.114	0.810 (1.000)	0.010	0.929 (1.000)	0.021	0.973 (1.000)
PRKCB	100227442	**0.376**	0.763 (1.000)	**0.222**	1.000 (1.000)	**0.161**	0.945 (1.000)	**0.425**	0.928 (1.000)
SHH	100222391	-0.265	0.600 (1.000)	0.148	0.772 (1.000)	-0.947	**0.018** (0.681)	-0.231	0.633 (1.000)
SLC7A11	100223276	**-0.693**	0.102 (1.000)	**-0.228**	0.610 (1.000)	**-0.137**	0.840 (1.000)	**-0.467**	0.189 (1.000)
TCF7	100221008	**-0.603**	0.144 (1.000)	**-0.643**	0.152 (1.000)	**-0.275**	0.451 (1.000)	**-0.301**	0.359 (1.000)
WNT16	100218349	0.479	0.908 (1.000)	-0.656	1.000 (1.000)	1.600	**0.040** (0.956)	-0.044	1.000 (1.000)
WNT5A	100219241	**-0.411**	0.132 (1.000)	**-0.183**	0.702 (1.000)	**-0.021**	0.926 (1.000)	**-0.163**	0.455 (1.000)
WNT7A	100220584	**-0.405**	0.449 (1.000)	**-0.356**	0.592 (1.000)	**-0.202**	0.607 (1.000)	**-0.595**	0.149 (1.000)

Table 7: Melanogenesis pathway genes that are significantly differentially expressed between orange and gray patches in Wild-type Zebra Finch. Comparisons are between the sexes (orange male cheeks vs gray female cheeks) and within one sex (orange male cheeks vs gray male crown feathers). Positive fold change represents upregulation in orange relative to gray, and negative fold change the opposite. P-values and false discovery rate corrections are bolded when significant (< 0.05).

Gene	GeneID	Orange male cheek vs. gray female cheek		Orange male cheek vs. Gray male crown	
		Log Fold Change	p-value (FDR)	Log Fold Change	p-value (FDR)
ASIP	100218186	-0.403	0.484 (1.000)	2.650	**0.001** (0.393)
CREB3	100222350	0.833	**0.039** (0.872)	-0.383	0.320 (1.000)
GNAI2	100225910	0.024	0.934 (1.000)	-0.636	**0.020** (1.000)
GNAQ	100230245	1.200	**0.000 (0.007)**	0.164	0.502 (1.000)
HRAS	100190361	-0.833	**0.029** (0.765)	-0.891	**0.017** (1.000)
KIT	100221238	1.883	**0.000 (0.005)**	0.632	0.174 (1.000)
LEF1	100228376	0.627	0.056 (0.965)	0.792	**0.016** (1.000)
NDP	100224175	-0.131	0.835 (1.000)	1.036	**0.011** (1.000)
OCA2	100228502	-1.509	0.171 (1.000)	-3.785	**0.000 (0.000)**
TYR	100225893	1.611	**0.005** (0.280)	0.803	0.119 (1.000)
TYRP1	100218715	-0.791	0.217 (1.000)	-3.931	**0.000 (0.000)**
WNT6	100230318	-0.605	0.145 (1.000)	-1.155	**0.036** (1.000)

A novel candidate gene for loss of sexual dichromatism in Zebra Finch plumage

Abstract

Sexual dimorphism is evolutionarily labile in many clades of organisms. Identifying the genetic mechanisms for transitions in sexual dimorphism could help explain this evolutionary lability. Here we investigated the genetic basis of loss of dimorphism in a domesticated color morph of the Zebra Finch (*Taeniopygia guttata*). The Blackcheek morph, a simple recessive autosomal mutation, has a sexually monomorphic black cheek patch, whereas the Wild-type Zebra Finch is sexually dimorphic in this trait. Using whole genome resequencing of Wild-type and Blackcheek finches, we identified a major peak of divergence between the morphs containing the coding sequences of ten genes. Two genes, GATD3A and Norrie Disease Protein or NDP, were differentially expressed in cheek feathers between the morphs. While GATD3A has no previous known link to pigmentation, NDP has previously been linked to pattern differences in bird plumage. NDP is a signaling molecule that could regulate the transcription of multiple melanogenesis genes, making it a strong candidate locus for this mutation. We describe patterns of gene expression in cheek feathers between the morphs and sexes of Zebra Finch, and provide hypotheses for how downregulation of NDP in the Blackcheek mutation may act to suppress sexual dimorphism in plumage pigmentation. This work demonstrates that a loss of sexual dimorphism in a single plumage ornament is possibly caused by a mutation changing the expression of a single gene. Thus sexual dimorphism can be lost repeatedly and rapidly in finches and other groups by relatively simple genetic changes.

Introduction

Sexual dimorphism is a pervasive phenomenon that can contribute substantially to morphological diversity in animals (Butler et al. 2007). Despite the constraint of a genome largely shared between the sexes, sexual dimorphism in many cases evolves rapidly in response to sexual and ecological selection (Zarkower 2001, Ellegren and Parsch 2007, Chenoweth and McGuigan 2010, Gordon and Ruvinsky 2012, Griffin et al.

2013). Comparative analyses have revealed that sexual dimorphism can be gained or lost repeatedly across closely related species (Wiens 2001). This pattern is found across the tree of life, but is particularly prominent in groups such as birds (Price and Eaton 2014), lizards (Wiens 1999), frogs (Bell and Zamudio 2012), and insects (Emlen et al. 2005). Such rapid change is likely a result of the evolutionary lability of the regulatory architecture generating sexual dimorphism, as well as strong selection on dimorphic traits (Chenoweth and McGuigan 2010). However, in many cases we still lack a detailed understanding of how, mechanistically, variation in sexual dimorphism arises. A more detailed understanding of the mechanistic underpinnings of sexual dimorphism is needed in a diversity of non-model organisms, such that we may understand the processes by which dimorphism may rapidly evolve (Zarkower 2001, Williams and Carroll 2009, Chenoweth and McGuigan 2010).

Sexually dimorphic pigmentation (or sexual dichromatism) in birds is an excellent study system for such work. We have a growing understanding of the mechanisms producing melanin, the most widespread biological pigment, fueled by long focus on melanin production in model organisms and disease research coupled with a relatively conserved developmental basis for melanogenesis across birds and mammals (Hill and McGraw 2006a,b, Hoekstra 2006, Hubbard et al. 2010, D'Alba and Shawkey 2019). The mechanisms by which pigmentation is regulated in sex-specific patterns to generate sexual dichromatism are still poorly understood, however. In some birds, plumage dichromatism appears to be controlled by levels of circulating gonadal or gonadotropic hormones (Kimball 2006). The precise mechanisms by which hormones are involved vary across species (Kimball 2006), a pattern observed in other animal groups that show hormone-mediated sexual dichromatism (Hayes 1997). Some sexually dichromatic birds do not appear to regulate their plumage pigmentation with sex hormones at all (Kimball 2006). Sexual dichromatism in bird plumage evolves rapidly in response to sexual and ecological selection pressures on both male and female plumage (Burns 1998, Badyaev and Hill 2003, Hill and McGraw 2006b, Hofmann et al. 2008, Price and Eaton 2014), showing that the mechanisms generating sexual dichromatism are flexible, and either easily gained, easily lost, or both.

We investigate here the genetic basis of a derived loss of sexual dichromatism in the plumage coloration of a songbird, the Zebra Finch (Estrildidae: *Taeniopygia guttata*). As in other avian groups, sexual dimorphism has evolved repeatedly in the Estrildid finches, with many close relatives of Zebra Finch being sexually monomorphic (Clement 1993, Forshaw and Shephard 2012, Gomes et al. 2016). Wild-type Zebra Finches are mostly gray with a pale belly, with males having additional black, brown, and orange plumage ornaments that females lack (**Figure 1**). In other estrildid finches, plumage dimorphism is regulated by gonadotropin hormones, with luteinizing hormone inducing colorful male-like plumage (Thapliyal and Tewary 1963, Kimball 2006). However, previous experiments have shown that in Zebra Finches, sexually dichromatic plumage is unresponsive to circulating hormone levels (Adkins-Regan et al. 1990; E Adkins-Regan, pers. comm.). As a result, Zebra Finches must have the sexual identity of feather follicles set by mechanisms other than circulating hormones, and could be fruitful targets of genetic studies looking for candidate loci associated with such regulation.

Domestic color morphs of Zebra Finches are an underutilized but potent source of genetic variation for investigating the genetic basis of loss of sexual dichromatism. Zebra Finches were domesticated c. 75 years ago, and a number of plumage mutations have arisen in captivity in the following decades (**Figure 1**; Landry 1997). Some of these mutations are pigment dilutions or knockouts, but, interestingly, some mutations generate pigment and pattern variation that mimics plumage variation found among related Estrildid finch species. In particular, several mutants (Blackcheek, Graycheek, Cheekless, Eumo, etc; **Figure 1**) represent a loss of sexual dimorphism. In these mutants, the cheek patch, an ornament that is sexually dimorphic in the Wild-type, is modified so that both sexes express similar cheek phenotypes. In some mutants (Cheekless, Eumo), males lose a cheek patch and resemble females in this trait, but maintain other sexually dimorphic plumage ornaments. In other mutants (Penguin, Graycheek, Blackcheek), females gain male-like cheek patches without gaining other sexually dimorphic ornaments expressed by the Wild-type male. These domestic mutants represent a powerful system for understanding the loci that underlie changes in sexual dichromatism of specific plumage elements, and they may shed light on the processes underlying rapid evolution of sexual dimorphism across other species in the family. Using domestic variation to understand

pigmentation in birds has been expanding, with recent efforts focusing on identifying the genetic basis for domestic variation that reflects wild phenotypes (Lopes et al. 2016, Mundy et al. 2016, Cooke et al. 2017, Vickrey et al. 2018).

Here we investigate the genetic basis of one specific plumage mutation – the Blackcheek Zebra Finch (**Figure 1**) – to better understand the genetic mechanisms that underlie derived losses of sexual dichromatism in birds. The Blackcheek mutation changes the Wild-type orange cheek patch in males (highly concentrated pheomelanin; McGraw and Wakamatsu 2004) to black in the mutant (highly concentrated eumelanin). The female mutant gains a black cheek patch, resembling the males, but otherwise remains dimorphic in the rest of the plumage. Thus, the Blackcheek mutant represents a loss of sexual dimorphism in one specific plumage patch, but not in the entire plumage, suggesting local regulatory control of dimorphism. Moreover, the mutant Blackcheek phenotype closely resembles phenotypes present in other Estrildid finches, such as the Black-cheeked Waxbill (*Estrilda charmosyna*) which has non-dimorphic black cheeks on a mostly gray plumage.

The Blackcheek mutation was discovered in the 1970's in Europe (Landry 1997). Breeders identified it as an autosomal recessive mutation (Landry 1997), and that simple Mendelian inheritance makes clear predictions for the patterns of genomic diversity and divergence in the causal locus. Selective breeding on a new recessive mutation should sweep the causal variant to fixation, resulting in long haplotypes with negligible nucleotide diversity in the causal region. This selection would result in allele frequency divergence (Fst) from the wild-type in the causal region, but no increase in absolute genetic divergence (Dxy) from the wild-type due to the mutation's recent origin within the domestic wild-type population (Cruickshank and Hahn 2014). Furthermore, because the phenotypic effects of this mutation are localized to specific plumage patches, we predict that a causal variant will be regulatory in nature, as coding mutations are more likely to be expressed more widely in the plumage. The causal Blackcheek variant is predicted to induce a number of gene expression changes relative to the wild-type in cheek feathers in both sexes due to a change in pigmentation from the wild-type in both sexes. These predictions make the Blackcheek mutation identifiable with a combination of genome scans and gene expression analysis. Thus, the two goals of this study are: 1)

use whole-genome sequencing to identify candidate loci for the Blackcheek mutation, and 2) use genome-wide patterns of gene expression to identify the regulatory changes in feather pigment production associated with the candidate genetic mutations.

Methods

Sample collection

We obtained Wild-type and Blackcheek Zebra Finches from commercial wholesalers. Birds were group housed and maintained by animal care staff at UIUC (IACUC Protocol #14134) and UMT (AUP Protocol #039-15) according to their standard procedures, including *ad libitum* food and water and a 12hr light/dark cycle. After at least 48hrs recovery from transport stress, we stimulated molt by manually plucking ten feathers from a small contiguous patch on the cheek of each individual. We determined through preliminary experiments that an optimal time for feather regrowth was eleven days, at which point the tip of the growing feather was just visible in the sheath, but the pigmented part of the feather was still growing and thus pigment production is still occurring. At the eleven day mark, birds were anesthetized with isoflurane and euthanized by cervical dislocation. The regrowing feather tissues were immediately removed as a contiguous patch, including the developing feathers, feather follicles, and skin surrounding them, but excluding mature feathers. Pectoral muscle tissue samples were also removed, and both feather and muscle tissues were snap frozen in liquid nitrogen. All tissues were subsequently stored at -80°C until extraction.

Genome sequencing and analysis

We extracted whole DNA for genomic analysis from pectoral muscle tissues for five males and five females each of Wild-type and Blackcheek finches (n = 20 total; n = 5/sex/morph). We extracted whole DNA with a QIAGEN DNeasy kit following manufacturer protocol. Library prep was conducted by Admera Health, LLC (South Plainfield, NJ, USA), using KAPA Hyper Prep Kits. The twenty individual genomes were sequenced by Admera Health in one multiplexed pool on two and half lanes of 2x150bp paired-end Illumina HiSeq X.

After demultiplexing, we trimmed adapter sequences, trimmed 5' and 3' ends of N's, dropped reads below 20bp in length, and filtered out reads below a Phred score of 15 averaged across 4bp windows using Trimmomatic v0.36 (Bolger et al. 2014). We merged paired-end reads overlapping more than 10bp with fewer than 2 mismatches using FLASH2 (Magoč and Salzberg 2011). We aligned sequences to the Zebra Finch reference genome (assembly taeGut3.2.4, Warren et al. 2010) with bowtie2 v2.3.4.3 (Langmead and Salzberg 2012) with the –very-sensitive-local option and default parameters. We then used Picard Tools v2.18.11 (Broad Institute 2018) to convert the aligned .sam files to .bam format, mark PCR duplicates, sort and index reads, and assign read groups.

We called variants for individual genomes separately with the function HaplotypeCaller in GATK v4.0.6.0 (McKenna et al. 2010, DePristo et al. 2011, Van der Auwera et al. 2013). Individual gvcf files were then combined with the CombineGVCFs function, and the variants were jointly recalled with the GenotypeGCVFs function. We hard filtered the jointly called variants following the GATK best practices ($QD < 2$, $FS > 60$, $MQ < 40$, $MQRankSum < -12.5$, $ReadPosRankSum < -8.0$; Van der Auwera et al. 2013). We filtered the joint variants further with vcftools v.0.1.16 (Danecek et al. 2011) for a minimum minor allele frequency of 0.1, a minimum mean read depth of 2, a maximum 30% missing data, and a minimum quality score of 20.

We used vcftools v0.1.16 (Danecek et al. 2011) to calculate nucleotide diversity (pi) and mean read depth per population, and Fst between Wild-type and Blackcheek, in 20kb sliding-windows with 10kb steps. We investigated smaller (10kb and 5kb) and non-overlapping window sizes and found qualitatively similar results. We Z-transformed the Fst values in R with the function scale. We calculated absolute divergence (Dxy) between Wild-type and Blackcheek finches with custom python scripts based on scripts by Simon Martin (https://github.com/simonhmartin/genomics_general). We phased haplotypes with beagle v4.1 (Browning and Browning 2007) and converted the phased vcf to a .hap and .map format via a custom python script for input into the R package rehh v2.0.2 (Gautier and Vitalis 2012). We used the functions *data2haplohh*, *scan_hh*, and *ies2xpehh* from rehh to calculate and plot the cross-population extended haplotype homozygosity (XP-EHH) across genomic regions of interest for Blackcheek vs Wild-type haplotypes.

Transcriptome sequencing and analysis

　　We extracted total RNA from frozen developing feather tissues using TRI Reagent (Sigma-Aldrich, St. Louis, MO, USA) following manufacturer protocols. We generated Illumina sequencing libraries following the Lohman et al. (2016) Tagseq protocol. We modified this protocol by including a custom oligo with a longer degenerate sequence for detecting PCR duplicates (sequence: ACC CCA TGG GGC TAC ACG ACG CTC TTC CGA TCT NNMWNN GGG). TagSeq libraries were multiplexed with Illumina index adapters and randomly divided into two normalized pools, each of which was sequenced on one lane of 100 nucleotide single-read Illumina HiSeq 2500 at Genomic Sequencing and Analysis Facility at University of Texas at Austin.

　　After demultiplexing, we used custom perl scripts (Matz 2017) and the FASTX-Toolkit (http://hannonlab.cshl.edu/fastx_toolkit/index.html) to remove PCR duplicates, trim adapter sequences, discard reads shorter than 20 nucleotides, trim poly-A tails, and set a minimum quality. We aligned reads to the Zebra Finch reference genome using bwa-mem v0.7.15-r1140 (Li and Durbin 2009, Li 2013). We used featureCounts v.1.5.2 (Liao et al. 2014) to generate read count tables for each library. These counts were then normalized by library size for analysis with the edgeR v.3.12.1 (Robinson et al. 2010, McCarthy et al. 2012) functions *calcNormFactors* and *cpm*.

　　We made six general comparisons of differentially expressed genes: differences between Wild-type and Blackcheek cheek feather expression (with sexes combined, and the two sexes analyzed separately), and differences between the sexes in cheek feather expression (with morphs combined, and the two morphs analyzed separately). We used the normalized read counts to test for differentially expressed genes (with the edgeR function exactTest and a False Discovery Rate of 0.05) in the whole transcriptome for these six comparisons. We converted Gene IDs to Ensembl Gene IDs with the db2db function on the biological Database network (Mudunuri et al. 2009), and tested each set of differentially expressed genes for gene ontology (GO) enrichment using g:Profiler (Reimand et al. 2016), using Taeniopygia guttata as the organism.

　　We repeated these analyses for two subsets of genes. First, we identified a list of individual candidate genes by presence in the divergence peaks identified in the genomic

analysis. Second, we identified the set of genes contained in the melanogenesis network, as identified with the KEGG melanogenesis network for *Taeniopygia guttata* (Kanehisa and Goto 2000, Kanehisa et al. 2016) with the addition of several novel candidate genes identified from the literature (**Table 1**). We tested these two sets of genes individually with t-tests in R for differential expression in the six population comparisons as above.

We examined patterns of correlated gene expression by conducting weighted gene coexpression network analysis on the normalized and log-transformed transcriptomes using WGCNA v.1.6.1 (Langfelder and Horvath 2008). We detected modules of coexpressed genes with the WGCNA function *blockwiseModules* with a soft-thresholding power of $\beta=6$ and default parameters. For each gene coexpression module, we treated the first axis of a principal components analysis of gene expression (PC1 or module eigengene) as a proxy for overall module expression, and tested for significant differences among the six population comparisons as above using t-tests. For gene coexpression modules that differed significantly in module expression between groups, we performed GO enrichment tests on the module gene lists as above.

Results

Zebra Finch genome sequencing resulted in mean coverage depth after filtering of 9.5X in the Wild-type and 8.4X in the Blackcheek morph. After filtering steps, a total of 15,338,353 single nucleotide polymorphisms (SNPs) were retained for analysis. Genome-wide mean nucleotide diversity was similar in both morphs (0.0040 in Wild-type vs 0.0045 in Blackcheek), suggesting that the Blackcheek mutant line is not more strongly inbred than the Wild-type lines. Mean genome-wide Fst between Wild-type and Blackcheek was relatively high, at 0.164, consistent with their being population structure across different captive-bred lines of finch (Hoffman et al. 2014). Sliding-window scans of Z-transformed Fst revealed a heterogenous landscape of divergence across the genome, with four peaks having a Z-score of five standard deviations above the genome-wide mean (**Figure 2**).

The largest and highest Fst peak was a 1Mb wide region located on Chromosome 1 (**Figure 3a**). This Fst peak is also associated with a peak of absolute divergence (measured as Dxy) between Wild-type and Blackcheek (**Figure 3b**). The cross-

100

population extended haplotype homozygosity scores (XP-EHH; **Figure 3c**) are strongly negative in this region, indicating that the Blackcheek mutant has longer inferred haplotypes in this region than Wild-type, consistent with recent artificial selection on this region in Blackcheek finches. Nucleotide diversity in this region was near the genome-wide average for Wild-type, but near zero for Blackcheek across the highest portion of the Fst peak (**Figure 3d**). Blackcheek nucleotide diversity across this region was among the lowest across the genome in the sliding-window analysis (**Figure 4**). There was no apparent difference in read depth between Wild-type and Blackcheek at this location, suggesting that the peak is not associated with a structural copy-number variant (**Figure 3e**). Although Fst is elevated in a much larger region of this chromosome (**Figure 3a**), we used the overlap of very low Blackcheek nucleotide diversity (**Figure 3d**) and the plateau of highest Fst values to narrow our focus to the 1Mb region from position 4,900,000-5,900,000 as the major divergence peak for further analysis. We identified ten genes located within this region, two of which were significantly differentially expressed between Wild-type and Blackcheek finches (**Table 2**, **Figure 5**).

Three other minor Fst peaks across the genome reached a Z-score of at least 5 (**Figures 6-8**). These peaks were much smaller in width (max 40kb), were not associated with read depth variation, and did not show differences in nucleotide diversity between Blackcheek and Wild-type (**Figures 6-8**). There were no annotated Zebra Finch genes within 1Mb upstream or downstream of the minor peak on Chromosome 1 (**Figure 6**). The first minor peak on Chromosome 1A (**Figure 7**) was located adjacent to two genes (KCND2 and LOC105758561), while the second minor peak on Chromosome 1A (**Figure 8**) was located entirely within the span of one gene (ST8SIA1). None of these three genes were significantly differentially expressed between Wild-type and Blackcheek or between the sexes (**Table 3**).

We scanned read depth across the genome to identify possible copy number variants between Wild-type and Blackcheek. We identified one narrow read depth variant, on Chromosome 1 (422000:425000), where the read depth in Wild-type peaks at 54X but Blackcheek read depth does not greatly exceed the genome-wide average of 9X. Using the Ensembl Zebra Finch genome browser, a TBLASTN scan of vertebrate cDNAs revealed this region to map to the mammalian heavy neurofilament (NF-H) gene, but this

gene is not annotated in Zebra Finch or Chicken genomes. We plotted raw read depth with our filtered transcriptome reads to this region to determine if an un-annotated gene was expressed at this location. We found an average of 0.2 reads per individual across this region in both morphs, indicating that NF-H is not functionally expressed in growing Zebra Finch feathers, and the copy number variant between Wild-type and Blackcheek at this location is unlikely to have functional significance in determining plumage coloration.

Weighted gene coexpression network analysis of Zebra Finch cheek expression identified 32 coexpression modules, ranging in size from 70 - 3,739 genes in each module and assigning 84.9% of annotated Zebra Finch genes to a module (**Table 4**). Four modules showed significantly different expression between Blackcheek and Wild-type, while two modules showed significant differences in module expression between the sexes in both morphs (**Table 4**). GO terms that are significantly enriched in these six differentially expressed modules are summarized in **Table 5** (no GO term was enriched for ME12 or ME29). One module, ME18, was significantly enriched for melanin biosynthesis, containing the melanin-related genes NDP, TYRP1, and OCA2. This module was significantly different in its expression between morphs but not between the sexes (**Table 4**). Similarly, genes differentially expressed between morphs are significantly enriched for melanin biosynthesis, but only in males (**Table 5**). Overall gene expression changes across the melanogenesis network, both between morphs and between sexes, are summarized in **Figure 9**.

Discussion

Identifying the genetic and regulatory architecture of sexual dimorphism can help us understand how sexual dimorphism may be so evolutionary labile (Zarkower 2001, Williams and Carroll 2009, Chenoweth and McGuigan 2010). We used a combination of genomic and transcriptomic data to identify a candidate locus for the Blackcheek mutation, a derived loss of sexually dimorphic pigmentation in Zebra Finches (**Figure 1**). The Blackcheek mutation has been identified by breeders as a recessive autosomal locus (Landry 1997), which predicts that the causal mutation is fixed in Blackcheek. Such recessive mutations in finches are likely to be line-bred and maintained as separate

102

stocks, producing inbreeding and population structure as in other Zebra Finch morphs (Hoffman et al. 2014). Thus, we predicted our Blackcheek individuals would be homozygous for the causal recessive haplotype, with reduced genetic diversity and longer haplotypes relative to Wild-type stock due to artificial selection on this mutation. Our analysis of genomic divergence between Wild-type and Blackcheek Zebra Finches revealed a heterogenous genomic landscape with multiple divergence peaks and a relatively high mean genome-wide Fst between populations, consistent with inbreeding generating population structure between these morphs. However, of the divergence peaks, only the largest and most divergent peak on Chromosome 1 combines elevated Fst between populations with higher extended haplotype homozygosity and substantially reduced nucleotide diversity in the Blackcheek (**Figure 3**).

These results suggest the major divergence peak on Chromosome 1 is the causal locus of the Blackcheek mutation. Of the ten genes located within this divergence peak, only two show differential expression between Wild-type and Blackcheek cheek feathers in either sex (**Table 2**). The gene GATD3A is more highly expressed in Blackcheek relative to Wild-type, while the gene NDP is under-expressed in Blackcheek (**Figure 5**). GATD3A, or glutamine amidotransferase like class 1 domain containing 3A, is a an ubiquitously expressed mitochondrial protein whose function is uncharacterized, and no link to pigmentation has previously been noted (Scott et al. 1997, Shin et al. 2004). Conversely, expression variation in the gene NDP (Norrie Disease Protein) has recently been linked to melanin-based pigment patterns in birds (Poelstra et al. 2015, Vickrey et al. 2018) and is thus a plausible candidate locus for the Blackcheek mutation.

NDP is a ligand of the Frizzled-4 (FZD4) receptor, which triggers the canonical Wnt/β-catenin signaling cascade (Hendrickx and Leyns 2008). NDP/FZD4 signaling has been implicated in multiple developmental roles. It is associated with development of vascularization in retina (Xu et al. 2004), ear (Xu et al. 2004), and uterus (Luhmann et al. 2005). It also has a role in neural progenitor cell proliferation in the retina (McNeill et al. 2013). NDP is involved in early embryonic axis specification in *Xenopus*, both through trigging of the Wnt signaling cascade and through mutual inactivation of other major signaling molecules like TGF-B and BMP (Xu et al. 2012). In these signaling contexts, NDP serves as an alternative FZD4 ligand to traditional Wnt signals, and can produce a

103

signaling effect independent of those produced by Wnt (Junge et al. 2009). NDP/FZD4 thus represents a versatile signaling module, potentially capable of being redeployed in multiple novel contexts during development.

NDP as a regulator of pigmentation

Recently, expression variation in NDP has been tied to melanin plumage patterning in crows (Poelstra et al. 2015) and pigeons (Vickrey et al. 2018). A copy-number variant in domestic pigeon breeds leads to over-expression of NDP, resulting in more dark barring on the wing through production of extra eumelanin on the wing covert feathers (Vickrey et al. 2018). Additionally, a missense mutation in NDP leads to patternless wings (lacking dark bars) in another pigeon breed (Vickrey et al. 2018). These mutations are known to have deleterious pleiotropic effects in these two pigeon breeds, including defects in vision and reproduction, consistent with the other known functions of NDP during development (Vickrey et al. 2018). NDP gene expression differences are associated with plumage patterning differences between two species of crows, where NDP is under-expressed in gray plumage relative to black (Poelstra et al. 2015). These two studies, combined with our data presented here, show that NDP expression is associated with plumage pigmentation in different contexts in different species, consistent with its role as a versatile signaling molecule.

The precise mechanisms by which NDP could regulate melanin pigmentation are not yet known, but we can make certain predictions based on review of melanogenesis pathways. Briefly, melanins are produced in specialized organelles, melanosomes, inside specialized cells, melanocytes. The two most common types of melanin used in integumentary pigmentation are black eumelanin and reddish-brown pheomelanin, and both are constructed from tyrosine as a precursor (D'Alba and Shawkey 2019). An initial rate-limiting step converts tyrosine to the intermediate dopaquinone with the enzyme tyrosinase (TYR). Dopaquinone is further converted to eumelanin through the actions of the enzymes tyrosinase-related protein 1 (TYRP1) and dopachrome tautomerase (DCT), or pheomelanin in the presence of cysteine (D'Alba and Shawkey 2019). Regulation of which melanin is produced is largely a function of the melanosome concentrations of TYR and cysteine (which is essential for pheomelanin but not eumelanin): higher TYR or

lower cysteine concentrations lead to higher production of eumelanin (Smit et al. 1997). Cysteine concentrations may be regulated in part by Slc7a11, a membrane-bound cysteine transporter in melanocytes (Chintala et al. 2005). TYR function and concentration in the melanosome is likely regulated by oculocutaneous albinism II gene (OCA2), a membrane-bound transporter localized to the melanosome and endoplasmic reticulum (Potterf et al. 1998, Brilliant 2001, Manga et al. 2001, Chen et al. 2002, Staleva et al. 2002, Toyofuku et al. 2002, Visser et al. 2014). Transcription of OCA2, and all three melanogenesis enzymes are all regulated by a major hub transcription factor, Microphthalmia-associated transcription factor or MITF (Cheli et al. 2009). MITF is itself regulated by at least three signaling cascades in the melanocyte (Figure 6), one of which is the canonical Wnt signaling cascade. The Wnt cascade acts through the intermediate transcription factors LEF1, TCF7, and TCF7L2, which regulate MITF (LEF1 also regulates OCA2 directly; Visser et al. 2014).

A functional hypothesis for NDP's role in pigmentation must explain how reduced NDP expression results in higher expression of eumelanin. In male Zebra Finches, the Blackcheek mutant changes the Wild-type orange cheek, which contains highly concentrated pheomelanin (McGraw and Wakamatsu 2004) into a black cheek, which contains high concentrations of eumelanin. In females, this mutation changes a gray cheek (low eumelanin) to a black cheek (high eumelanin). NDP, and its co-receptor LRP5, are both under-expressed in Blackcheek, likely leading to reduced activation of the Wnt signaling cascade even though the main receptor FZD4 is over-expressed in Blackcheek. There is no change in expression by morph or sex in the main regulator of melanogenesis, MITF, which is perhaps not surprising due to its central position as a regulator of dozens of other genes (Cheli et al. 2009, Poelstra et al. 2015). One target of MITF, the enzyme, TYRP1, is upregulated in Blackcheek, consistent with higher production of black eumelanin (it is similarly upregulated when comparing other plumage colors to black feathers: **Chapter 2**). However, the rate-limiting step in switching from pheomelanogenesis to eumelanogenesis is the relative concentrations of TYR and cysteine. Contrary to expectations, TYR is not upregulated in Blackcheek, and SLC7A11, which transports cysteine into the cell, is not downregulated. However, OCA2, is upregulated in Blackcheek, as it is in Wild-type black feathers when compared

to other plumage colors (**Chapter 2**). Upregulation of OCA2 could facilitate additional transport of tyrosinase into the melanosome and facilitate tyrosinase function through regulation of melanosome pH, stimulating additional eumelanogenesis, even in the absence of increased TYR transcription (Potterf et al. 1998, Manga et al. 2001, Chen et al. 2002, Toyofuku et al. 2002, Visser et al. 2014).

OCA2 is a target of Wnt signaling activation in melanocytes, and therefore regulation of melanogenesis through OCA2 expression is a plausible hypothesis for linking NDP signaling to pigment production. However, we note two caveats to this hypothesis. First, although Blackcheek mutants expresses less NDP and thus potentially less Wnt signaling activation, OCA2 expression is increased. Second, previous studies in both pigeons (Vickrey et al. 2018) and crows (Poelstra et al. 2015) found higher NDP expression is associated with increased eumelanin pigmentation, the opposite pattern of what we found in Zebra Finches. We note that OCA2 has multiple regulators, and is targeted both by Wnt signaling directly through the transcription factor LEF1 and indirectly by MITF, which is regulated by additional signaling pathways (**Figure 9**; Visser et al. 2014). Thus there are multiple pathways by which NDP could regulate melanogenesis target genes. An alternative hypothesis is that a reduction in NDP signaling could be compensated for by an increase in Wnt-activated signaling of the same pathways. We note that some Wnt signals are upregulated and some Frizzled receptors are downregulated in the Blackcheek mutant (**Figure 9**), indicating potential shifts in Wnt activated signaling in addition to the reduction in NDP. Thus, a reduction of NDP may not necessarily lead to an overall reduction of Wnt activated signaling, but instead, to a shift in its regulation or that of its transcriptional targets (Junge et al. 2009). Clearly, further study is needed to elucidate these signaling mechanisms and provide clearer functional links between signal activators and pigment production.

Tissue- and sex-specific regulation of pigmentation through NDP

There are clear hypotheses for how NDP expression might be involved in generating pigmentation variation. It is less clear how downregulation of NDP in the Blackcheek mutant might lead to loss of dichromatism in specific plumage patches. The phenotypic effects of the Blackcheek mutation are localized to specific plumage patches,

as are NDP mutations in pigeons (Vickrey et al. 2018). However, NDP expression in pigeon mutants is elevated across the plumage, not just in the wing patch with pattern differences (Vickrey et al. 2018). This strongly implies that NDP expression is interacting with other tissue-specific *cis*- or *trans*- elements, such that global change in NDP expression is only manifested as a phenotypic pigmentation change in one patch. Since we only have expression data for cheek feathers, we cannot assess whether Blackcheek NDP expression is reduced solely in the cheek feathers, or is reduced systematically throughout the mutant finch plumage. Blackcheek males also exhibit darkened flank coloration (**Figure 1**; Landry 1997), suggesting that the phenotypic effects of the NDP mutation may not only localized to the cheek. However, unlike in pigeons (Vickrey et al. 2018), pleiotropic effects on vision or reproduction have not been described in Blackcheek finches (Landry 1997). Additional study is needed to investigate the systemic and tissue-specific effects of changing NDP expression.

NDP expression is not sexually dimorphic in the growing cheek feathers of either morph (**Table 2**), so it is not intuitive how downregulation of NDP expression may drive a loss in sexual dimorphism. One possibility is that changing levels of NDP expression interact with other sexually dimorphic loci. We did not detect sex differences in expression in the known regulators or co-receptors of NDP/FZD4 (**Table 1**). In the Wnt signaling cascade downstream of NDP/FZD4, one gene, GNAQ, is significantly different between the sexes (being over-expressed in males) and is the only melanogenesis pathway gene to be significantly different between the sexes in both morphs. GNAQ is over-expressed in males in other Wild-type plumage patches as well (**Chapter 2**), and there is no difference between Wild-type and Blackcheek in this sex bias. Interestingly, this gene forms a potential branching point in canonical Wnt signaling and could hypothetically drive sex-specific differences in the expression of targets of Wnt signaling (discussed in **Chapter 2**). Therefore, one hypothesis for loss of dimorphism in Blackcheek is that changing levels of NDP-activated Wnt signaling could act through sex-biased GNAQ expression to produce differential expression downstream in the signaling cascade in males, even though the expression of NDP itself is not sexually dimorphic. Reduction of NDP expression in the Blackcheek mutant could then remove

those sex-specific responses. More work is needed to elucidate if GNAQ is operating in such a fashion in Zebra Finch melanocytes.

Two additional melanogenesis genes show sex-specific gene expression. KIT, which initiates a MAPK signaling pathway, is over-expressed in Wild-type males but is not dimorphic in expression in Blackcheek. CREB3, an intermediate step in cAmp-dependent signaling, is not divergent between the sexes in Wild-type, but is overexpressed in Blackcheek males. Both pathways regulate MITF, neither shows downstream sex-specific expression differences, and neither are known targets of NDP signaling. Thus, we currently lack direct evidence for how, mechanistically, NDP expression can be a driver of sexual dimorphism in developing feather gene expression.

The link between NDP expression and sexual dimorphism could be investigated further in future work by considering the timing of sexual divergence in pigmentation. Juvenile Zebra Finches have a female-like plumage and sexes are indistinguishable until the molt into adult plumage, whereupon male finches develop their sex-specific plumage ornaments. In the Blackcheek mutation, the black cheeks in both sexes are present even in the juvenile stage, whereas the other sexually dichromatic ornaments develop in adult plumage as normal (Landry 1997). Upon reaching adulthood, the sexual dimorphism in plumage is set, and unresponsive to sex hormone manipulations as it is in some other sexually dichromatic bird species (Adkins-Regan et al. 1990; E Adkins-Regan, pers. comm.). It seems then that the Blackcheek mutation is acting to change the 'base' plumage in both sexes, and prevents the onset of sexual development in cheek patch of the male. Investigating gene expression patterns before and after the onset of sexual development could be fruitful in identifying these processes, and provide better links between NDP expression, sexual dimorphism, and pigmentation.

Origin of the Blackcheek mutation

The major divergence peak containing NDP on Chromosome 1 has many of the population genetic signatures associated with a new recessive mutation undergoing selective breeding (namely, low nucleotide diversity, high Fst relative to the wild-type, and longer haplotypes). However, the Chromosome 1 divergence peak is also associated with a peak in absolute divergence (Dxy; **Figure 3b**), inconsistent with a recent origin of

a *de novo* mutation. Since Dxy is expected to scale with mutation rate, elevated Dxy could result from an elevated mutation rate in the region of the divergence peak (Nei 1987, Cruickshank and Hahn 2014), but this explanation seems unlikely for such a large region. Alternatively, the Dxy peak could indicate an area of the Blackcheek genome with an older divergence time from the wild-type genomic background relative to the rest of the Blackcheek genome (Cruickshank and Hahn 2014). The latter explanation conflicts with the relatively recent (1970's) origin of Blackcheek from captive stock (Landry 1997) but details of this origin are scarce.

Distinguishing among these hypotheses will require additional analyses. The effect of mutation rate on Dxy can be controlled with a relative node depth test, in which Dxy is scaled to an outgroup (Feder et al. 2005, Cruickshank and Hahn 2014). If a divergence peak occurs in relative node depth as well as Dxy, a mutational origin is unlikely. Whole genomes are now available for other estrildid finches, such as the Bengalese Finch (*Lonchura striata*; Colquitt et al. 2018), as well as more distantly related bird species, which could provide suitable outgroups for this test.

An older divergence time for the Blackcheek haplotype relative to the rest of the Blackcheek mutation can be explained by two hypotheses. One is that the Blackcheek mutation is derived from old standing variation within Zebra Finch, which was only recently identified by breeders and selected for. Recessive traits can segregate within a population at low frequency, and this type of ancestral polymorphism could explain the Dxy pattern observed in Blackcheek. However, the Blackcheek phenotype has not been observed among wild Zebra Finches to the best of our knowledge. The alternative hypothesis is that the Blackcheek mutation was introgressed through hybridization in captivity with another finch species. Although this has not been recorded in the literature for Zebra Finch morphs, color phenotypes introgressed from other species through selective breeding has been documented in canaries (Lopes et al. 2016) and pigeons (Vickrey et al. 2018).

Distinguishing introgression from standing variation can be accomplished through a combination of haplotype dating (Vickrey et al. 2018) and topology-based tests. Multiple Estrildid finches have black cheeks, masks, or hoods (Clement 1993) and could be candidates for introgression. Of those species more commonly found in captivity, the

Black-cheeked Waxbill (*Estrilda charmosyna*) is most similar in phenotype to the Blackcheek mutation in that it has sexually monomorphic black cheeks. Luckily, the phylogeny of Estrildidae and the available genomic resources make a topology test of introgression straightforward. Zebra Finch is a member of the Australian grassfinch clade of Estrildid finches, which is sister to the two remaining groups of Estrildids, the manikins and waxbills (Gomes et al. 2016). All of the Estrildid species with black cheeks, masks, or hoods fall into these latter two clade, as well as the other sequenced estrildid genome (*Lonchura*; Colquitt et al. 2018). Therefore, a topology-based scan test across the genome with wild-type and Blackcheek Zebra Finches, *Lonchura*, and a non-Estrildid outgroup would reveal one of two patterns: the two Zebra Finch alleles would be each others closest relatives across most of the genome, whereas the Blackcheek allele would be more closely related to the *Lonchura* allele if it introgressed from a species in that clade. Conducting these tests will be important in future work to determine the evolutionary origin of the Blackcheek mutation in Zebra Finches.

Conclusion

Sexual dimorphism is gained and lost rapidly in many organisms (Wiens 2001). Here, we have presented evidence that these changes can be induced by a simple mutation that changes the regulation of one signaling pathway gene. The derived loss of sexual dimorphism in one plumage ornament in Zebra Finch is caused by a simple recessive autosomal mutation that causes a reduction in expression of the gene NDP. We discussed plausible hypotheses for how NDP expression may act on melanin pigmentation in the mutant finch, and how NDP-induced signaling pathways may be able to induce sexual dimorphism. This work adds to a growing body of literature supporting a role for NDP in regulation of melanin in birds (i.e. Poelstra et al. 2015, Vickrey et al. 2018). The exact mechanisms by which NDP acts on melanin production remain to be fully elucidated, but this system may be explored further to investigate those mechanisms.

First, a backcross breeding design could be useful for fine-scale mapping of the Blackcheek causal mutation and allele-specific expression, narrowing in on cis- and trans-acting factors regulating NDP expression. Gene expression studies should

additionally be expanded to other plumage patches, allowing further insight into tissue-specific regulation, and to earlier developmental stages to identify the establishment of sex-specific pigmentation at different stages. Additional candidate genes for sexual dichromatism in Zebra Finches can be identified by repeating these approaches in other morphs that present simple Mendelian loci for sexual pigmentation changes (**Figure 1**; Landry 1997). A combined look at sex-specific regulatory structures and tissue-specific regulation and development of pigmentation phenotypes in these finches will aid in the understanding the mechanisms of sexual dichromatism, and will aid the ultimate goal of understanding the evolution of such variation in the diversity of wild species (**Figure 1**; Zarkower 2001, Williams and Carroll 2009, Chenoweth and McGuigan 2010).

Acknowledgements

References

Adkins-Regan, E, M Abdelnabi, M Mobarak, and MA Ottinger (1990) Sex steroid levels in developing and adult male and female zebra finches (Poephila guttata). *General and Comparative Endocrinology* **78**:93-109.

Badyaev, AV, and GE Hill (2003) Avian sexual dichromatism in relation to phylogeny and ecology. *Annual Review of Ecology Evolution and Systematics* **34**:27-49.

Bell, RC, and KR Zamudio (2012) Sexual dichromatism in frogs: natural selection, sexual selection and unexpected diversity. *Proceedings of the Royal Society of London B* **279**:4687-4693.

Bolger, AM, M Lohse, and B Usadel (2014) Trimmomatic: a flexible trimmer for Illumina sequence data. *Bioinformatics* **30**:2114-2120.

Brilliant, M.H. (2001). The mouse p (pink-eyed dilution) and human P genes, oculocutaneous albinism type 2 (OCA2), and melanosomal pH. *Pigment Cell Research* **14**:86–93.

Broad Institute (2018) Picard Tools v.2.18.11 http://broadinstitute.github.io/picard/

Browning, SR, and BL Browning (2007) Rapid and accurate haplotype phasing and missing-data inference for whole-genome association studies by use of localized haplotype clustering. *The American Journal of Human Genetics* **81**:1084-1097.

Burns, KJ (1998) A phylogenetic perspective on the evolution of sexual dichromatism in tanagers (Thraupidae): the role of female versus male plumage. *Evolution* **52**:1219-1224.

Butler, MA, SA Sawyer, and JB Losos (2007) Sexual dimorphism and adaptive radiation in *Anolis* lizards. *Nature* **447**:202-205.

Cheli, Y, M Ohanna, R Ballotti, and C Bertolotto (2009) Fifteen-year quest for microphthalmia-associated transcription factor target genes. *Pigment Cell Melanoma Research* **23**:27-40.

Chen, K., Manga, P., and Orlow, S.J. (2002). Pink-eyed dilution protein controls the processing of tyrosinase. *Molecular Biology of the Cell* **13**:1953–1964.

Chenoweth, SF, and K McGuigan (2010) The genetic basis of sexually selected variation. *Annual Review of Ecology, Evolution, and Systematics* **41**:81-101.

Chintala, S, W Li, ML Lamoreux, S Ito, K Wakamatsu, EV Sviderskaya, DC Bennett, Y-M Park, WA Gahl, M Huizing, RA Spritz, S Ben, EK Novak, J Tan, and RT Swank (2005) Slc7a11 gene controls production of pheomelanin pigment and proliferation of cultured cells. *PNAS* **102**:10964-10969.

Clement, P (1993) *Finches & Sparrows: An Identification Guide*. Princeton University Press.

Colquitt, BM, DG Mets, and MS Brainard (2018) Draft genome assembly of the Bengalese finch, Lonchura striata domestica, a model for motor skill variability and learning. *GigaScience* **7**:giy008

Cooke, TF, CR Fischer, P Wu, T-X Jiang, KT Xie, J Kuo, E Doctorov, A Zehnder, C Khosla, C-M Chuong, and CD Bustamante (2017) Genetic mapping and biochemical basis of yellow feather pigmentation in budgerigars. *Cell* **171**:427-439.

Cruickshank, TE, and MW Hahn (2014) Reanalysis suggests that genomic islands of speciation are due to reduced diversity, not reduced gene flow. *Molecular Ecology* **23**:3133-3157.

D'Alba, L, and MD Shawkey (2019) Melanosomes: biogenesis, properties, and evolution of an ancient organelle. *Physiological Reviews* **99**:1-19.

Danecek, P, A Auton, G abecasis, CA Albers, E Banks, MA DePristo, R Handsaker, G Lunter, GT Marth, ST Sherry, G McVean, R Durbin, and 1000 Genomes Project Analysis Group (2011) The variant call format and VCFtools. *Bioinformatics* **27**:2156-2158.

DePristo, MA, E Banks, R Poplin, KV Garimella, JR Maguire, C Hartl, AA Philippakis, G del Angel, MA Rivas, M Hanna, A McKenna, TJ Fennell, AM Kernytsky, AY Sivachenko, K Cibulskis, SB Gabriel, D Altshuler, and MJ Daly (2011) A framework for variation discovery and genotyping using next-generation DNA sequencing data. *Nature Genetics* **43**:491-498.

Ellegren, H, and J Parsch (2007) The evolution of sex-biased genes and sex-biased gene expression. *Nature Reviews Genetics* **8**:689-698.

Emlen, DJ, J Hunt, and LW Simmons (2005) Evolution of sexual dimorphism and male dimorphism in the expression of beetle horns: phylogenetic evidence for modularity, evolutionary lability, and constraint. *The American Naturalist* **166**:S42-S68.

Feder, JL, X Xie, J Rull, S Velez, A Forbes, B Leung, H Dambroski, KE Filchak, and M Aluja (2005) Mayr, Dobzhansky, and Bush and the complexities of sympatric speciation in Rhagoletis. *Proceedings of the National Academy of Science* **102**:6573-6580.

Forshaw, JM, and M Shephard (2012) *Grassfinches in Australia*. CSIRO Publishing.

Gautier, M, and R Vitalis (2012) rehh: an R package to detect footprints of selection in genome-wide SNP data from haplotype structure. *Bioinformatics* **28**:1176-1177.

Gomes, ACR, MD Sorenson, and GC Cardoso (2016) Speciation is associated with changing ornamentation rather than stronger sexual selection. *Evolution* **70**:2823-2838.

Gordon, KL, and I Ruvinsky (2012) Tempo and mode in evolution of transcriptional regulation. *PLoS Genetics* **8**:e1002432

Griffin, RM, R Dean, JL Grace, P Ryden, and U Friberg (2013) The shared genome is a pervasive constraint on the evolution of sex-biased gene expression. *Molecular Biology and Evolution* **30**:2168-2176.

Hayes, TB (1997) Hormonal mechanisms as potential constraints on evolution: examples from the Anura. *Integrative and Comparative Biology* **37**:482-490.

Hendrickx, M, and L Leyns (2008) Non-conventional Frizzled ligands and Wnt receptors. *Development, Growth, and Differentiation* **50**:229-243.

Hill, GE, and KJ McGraw (2006a) *Bird Coloration Volume I: Mechanisms and Measurement*. Harvard University Press, Cambridge, MA, USA.

Hill, GE, and KJ McGraw (2006b) *Bird Coloration Volume II: Function and Evolution*. Harvard University Press, Cambridge, MA, USA.

Hoekstra, HE (2006) Genetics, development and evolution of adaptive pigmentation in vertebrates. *Heredity* **97**:222-234.

Hoffman, JI, ET Krause, K Lehmann, and O Kruger (2014) MC1R genotype and plumage colouration in the Zebra Finch (Taeniopygia guttata): population structure generates artefactual associations. *PLoS ONE* **9**:e86519

Hofmann, CM, TW Cronin, and KE Omland (2008) Evolution of sexual dichromatism. 1. Convergent losses of elaborate female coloration in New World orioles (Icterus spp.). *The Auk* **125**:778-789.

Hubbard, JK, JAC Uy, ME Hauber, HE Hoekstra, and RJ Safran (2010) Vertebrate pigmentation: from underlying genes to adaptive function. *Trends in Genetics* **26**:231-239.

Jeronimo, S, M Khadraoui, D Wang, K Martin, JA Lesku, KA Robert, E Schlicht, W Forstmeier, and B Kempenaers (2018) Plumage color manipulation has no effect on social dominance or fitness in zebra finches. *Behavioral Ecology* **29**:459-467.

Jones, MR, LS Mills, PC Alves, CM Callahan, JM Alves, DJR Lafferty, FM Jiggins, JD Jensen, J Melo-Ferreira, and JM Good (2018) Adaptive introgression underlies polymorphic seasonal camouflage in snowshoe hares. *Science* **360**:1355-1358.

Junge, HJ, S Yang, JB Burton, K Paes, X Shu, DM French, M Costa, DS Rice, and W Ye (2009) TSPAN12 regulates retinal vascular development by promoting Norrin- but not Wnt-induced FZD4/B-Catenin signaling. *Cell* **139**:299-311.

Kanehisa, M, and S Goto (2000) KEGG: Kyoto Encyclopedia of Genes and Genomes. *Nucleic Acids Research* **28**:27-30.

Kanehisa, M, Y Sato, M Kawashima, M Furumichi, and M Tanabe (2016) KEGG as a reference resource for gene and protein annotation. *Nucleic Acids Research* **44**:D457-D462.

Kimball, RT (2006) Hormonal control of coloration. In: Hill, GE, and KJ McGraw (2006a) *Bird Coloration Volume I: Mechanisms and Measurement*. Harvard University Press, Cambridge, MA, USA.

Landry, G (1997) *An Almost complete Guide to: The Varieties and Genetics of the Zebra Finch*. 3rd Edition: 2017. Poule d'eau Publishing, Franklin, Louisiana, USA.

Langfelder, P, and S Horvath (2008) WGCNA: an R package for weighted correlation network analysis. *BMC Bioinformatics* **9**:559

Langmead, B, and SL Salzberg (2012) Fast gapped-read alignment with Bowtie 2. *Nature Methods* **9**:357-359.

Li, H (2013) Aligning sequence reads, clone sequences and assembly contigs with BWA-MEM. *arXiv*:1303.3997v2 [q-bio.GN]

Li, H, and R Durbin (2009) Fast and accurate short read alignment with Burrows-Wheeler transform. *Bioinformatics* **25**:1754-1760.

Liao, Y, GK Smyth, and W Shi (2014) featureCounts: an efficient general purpose program for assigning sequence reads to genomic features. *Bioinformatics* **30**:923-930.

Lohman, BK, JN Weber, and DI Bolnick (2016) Evaluation of TagSeq, a reliable low-cost alternative for RNAseq. *Molecular Ecology Resources* **16**:1315-1321.

Lopes, RJ, JD Johnson, MB Toomey, MS Ferreira, PM Araujo, J Melo-Ferreira, L Andersson, GE Hill, JC Corbo, and M Carniero (2016) Genetic basis for red coloration in birds. *Current Biology* **26**:1427-1434.

Luhmann, UFO, D Meunier, W Shi, A Lüttges, C Pfarrer, R Fundele, and W Berger (2005) Fetal loss in homozygous mutant Norrie disease mice: a new role of Norrin in reproduction. *Genesis: The Journal of Genetics and Development* **42**:253-262.

Magoč, T, and SL Salzberg (2011) FLASH: fast length adjustment of short reads to improve genome assemblies. *Bioinformatics* **27**:2957-2963.

Manga, P., Boissy, R.E., Pifko-Hirst, S., Zhou, B.K., and Orlow, S.J. (2001). Mislocalization of melanosomal proteins in melanocytes from mice with oculocutaneous albinism type 2. *Experimental Eye Research* **72**:695–710.

Matz, M (2017) Genome-wide gene expression profiling with tag-based RNA-seq (TagSeq). Github repository: https://github.com/z0on/tag-based_RNAseq

McCarthy, DJ, Y Chen, and GK Smyth (2012) Differential expression analysis of multifactor RNA-Seq experiments with respect to biological variation. *Nucleic Acids Research* **40**:4288-4297.

McGraw, KJ, and K Wakamatsu (2004) Melanin basis of ornamental feather colors in male Zebra Finches. *The Condor* **106**:686-690.

McKenna, A, M Hanna, E Banks, A Sivachenko, K Cibulskis, A Kernytsky, K Garimella, D Altshuler, S Gabriel, M Daly, and MA DePristo (2010) The Genome Analysis Toolkit: A MapReduce framework for analyzing next-generation DNA sequencing data. *Genome Research* **20**:1297-1303.

McNeill, B, C Mazerolle, EA Bassett, AJ Mears, R Ringuette, P Lagall, DJ Picketts, K Paes, D Rice, and VA Wallace (2013) Hedgehog regulates Norrie disease protein to drive neural progenitor self-renewal. *Human Molecular Genetics* **22**:1005-1016.

Mudunuri, U, A Che, M Yi, and RM Stephens (2009) bioDBnet: the biological database network. *Bioinformatics* **25**:555-556.

Mundy, NI, J Stapley, C Bennison, R Tucker, H Twyman, K-W Kim, T Burke, TR Birkhead, S Andersson, and J Slate (2016) Red carotenoid coloration in the Zebra Finch is controlled by a cytochrome P450 gene cluster. *Current Biology* **26**:1-6.

Nei, M (1987) *Molecular Evolutionary Genetics*. Columbia University Press, New York.

Poelstra, JW, N Vijay, MP Hoeppner, and JBW Wolf (2015) Transcriptomics of colour patterning and coloration shifts in crows. *Molecular Ecology* **24**:4617-4628.

Potterf, S.B., Furumura, M., Sviderskaya, E.V., Santis, C., Bennett, D.C., and Hearing, V. (1998). Normal tyrosine transport and abnormal tyrosinase routing in pink-eyed dilution melanocytes. *Experimental Cell Research* **244**:319–326.

Price, JJ, and MD Eaton (2014) Reconstructing the evolution of sexual dichromatism: current color diversity does not reflect past rates of male and female change. *Evolution* **68**:2026-2037.

Reimand, J, T Arak, P Adler, L Kolberg, S Reisberg, H Peterson, J Vilo (2016) g:Profiler – a web server for functional interpretation of gene lists (2016 update). *Nucleic Acids Research* **44**:W83-W89.

Robinson, MD, DJ McCarthy, GK Smyth (2010) edger: a Bioconductor package for differential expression analysis of digital gene expression data. *Bioinformatics* **26**:139-140.

Scott, HS, H Chen, C Rossier, MD Lalioti, SE Antonarakis (1997) Isolation of a human gene (HES1) with homology to an Escherichia coli and a zebrafish protein that maps to chromosome 21q22.3. *Human Genetics* **99**:616-623.

Shin, J-H, R Weitzdoerfer, M Fountoulakis, and G Lubec (2004) Expression of cystathionine β-synthase, pyridoxal kinase, and ES1 protein homolog (mitochondrial precursor) in fetal Down syndrome brain. *Neurochemistry International* **45**:73-79.

Smit, NP, HVan der Meulen, HK Koerten, RM Kolb, AM Mommaas, EG Lentjes, and S Pavel (1997) Melanogenesis in cultured melanocytes can be substantially influenced by L-tyronsine and L-cysteine. *The Journal of Investigative Dermatology* **109**:796-800

Staleva, L., Manga, P., and Orlow, S.J. (2002). Pink-eyed dilution protein modulates arsenic sensitivity and intracellular glutathione metabolism. *Mol. Biol. Cell* **13**, 4206–4220

Thapliyal, JP, and PD Tewary (1963) Effect of estrogen and gonadotropic hormones on the plumage pigmentation in Lal Munia (Estrilda amandava). *Naturwissenschaften* **50**:529.

Toyofuku, K., Valencia, J.C., Kushimoto, T., Costin, G.E., Virador, V.M., Vieira, W.D., Ferrans, V.J., and Hearing, V.J. (2002). The etiology of oculocutaneous albinism (OCA) type II: the pink protein modulates the processing and transport of tyrosinase. *Pigment Cell Research* **15**:217–224.

Van der Auwera, GA, MO Carneiro, C Hartl, R Poplin, G del Angel, A Levy-Moonshine, T Jordan, K Shakir, D Roazen, J Thibault, E Banks, KV Garimella, D Altshuler, S Gabriel, and M DePristo (2013) From FastQ data to high-confidence variant calls: the Genome Analysis Toolkit Best Practices pipeline. *Current Protocols in Bioinformatics* **43**:11.10.1-11.10.33.

Vickrey, AI, R Bruders, Z Kronenberg, E Mackay, RJ Bohlender, ET Maclary, R Maynez, EJ Osborne, KP Johnson, CD Huff, M Yandell, and MD Shapiro (2018) Introgression of regulatory alleles and a missense coding mutation drive plumage pattern diversity in the rock pigeon. *eLife* **7**:e34803

Visser, M, M Kayser, F Grosveld, and R-J Palstra (2014) Genetic variation in regulatory DNA elements: the case of OCA2 transcriptional regulation. *Pigment Cell Melanoma Research* **27**:169-177.

Warren, WC, DF Clayton, H Ellegren, AP Arnold, LW Hillier, A Künstner, S Searle, S White, AJ Vilella, S Fairley, A Heger, L Kong, CP Ponting, ED Jarvis, CV Mello, P Minx, P Lovell, TAF Velho, M Ferris, CN Balakrishnan, S Sinha, C Blatti, SE London, Y Li, Y-C Lin, J George, J Sweedler, B Southey, P Gunaratne, M Watson, K Nam, N Backström, L Smeds, B Nabholz, Y Itoh, O Whitney, AR Pfenning, J Howard, M Völker, BM Skinner, DK Griffin, L Ye, WM McLaren, P Flicek, V Quesada, G Velasco, C Lopez-Otin, XS Puente, T Olender, D Lancet, AFA Smit, R Hubley, MK Konkel, JA Walker, MA Batzer, W Gu, DD Pollock, L Chen, Z Cheng, EE Eichler, J Stapley, J Slate, R Ekblom, T Birkhead, T Burke, D Burt, C Scharff, I Adam, H Richard, M Sultan, A Soldatov, H Lehrach, SV Edwards, S-P Yang, X Li, T Graves, L Fulton, J Nelson, A Chinwalla, S Hou, ER Mardis, and RK Wilson (2010) The genome of a songbird. *Nature* **464**:757-762.

Wiens, JJ (1999) Phylogenetic evidence for multiple losses of a sexually selected character in phrynosomatid lizards. *Proceedings of the Royal Society of London B* **266**:1529-1535.

Wiens, JJ (2001) Widespread loss of sexually selected traits: how the peacock lost its spots. *TRENDS in Ecology & Evolution* **16**:517-523.

Williams, TM, and SB Carroll (2009) Genetic and molecular insights into the development and evolution of sexual dimorphism. *Nature Reviews Genetics* **10**:797-804.

Xu, Q, Y Wang, A Dabdoub, PM Smallwood, J Williams, C Woods, MW Kelley, L Jiang, W Tasman, K Zhang, and J Nathans (2004) Vascular development in the retina and inner ear: control by Norrin and Frizzled-4, a high-affinity ligand-receptor pair. *Cell* **116**:883-895

Xu, S, F Cheng, J Liang, W Wu, and J Zhang (2012) Maternal xNorrin, a canonical Wnt signaling agonist and TGF-B antagonist, controls early neuroectoderm specification in Xenopus. *PLoS Biology* **10**:e1001286.

Zarkower, D (2001) Establishing sexual dimorphism: conservation amidst diversity? *Nature Reviews Genetics* **2**:175-185.
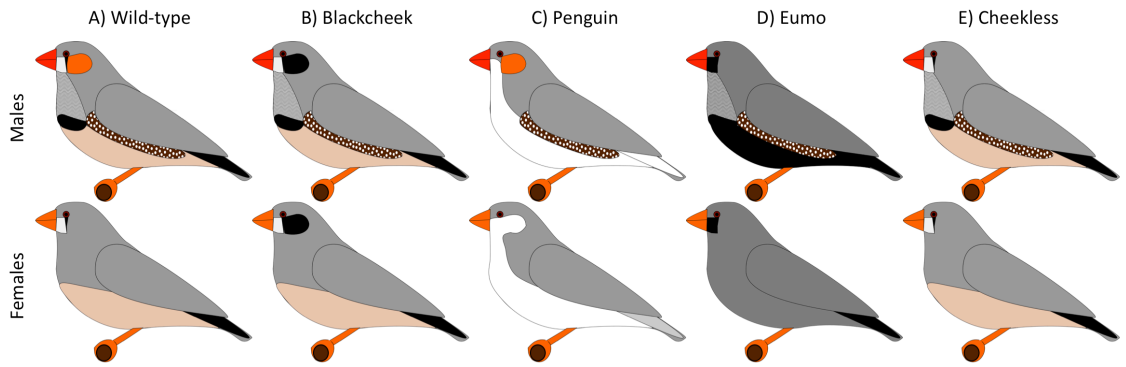
Figures

Figure 1: Captive-bred color mutants in Zebra Finch (A-E). The Wild-type finch (A) is sexually dimorphic in the cheek, breast, and flank plumage. In some domestic mutations, females may express a cheek patch (B,C), or males may lose expression of the cheek patch (D,E). In several of these mutants, the cheek becomes sexually monomorphic (B,D,E), representing a derived loss of sexual dimorphism in a single plumage patch while remaining dimorphic in the breast and flanks. Here, we investigate the genetic basis of one such mutant, the Blackcheek Zebra Finch (B).

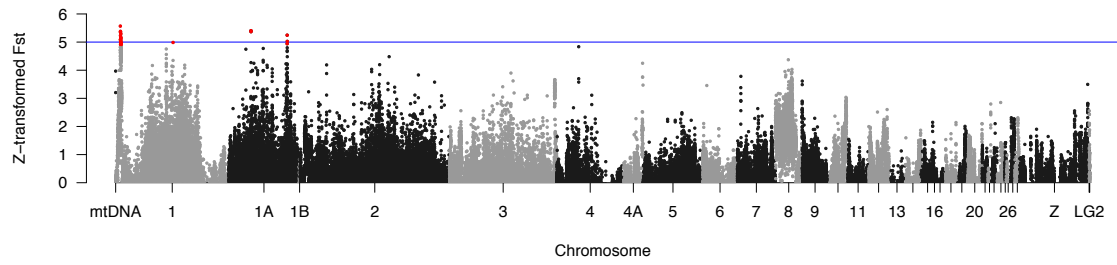**Figure 2:** Z-transformed Fst between Wild-type and Blackcheek Zebra Finches (n=20 total; n=5/morph/sex) scanned across the genome in overlapping sliding windows of 20kb with 10kb increments. The blue line represents an arbitrary cutoff for divergence peaks of a Z-score of 5. Four divergence peaks above that cutoff are highlighted in red.
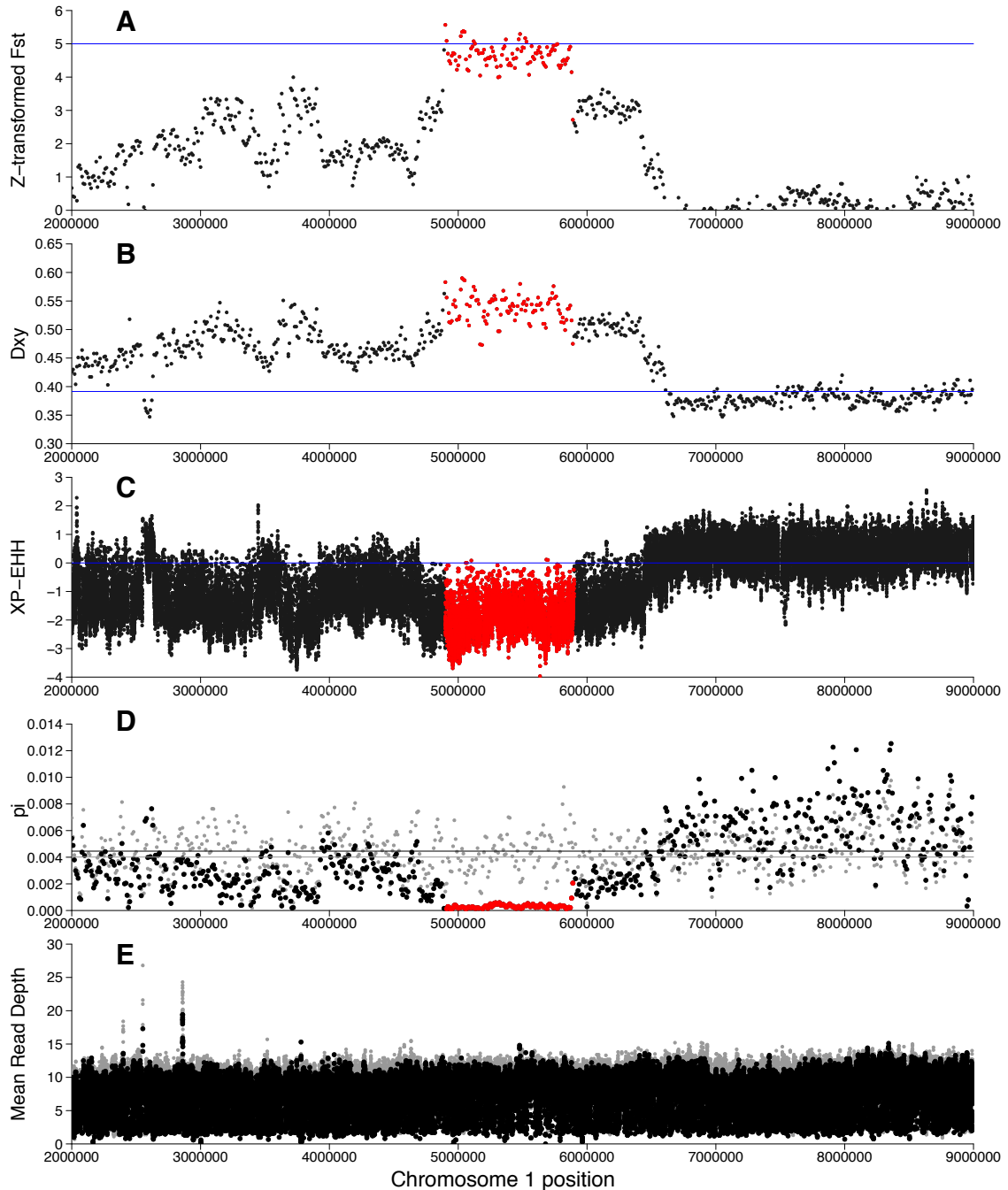
Figure 3: Major divergence peak (highlighted in red) between Wild-type and Blackcheek Zebra Finches on Chromosome 1. **A**) Z-transformed Fst between Wild-type and Blackcheek Zebra Finches in overlapping sliding windows of 20kb length with 10kb increments. Blue line indicates an arbitrary cutoff of a Z-score of 5. **B**) Absolute divergence (Dxy) in 20kb windows with 10kb increments. Genome-wide mean Dxy indicated with a blue line. **C**) Cross-population extended haplotype homozygosity (XP-EHH) between Wild-type and Blackcheek Zebra Finches. Values below zero (marked with a blue line) have higher integrated extended haplotype homozygosity in Blackcheek relative to Wild-type. **D**) Nucleotide diversity (pi) in Wild-type (gray) and Blackcheek

(black) populations, calculated in 20kb windows with 10kb increments. Genome-wide average pi for Wild-type and Blackcheek are shown in gray and black lines, respectively. **E**) Mean read depth for Wild-type (gray) and Blackcheek (black) populations.

Figure 4: Relationship of nucleotide diversity and Fst between Wild-type and Blackcheek Zebra Finches. Points represent mean values for each 20kb window scanned in overlapping 10kb increments across the genome. Windows from the major divergence peak (**Fig 3**; Chr1:4900000-5900000) are highlighted in red. Horizontal dotted line represents the genome-wide mean for nucleotide diversity in Blackcheek, and vertical dotted line represents the genome-wide mean for nucleotide diversity in Wild-type.
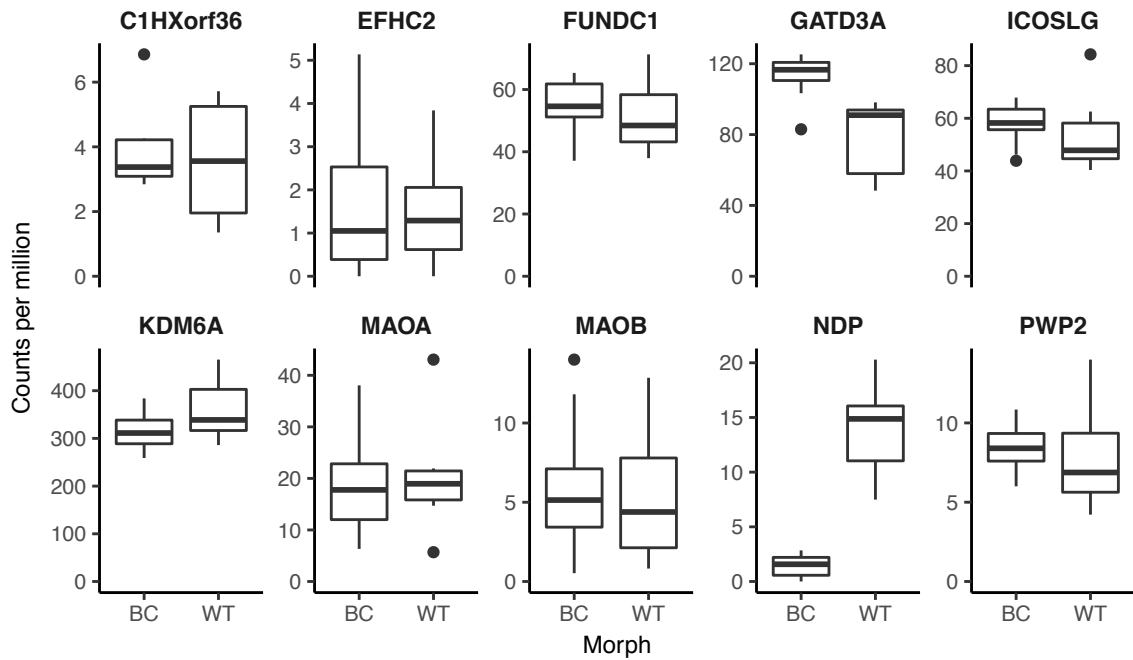
Figure 5: Differential expression of the ten candidate genes contained within the major divergence peak (**Figure 3**). Differential expression was tested between Blackcheek (BC; n = 9) and Wild-type (WT; n = 10) cheek feathers. Counts data are normalized by library size as counts per million. Sexes were combined for this analysis. Only GATD3A and NDP are differ significantly in expression between morphs ($p < 0.05$; see **Table 2**).

Figure 6: Minor divergence peak between Wild-type and Blackcheek Zebra Finches on Chromosome 1. **A)** Z-transformed Fst between Wild-type and Blackcheek Zebra Finches in overlapping sliding windows of 20kb length with 10kb increments. Blue line indicates an arbitrary cutoff of a Z-score of 5. **B)** Absolute divergence (Dxy) in 20kb windows with 10kb increments. Genome-wide mean Dxy indicated with a blue line. **C)** Nucleotide diversity (pi) in Wild-type (gray) and Blackcheek (black) populations, calculated in 20kb windows with 10kb increments. Genome-wide average pi for Wild-type and Blackcheek

are shown in gray and black lines, respectively. **D**) Mean read depth for Wild-type (gray) and Blackcheek (black) populations.
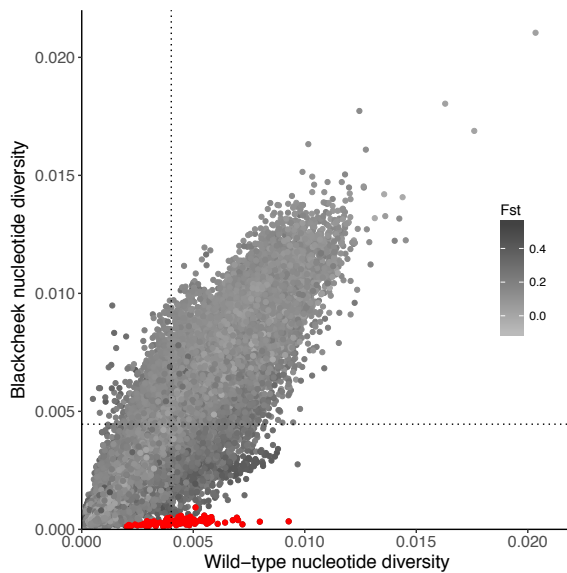
Figure 7: First minor divergence peak between Wild-type and Blackcheek Zebra Finches on Chromosome 1A. **A**) Z-transformed Fst between Wild-type and Blackcheek Zebra Finches in overlapping sliding windows of 20kb length with 10kb increments. Blue line indicates an arbitrary cutoff of a Z-score of 5. **B**) Absolute divergence (Dxy) in 20kb windows with 10kb increments. Genome-wide mean Dxy indicated with a blue line. **C**) Nucleotide diversity (pi) in Wild-type (gray) and Blackcheek (black) populations, calculated in 20kb windows with 10kb increments. Genome-wide average pi for Wild-

type and Blackcheek are shown in gray and black lines, respectively. **D**) Mean read depth for Wild-type (gray) and Blackcheek (black) populations.

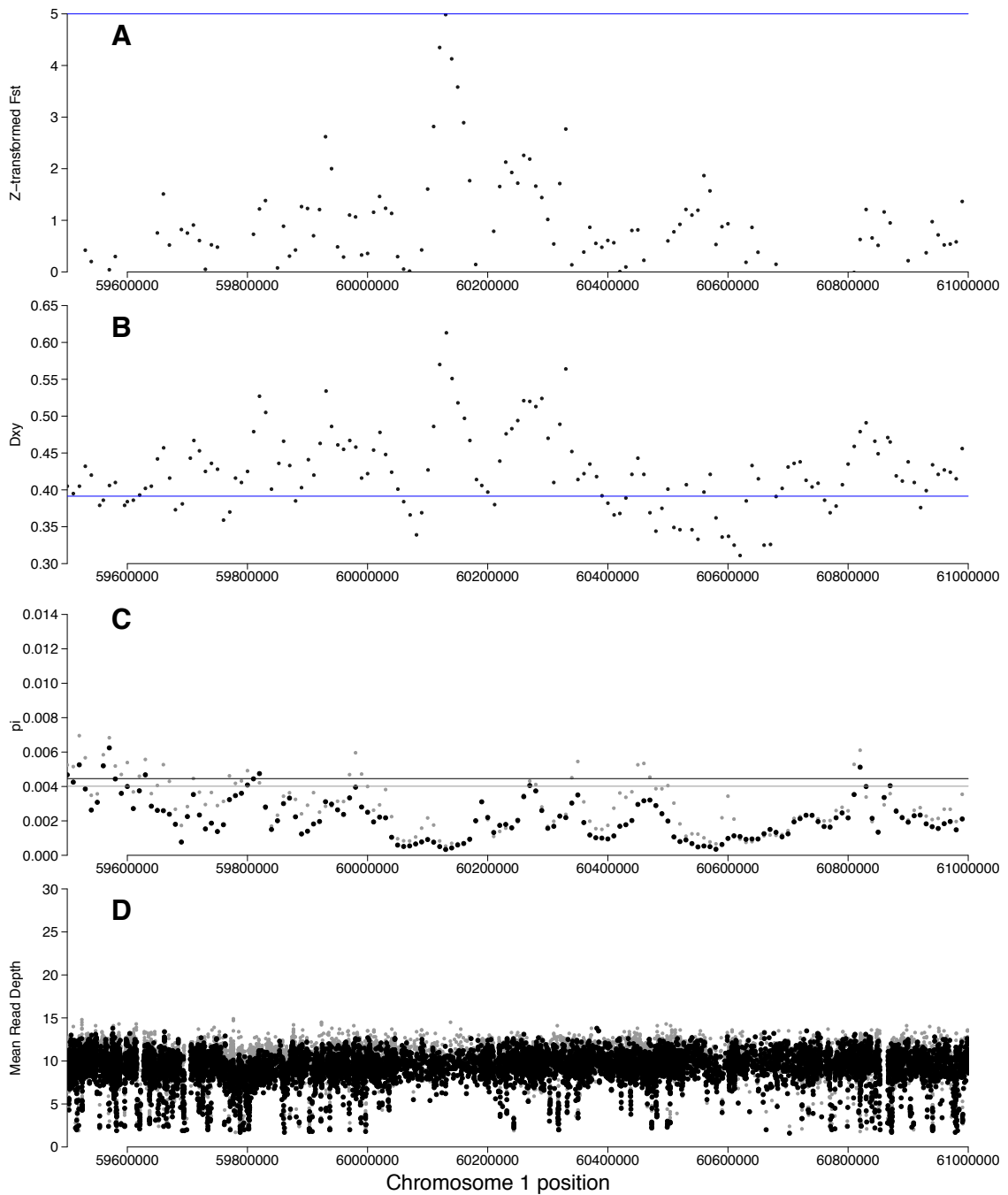**Figure 8**: Second minor divergence peak between Wild-type and Blackcheek Zebra Finches on Chromosome 1A. **A**) Z-transformed Fst between Wild-type and Blackcheek Zebra Finches in overlapping sliding windows of 20kb length with 10kb increments. Blue line indicates an arbitrary cutoff of a Z-score of 5. **B**) Absolute divergence (Dxy) in 20kb windows with 10kb increments. Genome-wide mean Dxy indicated with a blue line. **C**) Nucleotide diversity (pi) in Wild-type (gray) and Blackcheek (black) populations, calculated in 20kb windows with 10kb increments. Genome-wide average pi for Wild-

type and Blackcheek are shown in gray and black lines, respectively. **D**) Mean read depth for Wild-type (gray) and Blackcheek (black) populations.
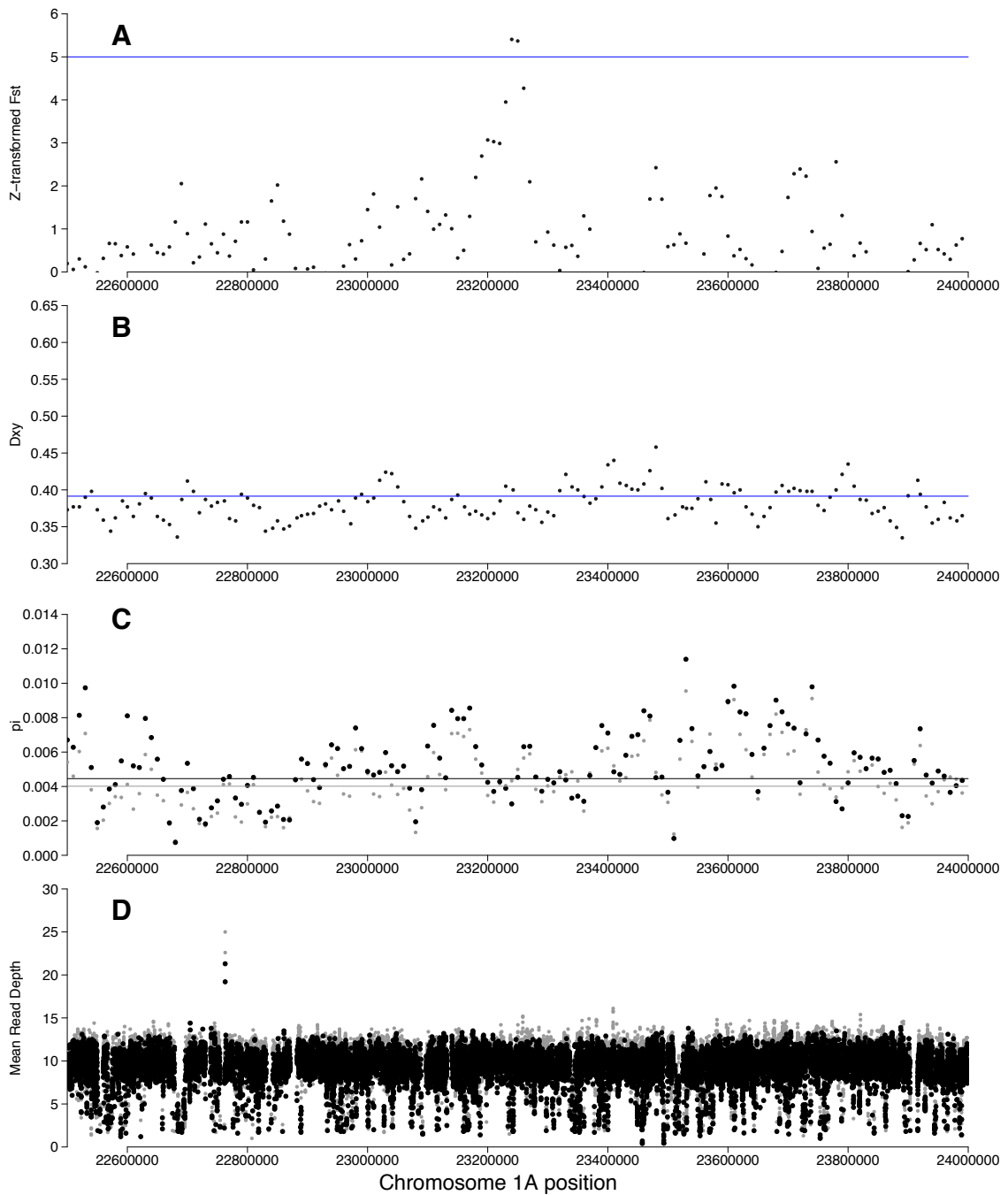
Figure 9: Divergence in gene expression between Wild-type (WT) and Blackcheek (BC) Zebra Finches in the melanogenesis network. The network is based on the KEGG melanogenesis pathway for Zebra Finch, with additional candidate genes and interactions added (**Table 1**). The endothelin signaling pathway has been omitted as no expression differences were found and it is not involved in MITF or OCA2 regulation.

Tables

Table 1: Candidate genes and interactions added to KEGG Zebra Finch melanogenesis pathway in **Figure 9**.

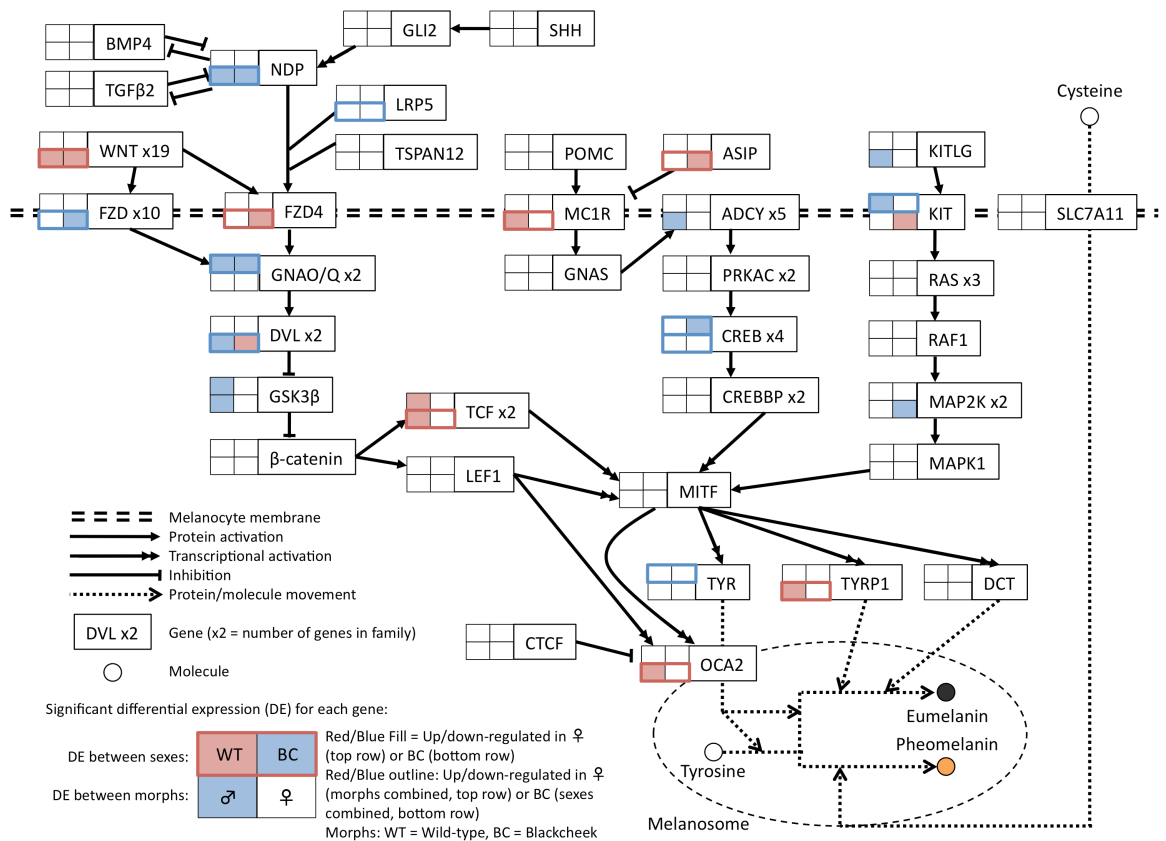| Gene name	Gene description	Gene ID	Function	Citation
NDP	Norrie disease protein	100224175	Fzd4 ligand	Hendrickx and Leyns (2008)
Shh	Sonic hedgehog signaling molecule	100222391	Induces signaling cascade to activate NDP transcription	McNeill et al. (2013)
Gli2	GLI family zinc finger 2	100221648	Induced by Shh signaling to bind to NDP promoter and initiate transcription	McNeill et al. (2013)
TGFB2	Transforming growth factor beta 2	100231617	Mutual inhibitor of NDP through direct binding	Xu et al. (2012)
BMP4	Bone morphogenetic protein 4	100221891	Mutual inhibitor of NDP through direct binding	Xu et al. (2012)
LRP5	LDL receptor related protein 5	100220027	Co-receptor required for NDP/FZD4 signaling activation	Xu et al. (2004)
TSPAN12	Tetraspanin 12	100220256	Co-receptor required for NDP/FZD4 signaling activation	Junge et al. (2009)
FZD4	Frizzled class receptor 4	100231781	Receptor for NDP and WNT; triggers canonical WNT signaling	Hendrickx and Leyns (2008)
MITF	Melanocyte inducing transcription factor	100232286	Target of NDP/FZD4 signaling; Enhances OCA2 expression	Visser et al. (2014)
LEF1	Lymphoid enhancer binding factor 1	100228376	Transcription factor of OCA2 and MITF activated by NDP/FZD4 signaling	Visser et al. (2014)
OCA2	Oculocutaneous albinism type 2	100228502	Regulates Tyrosinase transportation and function	Visser et al. (2014)
CTCF	CCCTC-binding factor	100224119	Suppresses the enhancer region of OCA2	Visser et al. (2014)
Slc7a11	Solute carrier family 7 member 11	100223276	Regulates pheomelanin production by transporting cysteine into melanocyte	Chintala et al. (2005)

Table 2: Differential expression between morphs and sexes in the ten genes located in the major divergence peak (**Figure 3**; Chr1:4900000-5900000). Bold p-values are significant at alpha=0.05. P-values marked with an asterisk (*) are significant at alpha=0.05 after Bonferroni correction.

Gene name	Gene ID	Wild-type - Blackcheek			Male-female		
		Sexes combined	Male	Female	Morphs combined	Wild-type	Blackcheek
PWP2	100218390	0.571	0.878	0.179	0.648	0.514	0.603
GATD3A	100229868	**0.001***	**0.016**	**0.005**	0.238	0.109	0.474
ICOSLG	100228022	0.354	0.191	0.801	0.132	0.217	0.380
C1HXorf36	100227072	0.653	0.769	0.746	0.902	0.925	0.909
KDM6A	100231869	0.091	0.051	0.659	0.693	0.388	0.705
FUNDC1	100228946	0.636	0.721	0.816	0.933	0.961	0.895
EFHC2	100226100	0.711	0.474	0.943	0.803	0.520	0.897
NDP	100224175	**0.000***	**0.001***	**0.004**	0.702	0.804	0.514
MAOB	100223232	0.609	0.433	0.778	0.313	0.876	0.218
MAOA	100221249	0.858	0.844	0.361	0.223	0.688	0.222

Table 3: Differential expression between morphs and sexes in the three genes located in the minor divergence peaks (**Figures 6-8**). Bold p-values are significant at alpha=0.05.

Divergence peak	Gene name	Gene ID	Wild-type - Blackcheek			Male-female		
			Sexes combined	Male	Female	Morphs combined	Wild-type	Blackcheek
1A:2324000	KCND2	100232741	0.055	0.326	0.121	0.825	0.716	0.720
	LOC105758561	105758561	0.784	0.488	0.722	0.893	0.501	0.682
1A:61111000	ST8SIA1	100225976	0.374	0.834	0.331	0.392	0.881	0.222

Table 4: Differences in module expression across Zebra Finch morphs and sexes. Module expression is summarized as the module eigengene (PC1 score) from modules identified by weighted gene coexpression network analysis (WGCNA). Bold p-values are significant at alpha=0.05. P-values marked with an asterisk (*) are significant at alpha=0.05 after Bonferroni correction.

| Module | Gene Count | Wild-type-Blackcheek | | | Male-female | | |
		Sexes combined	Male	Female	Morphs combined	Wild-type	Blackcheek
ME1	3739	0.354	0.134	0.642	0.542	0.174	0.528
ME2	1529	0.165	0.103	0.951	0.619	0.173	0.529
ME3	982	0.920	0.217	0.219	0.456	0.128	0.397
ME4	845	0.399	0.430	0.866	0.298	0.384	0.434
ME5	759	0.343	0.399	0.428	0.299	0.151	0.411
ME6	652	0.299	0.913	0.314	0.592	0.467	0.410
ME7	608	0.218	0.364	0.256	0.499	0.506	0.857
ME8	534	0.266	0.855	0.233	0.786	0.581	0.192
ME9	498	0.332	0.318	0.608	0.498	0.145	0.382
ME10	484	0.501	0.974	0.386	0.833	0.768	0.523
ME11	467	0.650	0.966	0.534	0.786	0.631	0.830
ME12	402	**0.036**	0.275	**0.004**	0.915	0.860	0.759
ME13	335	0.229	0.267	0.303	0.307	0.340	0.752
ME14	315	0.489	0.385	0.083	0.446	0.278	0.354
ME15	312	0.759	0.060	0.944	**0.000***	**0.000***	**0.001***
ME16	286	0.285	0.417	0.245	0.473	0.507	0.752
ME17	244	0.235	0.363	0.140	0.418	0.449	0.768
ME18	239	**0.017**	0.053	0.262	0.922	0.709	0.441
ME19	222	**0.024**	0.130	0.183	0.803	0.906	0.937
ME20	211	0.441	0.374	0.949	0.904	0.531	0.635
ME21	166	0.323	0.516	0.292	0.289	0.281	0.559
ME22	158	0.326	0.358	0.883	0.433	0.498	0.410
ME23	137	0.134	0.171	0.236	0.171	0.186	0.591
ME24	134	0.376	0.534	0.438	0.333	0.406	0.518
ME25	116	0.404	0.997	0.428	0.261	0.342	0.373
ME26	114	0.232	0.244	0.354	0.386	0.878	0.416
ME27	113	0.365	0.899	0.375	0.382	0.387	0.741
ME28	104	0.307	0.329	0.975	0.594	0.111	0.453
ME29	96	0.950	0.443	0.296	**0.000***	**0.000**	**0.007***
ME30	92	0.296	0.332	0.705	0.364	0.457	0.366
ME31	79	**0.000***	0.064	**0.000***	0.778	0.401	0.109
ME32	70	0.337	0.544	0.397	0.377	0.676	0.411
Unassigned	2684	0.997	0.714	0.255	0.103	0.252	0.302

Table 5: Significantly enriched Gene Ontology (GO) terms in sets of differentially expressed genes. ME lists refer to correlated expression modules from **Table 4**. WT = Wild-type. BC = Blackcheek

Gene list	GO term ID	GO term description	p-value	n of term genes	n of query genes	n of common genes
ME15	GO:1901700	response to oxygen-containing compound	2.20E-02	502	172	19
	GO:1901701	cellular response to oxygen-containing compound	2.71E-02	376	172	16
	GO:0043226	organelle	7.30E-03	6192	172	105
	GO:0043227	membrane-bounded organelle	5.90E-04	5289	172	97
	GO:0031982	vesicle	4.04E-02	670	172	22
	GO:0005623	cell	5.07E-03	8485	172	132
	GO:0044464	cell part	6.41E-03	8420	172	131
	GO:0012505	endomembrane system	2.93E-02	1600	172	39
	GO:0005622	intracellular	5.61E-03	7424	172	120
	GO:0044424	intracellular part	1.34E-02	7011	172	114
	GO:0043229	intracellular organelle	5.60E-03	6081	172	104
ME18	REAC:R-TGU-2024101	CS/DS degradation	4.98E-02	9	91	3
	REAC:R-TGU-5662702	Melanin biosynthesis	1.84E-03	5	65	3
ME19	GO:0030030	cell projection organization	3.93E-02	628	132	18
	GO:0120036	plasma membrane bounded cell projection organization	3.45E-02	622	132	18
	GO:0007275	multicellular organism development	3.44E-02	2143	132	39
	GO:0050794	regulation of cellular process	3.47E-02	5578	132	76
ME31	GO:1903901	negative regulation of viral life cycle	2.02E-02	17	36	3
	GO:0045071	negative regulation of viral genome replication	2.54E-03	9	36	3
DE: WT-BC (Sexes combined)	GO:0009605	response to external stimulus	6.55E-03	813	74	16
	GO:0071496	cellular response to external stimulus	3.60E-02	107	74	6
	GO:0051704	multi-organism process	1.02E-02	648	74	14
	GO:0009607	response to biotic stimulus	3.08E-02	285	74	9
	GO:0043207	response to external biotic stimulus	1.83E-02	267	74	9
	GO:0051707	response to other organism	1.78E-02	266	74	9
	GO:0015670	carbon dioxide transport	4.85E-02	2	74	2
	GO:0006631	fatty acid metabolic process	1.30E-02	137	74	7
	GO:0043292	contractile fiber	7.19E-03	81	74	6
	GO:0044449	contractile fiber part	3.04E-03	70	74	6
	GO:0030016	myofibril	5.34E-03	77	74	6
	GO:0030017	sarcomere	2.14E-03	66	74	6
DE: WT-BC (males)	GO:0019755	one-carbon compound transport	2.40E-02	4	22	2
	GO:0015670	carbon dioxide transport	4.00E-03	2	22	2
	GO:0012506	vesicle membrane	3.29E-02	105	22	4
	REAC:R-TGU-1480926	O2/CO2 exchange in erythrocytes	4.17E-02	11	14	2
	REAC:R-TGU-1237044	Erythrocytes take up carbon dioxide and release oxygen	4.17E-02	11	14	2
	REAC:R-TGU-1247673	Erythrocytes take up oxygen and release carbon dioxide	1.60E-02	7	14	2
	REAC:R-TGU-5662702	Melanin biosynthesis	7.63E-03	5	14	2
DE: WT-BC (females)	GO:0009615	response to virus	3.94E-02	102	23	4